ANALYSIS OF COHESIN ARCHITECTURE AND FUNCTION IN *SACCHAROMYCES CEREVISIAE*

John Ignatius Mc Intyre

Thesis presented for the degree of Doctor of Philosophy to
University College London

June 2007

Chromosome Segregation Laboratory
Cancer Research UK London Research Institute
44 Lincoln's Inn Fields
London WC2A 3PX

ProQuest LLC
789 East Eisenhower Parkway
P.O. Box 1346
Ann Arbor, MI 48106-1346

If we knew what it was we were doing, it would not be called research, would it?

Albert Einstein

PUBLICATIONS ARISING FROM THIS THESIS

Lengronne, A., **Mc Intyre, J.**, Katou, Y., Kanoh, Y., Hopfner, K.P., Shirahige, K., and Uhlmann, F. Establishment of sister chromatid cohesion at the *S. cerevisiae* replication fork. Mol Cell. 2006 Sep 15;23(6):787-99

Mc Intyre, J., Muller, E.G.D., Weitzer, S., Snydsmann, B., Davis, T.N., and Uhlmann, F. *In vivo* analysis of cohesin architecture using FRET in the budding yeast *S. cerevisiae*. (EMBO J, in press).

ABSTRACT

In this thesis I have undertaken a detailed molecular analysis of a conserved protein complex instrumental in genome stability. I have used the budding yeast *Saccharomyces cerevisiae* in conjunction with FRET (Fluorescence resonance energy transfer) to come up with a refined molecular architecture of the cohesin complex. This analysis involved the construction of an extensive panel of strains combining pair-wise FRET donor and acceptor fluorophores on subunits of the cohesin complex. This study has revealed many new and interesting insights into the functioning of the complex, which would not have been possible by many conventional biochemical techniques. For example we have shown that cohesin complexes exist as monomers using this analysis. The Scc1 subunit could be mapped to the heads in a conformation somewhat different to current models. Current thinking depicts Scc1 as a bridge between the otherwise distal Smc1 and Smc3 heads. Here we show instead that Scc1 likely adopts a conformation with its C-terminus sitting in a groove between the Smc1 and Smc3 heads. It was also revealed that the Smc1 and Smc3 heads are constitutively together. We also provide new information on the mode of interaction of Pds5 with the cohesin complex.

Additionally I have generated mutant alleles of the Smc1 and Smc3 subunits of the cohesin complex. These mutant proteins are impaired in ATP hydrolysis. Such mutants have afforded us the opportunity to assess when during the cohesin cycle ATP hydrolysis is required. I have shown that ATP hydrolysis is crucial for cohesin loading onto chromatin, with the mutant alleles showing substantially reduced kinetics of chromatin recruitment. Additionally, ATPase activity seemed not to be required for either cohesion establishment or cohesin relocation along chromosomes.

This study provides us with crucial new molecular details on the functioning of the cohesin complex – a master regulator of genome stability.

TABLE OF CONTENTS

LIST OF FIGURES

CHAPTER 1

CHAPTER 2

CHAPTER 3

CHAPTER 4

CHAPTER 5

ABBREVIATIONS

aa, amino acid
ATP, adenosine triphosphate
ABC, ATP binding cassette
AFM, atomic force microscopy
APC, anaphase promoting complex
BSA, bovine serum albumin
bp, base pairs
CAR, cohesin associated region
CIP, calf intestinal phosphatase
ChIP, chromatin immunoprecipitation
CFP, cyan fluorescent protein
CSF, CFP spillover factor
D, dalton
    kDa, kilodalton
    mDa, megadalton
dNTP, deoxyribonucleotide triphosphate
DIC, differential interference contrast
DSB, double strand break
DNA, deoxyribonucleic acid
    ssDNA, single stranded DNA
    dsDNA, double stranded DNA
DNAse, deoxyribonuclease
DTT, dithiothreitol
ECL, enhanced chemiluminescence
EM, electron microscopy
EDTA, ethylenediamine tetraacetic acid
FACS, fluorescence activated cell sorting
FLIM, fluorescence lifetime imaging microscopy
FRAP, fluorescence recovery after photobleaching
FRET, fluorescence resonance energy transfer
g, gram
    mg, milligram
    μg, microgram
GAL1, galactose inducible promoter 1
GAP, GTPase activating protein
GFP, green fluorescent protein
GST, glutathione S-transferase
HA, hemagglutinin
HEPES, 4-(2-hydroxyethyl)-1-piperazineethanesulfonic acid
HRP, horseradish peroxidase
HU, hydroxyurea
Ig, immunoglobulin
IP, immunoprecipitation
IPTG, isopropyl β-D-1 thiogalactopyranoside
IR, ionizing radiation
L, litre
    ml, millilitre
    μl, microlitre
MAT, mating type
Mb, megabase

min, minute
NBD, nucleotide binding domain
NOC, nocodazole
OD, optical density
ORF, open reading frame
PEG, polyethylene glycol
PIPES, 1,4-Piperazinediethanesulfonic acid
PMSF, phenylmethanesulfonyl fluoride
PCR, polymerase chain reaction
RNA, ribonucleic acid
RNAi, RNA interference
RNAse, ribonuclease
RPM, revolutions per minute
SDS, sodium dodecyl sulphate
SMC, structural maintenance of chromosome
SFM, scanning force microscopy
SPB, spindle pole body
TEV, tobacco etch virus
Tris, 2-amino-2-hydroxymethyl-1,3-propanediol
UTR, untranscribed region
UV, ultraviolet
YFP, yellow fluorescent protein
YSF, YFP spillover factor
WHD, winged helix domain

ACKNOWLEDGEMENTS

I would first like to thank my supervisor Frank Uhlmann for what can only be described as his extreme enthusiasm for science. I am very indebted to Frank for his unflagging excitement and encouragement during my four years at Cancer Research UK.

I thank all members of the chromosome segregation laboratory for their continued support both in and out of the lab and for making the lab such a nice place to work. I especially thank the world's best scientific officer and my very good friend Chris for her dealing with my constant demands and whinging. Thanks also to all my friends within the LRI, especially Karen, Sean, Jonathan and Stuart.

Special mention must also go to both Eric Muller and Trisha Davis at the University of Washington, Seattle. Without their collaboration and advice with FRET, this project would never have been possible.

I will always be grateful to my parents who have always gave me every opportunity and always believed in me.

1 Chapter 1: Introduction

1.1 Sister chromatid cohesion

Since the dawn of cell biology, cytologists have marvelled at the magic of mitosis. How can a complex event such as the accurate distribution of chromosomes from an apparent mess of genetic material occur with such amazing fidelity? Walther Fleming, a German biologist was amongst the first to observe thread like molecules in the nuclei of cells that appeared to be dividing. Later these threads were named chromosomes and Fleming summarised the process, referring to it as "karyomitosis" (Fleming, 1882). Over one hundred years later we are only now beginning to have a conceptual understanding of the molecular machines that govern this transition. Many processes are important to this partitioning – the spindle, kinetochore-microtubule interactions and the spindle pole body. Beyond this of course is the requirement for an 'identity' mechanism to identify pairs of identical DNA molecules (termed sister chromatids). We now know that sister chromatids remain tightly paired and do not separate appreciably from the time of their genesis in S phase until anaphase onset. By merit of the fact that sister chromatids come in pairs enables the cells to bi-orient these sisters with spindles microtubules emanating from opposite poles of the cell. This ensures that one of each sister chromatid is dragged into each daughter cell hence ensuring they receive the correct genetic complement (Reviewed in (Nasmyth, 2002). Errors in this process, resulting in missing or supernumerary chromosomes (termed aneuploidy), are observed in most cancers (reviewed in (Jallepalli and Lengauer, 2001) and are the primary causative agent in spontaneous human miscarriages (Boue et al., 1975; Hassold et al., 1980). But is chromosome mis-segregation responsible for the initiation of tumorigenesis, or merely a consequence of the tumorigenic state? It has been documented that genetic instability can be observed at even the earliest stages in colorectal polyps (Shih et al., 2001). This of course does not absolutely define that loss of a specific genomic locus is the *raison d'être* in tumor formation, but nonetheless shows that chromosome instability occurs long in advance of these polyps ever becoming malignant.

Undoubtedly, a detailed molecular understanding of the players involved in chromosome segregation, but more importantly their concise mechanism of action will lead to a sounder footing on which to develop potential therapeutic agents.

1.2 SMC containing protein complexes

1.2.1 The cohesin complex

The cohesin complex is the primary mediator of chromosomal cohesion in eukaryotes. This ring shaped protein complex loads onto DNA before cohesion establishment in S phase and keeps sister chromatids cohered until the time of anaphase onset. Cohesins were discovered as a result of genetic screens in budding yeast to identify mutants that had precocious separation of sister chromatids before anaphase onset (Michaelis et al., 1997; Guacci et al., 1997b). Later studies identified the binding partners of Scc1 (Sister Chromatid Cohesion 1) as Smc1, Smc3 and Scc3 (Losada et al., 1998; Toth et al., 1999). Smc1 and Smc3 are members of the Structural Maintenance of Chromosome family that have diverse roles in many cellular processes from recombination, condensation, and gene dosage compensation (reviewed in Hagstrom and Meyer, 2003). Before considering how cohesin mediates cohesion of DNA molecules we must first consider the architecture of this conserved protein complex. Based on a large body of evidence, one very popular model of cohesin function is that of the 'embrace model'. This theory posits that cohesin complexes exist as large proteinacious rings that are capable of trapping within their inner circumference DNA replication products (Haering et al., 2002). This is based on a number of key pieces of evidence, each of which is discussed in greater detail below. (1) The first images of holo cohesin complexes were of both human and *Xenopus laevis* cohesins as visualised by electron microscopy (Anderson et al., 2002). Here it was shown that cohesins form ring shaped complexes with the coiled coil arms of both Smc1 and Smc3 encompassing most of the circumference of the cohesin ring. Cohesin, unlike condensin, had a more flexible hinge region, and the coiled coils emanated from the hinge in a variety of conformations and angles. Budding yeast cohesin complexes were seen to adopt a similar

conformation (Haering et al., 2002). Extensive biochemical characterisation of the yeast cohesin complex expressed in insect cells has also provided us with a detailed map of the interaction between subunits (Haering et al., 2002), with the Scc1 subunit thought to serve as a bridge between the heads of Smc1 and Smc3. Scc3 links to the heads of Smc1 and Smc3 in a manner dependent on Scc1. Furthermore, this study demonstrated that hetero-dimerisation of Smc1 and Smc3 is conferred by their hinge domains (See figure 1.1 for schematic). (2) A second major prediction of the ring model of cohesin is that cleavage of any part of the ring should liberate it from DNA. This is indeed the case and cleavage of either a protease site engineered version of Scc1 or Smc3 (TEV protease) results in cohesin dissociation from chromosomes and the separation of sister DNA molecules (Gruber et al., 2003). Similarly, the creation of 'open' cohesin complexes where Smc1 lacks its head or coiled coil domains fail to associate with DNA (Weitzer et al., 2003). (3) The third and final argument in favour of the ring model is the recent demonstration that cohesin complexes are topologically associated with circular minichromosomes in budding yeast. Cleavage of cohesin by TEV cleavable Scc1 leads to dissociation of this cohesin from the minichromosome. Conversely, cleavage of the DNA by restriction enzymes gives the same result (Ivanov and Nasmyth, 2005). These results are hard to reconcile with models where cohesin rings embrace chromatin directly (via direct protein-DNA interactions), but are wholly consistent with a topological ring around sister chromatids.

The Scc3 subunit of cohesin as mentioned, interacts with the cohesin complex in an Scc1 dependent manner and no direct interaction can be seen in the absence of Scc1 (Haering et al., 2002). Three homologues of Scc3 exist in human cells, SA1, SA2 which are required for mitotic cohesion (Losada et al., 2000; Sumara et al., 2000) and SA3 whose role is restricted to meiosis (Pezzi et al., 2000). SA2 phosphorylation has been shown to be instrumental for the prophase removal of cohesins in human cells (Hauf et al., 2005). In budding yeast, Scc3 is required for the generation of cohesion, and mutants in Scc3 display major cohesion defects when the protein is inactivated from G1 (Toth et al., 1999).

Scc1/Rad21/Mcd1 is the so called Kleisin subunit of the cohesin complex (Schleiffer et al., 2003) and is cleaved by separase at anaphase onset (Uhlmann et al., 1999). This is the basic mechanism underlying chromosome segregation in all known eukaryotes. Scc1 has been shown in *in vitro* expression systems to bind to the head domains of Smc1 and Smc3, and the N- and C-terminal cleavage products of Scc1 bind the Smc3 and Smc1 heads respectively (Haering et al., 2002). Some evidence suggests that Scc1 acts as a bridge between otherwise distal Smc1 and Smc3 heads (Gruber et al., 2003). In this study the authors reasoned that Scc1 exists as a bridge for the following reason. Following Scc1 cleavage at anaphase and the cleavage of Smc3 with TEV in the extract, immunoprecipitation of Scc1 C-terminus should co-immunoprecipitate both Scc1 N-terminus and the Smc3 head TEV cleavage fragment, assuming that the Smc1 and Smc3 heads interact directly. The authors conclude that since this IP does not pull down the Scc1 N-terminus or the Smc3 head, it follows that the Smc1 and Smc3 heads are not together when Scc1 is bound, i.e. Scc1 serves as a bridge between the heads. An equally plausible alternative is that since the IP is performed in the presence of Scc1 C-terminus cleavage product, something that has been shown to have extreme destabilising effects on the interaction between the Smc1 and Smc3 heads (Weitzer et al., 2003), this is why the IP failed to detect this interaction. A crystal structure has been obtained for the yeast Smc1 head co-crystallized along with a C-terminus fragment of Scc1 of some 115 amino acids (Haering et al., 2004). Key amongst the interesting features of this structure is the interaction between a so-called winged helix domain (WHD) on Scc1's extreme C-terminus and the terminal two β-strands on the Smc1 head. Indeed the mutation of even a single residue on this WHD can abolish the interaction with Smc1 and renders the protein non-functional.

Pds5 is another putative component of the cohesin complex but its exacting role in cohesion is somewhat obscure. Pds5 bears homology to BimD protein of *A. nidulans*, an essential protein required for both DNA repair and mitotic chromosome segregation (Holt and May, 1996; Denison et al., 1993). A homologue also exists in *S. macrospora* where it plays a role in mitotic and meiotic cohesion and the formation of the synaptonemal complex (van Heemst et al., 1999). In budding yeast too, Pds5 is essential and mutants display very

severe cohesion defects. Some conflicting evidence exists as to the interdependency of binding between Scc1 and Pds5. It seems clear that Scc1 is an absolute prerequisite for Pds5 recruitment onto chromosomes. In contrast there is evidence for and against the need for Pds5 for Scc1 binding in budding yeast (Panizza et al., 2000; Hartman et al., 2000). However it seems the case in *Xenopus* extracts that Pds5 is not required for Scc1 binding to DNA (discussed below). The proteins show strong colocalisation of binding sites on budding yeast chromosomes (Lengronne et al., 2004), and like other cohesin components Pds5 dissociates from chromatin at the metaphase to anaphase transition (Panizza et al., 2000; Hartman et al., 2000). Pds5 is not however essential in *Schizosaccharomyces pombe*, and remarkably this genetic background allows for the disruption of the otherwise essential cohesin establishment factor Eso1 (Eco1 in budding yeast) (Tanaka et al., 2001). In both *Xenopus* and mammalian cells Pds5 exists in two isoforms – Pds5a/Pds5b (Sumara et al., 2000; Losada et al., 2005). It interacts with the cohesin complex in a salt sensitive manner, but its depletion by RNAi in HeLa cells or *Xenopus* extracts results in only very subtle cohesion defects. Similar to results obtained by Hartmann *et al* but in contrast to those of Panizza *et al*, Pds5 depletion does not result in an apparent reduction of other cohesin components on chromatin (Losada et al., 2005). Pds5 is sumoylated in a cell cycle dependent manner, with sumoylation being high around G1/S and lowest at anaphase and G1. Furthermore, the over-expression of a sumo isopeptidase, Smt4 rescues the temperature sensitivity of three different alleles of Pds5 (Stead et al., 2003). However the nature of this rescue could be attributed to any number of pleiotropic effects the over-expression would have on other sumo-conjugated proteins. Topo II has also been found to be a high copy suppressor of Pds5 mutants but the functional significance or specificity of this result remains to be determined (Aguilar et al., 2005). Interesting is also the recent finding that Eco1/Ctf7 over expression suppresses the temperature sensitivity of Pds5 mutants and *vice versa* (Noble et al., 2006).

Chromosomal binding sites have been generated examining the pattern of cohesin binding in budding yeast. Cohesin binds to distinct sites along chromosome arms and show an enrichment around the centromeres (Tanaka et al., 1999; Blat and Kleckner, 1999; Megee et al., 1999). Cohesin binding sites

also correlate with an increased AT DNA content (Blat and Kleckner, 1999; Glynn et al., 2004). Cohesin recruitment to an ectopic centromere on a budding yeast chromosome depends on it having a functional kinetochore. For example, the repression of centromere function by GAL transcription through it prevents Scc1 recruitment. Similarly, the presence of mutant kinetochore proteins (Cse4, Mif2 or Ndc10) also fails to recruit Scc1 to an ectopic centromere (Tanaka et al., 1999). Cohesin sites on chromosome arms are of course not bound by kinetochore proteins (Megee et al., 1999), hence the mechanism of cohesin recruitment differs somehow between arm and centromeric regions. Importantly, it has been demonstrated that a centromere can direct binding of cohesin to adjacent chromatin, even if it is the case that these CEN flanking sequences do not bind cohesins normally. Amazingly, the excision of a centromere from its chromosome by expression of a site specific recombinase induces both the removal of cohesins from the centromere and the surrounding flanking regions. This occurs both if the centromere is excised from G1 or excised in G2 (Megee et al., 1999; Weber et al., 2004). This suggests that the centromere and its associated proteins promote the binding and the maintenance of cohesin at pericentric regions.

One of the earliest clues that transcription may be a determinant of cohesin positioning came from the observation that transcriptional repression of a centromere by strong transcription from the *GAL1* promoter abolished cohesin binding at this locus (Tanaka et al., 1999). Consistent with this is the binding of cohesins in boundary regions of silenced chromatin (Laloraya et al., 2000). More recent studies have shown that transcription is indeed a major determinant of cohesin positioning in budding yeast. Induction of transcription for example can actively remove cohesin from a previously untranscribed gene. Consistently, the vast majority of cohesin sites in budding yeast are associated with convergent transcription sites in intergenic regions. (Lengronne et al., 2004; Glynn et al., 2004). These characteristics are upheld in both meiosis of budding yeast (Glynn et al., 2004) and in fission yeast mitosis (Lengronne et al., 2004) indicating that this might be a universally conserved process in eukaryotes.

1.2.2 The condensin complex

The second SMC containing complex in eukaryotes is the condensin complex. As the name suggests, this complex plays a major role in chromosome condensation (Hirano, 2006). The core components of the complex - Smc2 (XCAP-E) and Smc4 (XCAP-C), are also members of the SMC family of proteins which also includes the cohesin core components (Hirano and Mitchison, 1994); (Saka et al., 1994). Genetic studies in *S. pombe, S. cerevisiae, Drosophila melanogaster* and *Caenorhabditis elegans* have shown the complex to be very important for chromosome condensation and segregation. Mutant phenotypes in these organisms show similar phenotypes, namely uncondensed nuclei and the presence of anaphase bridges (Saka et al., 1994; Strunnikov et al., 1995; Bhat et al., 1996). Condensin complexes from both human cells and *Xenopus* extracts have been visualised by electron microscopy. Condensin, in contrast to cohesin often displays a more closed conformation, with the arms emanating from the hinge at a smaller and less variable angle (Anderson et al., 2002). Condensin in addition to the SMC core contains an additional three subunits that are thought to have a regulatory role in condensin function (See table 1.1, Figure 1.1) (Kimura and Hirano, 2000). The CAP-D2 and CAP-G subunits of the complex are HEAT repeat containing proteins (Neuwald and Hirano, 2000) while the CAP-H component of the complex is thought to be the Kleisin subunit (Schleiffer et al., 2003). With respect to the biochemistry of condensin, this has been characterised most extensively using holo condensin complexes immunopurified from *Xenopus* extracts. Holo condensin has the ability to bind DNA independently of ATP hydrolysis (Kimura and Hirano, 1997; Strick et al., 2004). Instead condensin uses ATP hydrolysis to condense DNA. This requirement has been seen both for the positive supercoiling and the positive knotting of DNA (Kimura and Hirano, 1997; Kimura et al., 1999). Condensin has an ATPase activity which is stimulated by the presence of DNA (Kimura and Hirano, 1997), but this is strictly dependent on the presence of the non-SMC subunits of condensin (Kimura and Hirano, 2000; Stray and Lindsley, 2003). Furthermore, condensation *in vitro* and *in vivo* is also dependent on these non-SMC proteins (Kimura and Hirano, 2000). Structural studies of both condensin and DNA-condensin complexes have given us important insights as to how this complex works at a mechanistic level.

Circular plasmid DNA incubated in the presence of condensin, ATP and type II topoisomerases is seen to undergo a positive knotting reaction and these knotted DNA molecules can be seen by electron microscopy (Kimura et al., 1999). Single molecule studies have also highlighted the fact that the action of condensin is highly co-operative, and that halving the protein concentration in a single molecule reaction can completely abolish any condensation activity (Strick et al., 2004). This suggests that condensins work together, perhaps as some sort of superstructure in order to condense DNA. Condensin interaction with DNA has also been visualised by electron spectroscopic imaging (ESI). DNA is seen to wrap around a globular domain of the condensin complex (presumably the ATPase head) and does so in an ATP hydrolysis dependent manner with approximately 190bp of DNA being wound by a single condensin complex (Strick et al., 2004). Subunit interaction studies have also been performed with recombinant proteins, and bear some similarities to the results obtained for cohesin as discussed above. Human Smc2 and Smc4 form a heterodimer independently of the non-SMC subunits. The non-SMC subunits were also able to form subcomplexes (Onn et al., 2007). These results are consistent with results in *Xenopus* where distinct condensin complexes exist of 13s (holo condensin), 11s (CAP-D2, CAP-G and CAP-H) and 8s (CAP-E and CAP-C) (Hirano et al., 1997; Kimura and Hirano, 2000). Consistent with the fact that CAP-H is the Kleisin subunit is the finding that (1) its N- and C-terminus bind Smc2 and Smc4 respectively and (2) CAP-D2 or CAP-G binding to the holo complex is dependent on the presence of CAP-H. In contrast to cohesin, ATP binding seems not to be required for complex assembly for condensin (Onn et al., 2007). Two condensin complexes exist in higher eukaryotes named condensin I and condensin II. They share the same set of core SMC subunits and differ in their non-SMC subunits (Ono et al., 2003). Condensin I is approximately five times more abundant than condensin II but depletion of condensin II specific subunits nonetheless also results in chromosome condensation and structural defects, albeit subtly different to condensin I knockdown (Ono et al., 2003).

Condensin function is also regulated by different means in different organisms. In higher eukaryotes for example, although condensin II is seen in the nucleus throughout the cell cycle, condensin I is only recruited onto chromatin

after nuclear envelope breakdown (Ono et al., 2004). Additional levels of regulation also underlie condensin function in *Xenopus*. Holo condensin complexes isolated from interphase extracts have negligible condensation abilities compared to complexes isolated from mitotic extracts. This was shown to be due to stimulatory phosphorylation of CAP-D2 and CAP-H, by Cdc2, most likely in a direct manner (Kimura et al., 1998). Casein kinase has also recently been shown to have an inhibitory effect on condensin function in interphase through phosphorylation of CAP-C, CAP-G and CAP-H (Takemoto et al., 2006). Fission yeast condensin is also subject to stimulatory phosphorylation at the hands of Cdc2 (on Cut3/Smc4), but this phosphorylation is instrumental in nuclear targeting of condensin in mitosis (Sutani et al., 1999).

1.2.3 The Smc5/6 containing complex

The Smc5/6 complex also plays a key role in the maintenance of genome integrity, but its function seems to be more specific to the DNA damage response pathway (see figure 1.1 for schematic and table 1.1) (reviewed in (Lehmann, 2005). The founding member of the complex is the RAD18 gene (Smc6), identified in screens for radiation sensitive mutants in *S. pombe* (Nasim and Smith, 1975). The gene was subsequently cloned and identified as RAD18, an SMC like protein with putative coiled coils and ATP binding sites (Lehmann et al., 1995). A hypermorphic allele of RAD18, *rad18-X*, was shown to be both UV and IR sensitive. It was later shown that this hypermorphic allele is a single point mutant near the hinge region of Rad18 (Fousteri and Lehmann, 2000). Surprisingly, RAD18 was shown to be an essential gene in both *S. pombe* and *S. cerevisiae* (RHC18) (Lehmann et al., 1995) unlike other DNA damage proteins, indicating it had an essential function beyond the DNA damage response. *rad18* mutants are also defective in the repair of double strand breaks (DSBs) induced by ionizing radiation and undergo aberrant mitosis after apparently escaping from a checkpoint arrest. This is despite the fact that the DNA damage checkpoint is activated as determined by Chk1 phosphorylation (Verkade et al., 1999). Similarly, Rad18 shut-off from the thiamine repressible nmt1 promoter does result in checkpoint activation but cells nonetheless enter mitosis with aberrant

chromosomes, probably due to the inability to sustain a checkpoint response (Harvey et al., 2004). In budding yeast cells progressing through the cell cycle from G1 to G2/M at the non-permissive temperature in an *smc6-9* and *smc5-6* background show evidence of DNA damage as visualised by both the accumulation of DDC1 damage foci and Rad53 phosphorylation (Torres-Rosell et al., 2005).

The Smc5/6 complex was shown to exist in a high molecular weight complex in *S. pombe* and the Rad18 partner was identified as Spr18 (SMC partner of Rad18) (Fousteri and Lehmann, 2000). Subsequent studies identified four non-SMC components of the complex, all of which are essential, and mutations of which cause DNA sensitivity similar to that seen with Rad18. These non-SMC element (nse) proteins are Nse1, Nse2 (Mms 21 in *S. cerevisaie*), Nse3 (YDR288W in *S. cerevisiae*) and Nse4 (Rad62 in *S. pombe*) (Sergeant et al., 2005; Fujioka et al., 2002; Harvey et al., 2004; McDonald et al., 2003; Hu et al., 2005; Pebernard et al., 2004; Morikawa et al., 2004). So how does this complex act at a mechanistic level to facilitate DNA repair reactions? The overall picture is still somewhat vague, but there is some evidence that Smc5/6 functions by promoting recombination reactions within the cell in response to DNA damage. The earliest evidence for this came from the observation that the *S. pombe rad18-X* showed epistatic interaction with recombination proteins Rhp51 and Rad2 (Lehmann et al., 1995). In support of this notion in *S. cerevisiae* is the finding that the *smc6-56* allele does not show additive sensitivity to DSB inducing agent MMS in a Rad52 deletion background, indicating that Smc6 is indeed working in the same pathway as Rad52 i.e. that of homologous recombination (Onoda et al., 2004). Similarly, *rad62-1* is epistatic with Rhp51 (the homolog of the *S. cerevisiae* Rad51) (Morikawa et al., 2004), as are *nse1-1*, *nse1-2* and *nse1-3* (McDonald et al., 2003; Pebernard et al., 2004). Interestingly, homologous recombination itself seems not to be compromised in *rad62-1*, as assayed by the ability to recombine a functional auxotrophic *Leu1*$^{+}$ marker at the *leu1-32* locus in *S. pombe* (Morikawa et al., 2004). In contrast, intra-chromosomal recombination events are compromised in *A. thaliana* in a mutant of the putative plant RAD18 gene (Mengiste et al., 1999). Meiosis (which involves recombination synapse formation in Meiosis I) is also defective in *S. pombe* in an

nse1-1 mutant background, and shows decreased crossover events (Pebernard et al., 2004). Finally, this concept is corroborated by the recent finding in human cells that RNAi mediated knockdown of Nse2 results in a dramatic decrease in the frequency of sister chromatid exchange events to the same extent as knockdown of Scc1 (Potts et al., 2006).

Although no structural information exists on the architecture of the Smc5/6 complex by way of EM images or crystal structures, a significant amount of *in vitro* work has given a good picture of the interaction partners and general geometry of the complex (See figure 1.1 for schematic). Rad18 (Smc6) and Spr18 (Smc5) bind each other directly. Nse2, the RING finger component, binds to Spr18 via the head proximal coiled coils, but does not interact with Rad18. Nse1 in turn forms a complex with Nse3 but fails to bind Rad18, Spr18, Nse2 or Rad62. Instead it forms a stable complex with Nse3. Nse3 however can complex with Rad62/Nse4, indeed this seems to be Nse4's only binding partner. Hence two major subcomplexes exist – the Spr18/Rad18/Nse2 complex and a separate Nse1/Nse3/Rad62(Nse4) complex (Sergeant et al., 2005). Nse5 and Nse6 were later shown to form a subcomplex, that can interact with Smc5 or Smc6 alone, and do so with the coiled coils of Smc5 and Smc6 (Pebernard et al., 2006); (Palecek et al., 2006). Nse4 was identified as the Kleisin subunit of Smc5/6 based on predicted structural homology to domains in Scc1's N- and C-terminus. Remarkably, Nse4 interacts in the same manner with the ATPase heads of Smc5 and 6, as does Scc1 with Smc1 and Smc3. Specifically, the introduction of point mutants in the predicted helix-turn-helix of Nse4 C-terminus can abolish the interaction with Smc5 (Haering et al., 2004; Palecek et al., 2006). In contrast to the other subunits, Nse5 and 6 are not essential for growth in *S. pombe* but their deletion nonetheless results in DNA damage sensitive cells (Pebernard et al., 2006). These subunits in contrast are essential proteins in *S. cerevisiae* (Zhao and Blobel, 2005). Enzymatic activities have been assigned to subunits of the Smc5/6 complex. Nse1 for example has a RING finger domain which is found in E3 ubiquitin ligases but this putative activity remains to be characterised (McDonald et al., 2003; Fujioka et al., 2002). Nse2 has a zinc-finger motif, and possesses sumo-ligase activity specific to Smc5/6 components. Interestingly, a mutant form of Nse2 lacking sumo-ligase activity in *S. pombe*, could substitute for the wild

type Nse2 to support cell viability, but was nonetheless damage sensitive (Andrews et al., 2005). This is reminiscent of a C-motif mutant in Rad18, that can also support viability but confers damage sensitivity on cells (Fousteri and Lehmann, 2000). This remains unexplained, but one could speculate that the proteins do not use their enzymatic activities for their 'essential' function, and that these activities are reserved for participating in the DNA damage response. This could explain the gross reorganisation of the nucleus into a hollow sphere when either wild type or ATPase mutant versions of Rad18 are over-expressed in *S. pombe* (Harvey et al., 2004) i.e. an ATPase dead version of the complex retains the ability to alter nuclear structure.

Smc5/6 recruitment to chromosomes seems to be regulated temporally during the cell cycle. In both *Xenopus* egg extracts and budding yeast its association with chromosomes is not seen before DNA replication (Lindroos et al., 2006; Tsuyama et al., 2006). In *Xenopus*, this result is not surprising, given that Scc2/4 is also a prerequisite for the Smc5/6 loading reaction in budding yeast (Lindroos et al., 2006), and Scc2 itself is not loaded onto chromatin until DNA replication has begun in *Xenopus* extracts (Gillespie and Hirano, 2004). Cohesin itself is also recruited to DSBs (discussed in section 1.7), and in human cells at least this recruitment is dependent on the Smc5/6 complex (Potts et al., 2006). Smc5/6 is also recruited to DSBs in budding yeast (De Piccoli et al., 2006; Lindroos et al., 2006) but this recruitment is independent of Scc2, but depends instead on the presence of Mre11 (Lindroos et al., 2006).

	S. cerevisiae	*S. pombe*	*H. sapiens*
Cohesin			
Molecular function = Chromosomel cohesion, DNA DSB repair			
Smc1	Smc1	Psm1	hSmc1α/hSmc1β
Smc3	Smc3	Psm3	hSmc3
Scc1*	Scc1/Mcd1	Rad21	hRad21
Scc3	Scc3	Psc3	hSA1/hSA2
Pds5	Pds5	Pds5	hPds5a/hPds5b
Rec8 (Meiotic)	Rec8	Rec8	hRec8
Condensin			
Molecular function = DNA condensation, some chromosomal cohesion, rDNA segregation			
Smc2	Smc2	Cut14	hSmc2/hCAP-E
Smc4	Smc4	Cut3	hSmc4/hCAP-C
Cap-D2	Ycs4	Cnd1	hCAP-D2
Cap-G	Ycg1/Ycs5	Cnd3	hCAP-G
Cap-H*	Brn1	Cnd2	hCAP-H
Smc5/6 complex			
Molecular function = DNA damage response, rDNA segregation			
Smc5	Smc5	Spr18	hSmc5
Smc6	Rhc18	Rad18	hSmc6
Nse1	Nse1	Nse1	hNse1
Nse2	Mms21	Nse2	hNse2
Nse3	YDR288W	Nse3	?
Nse4*	Qri2	Nse4/Rad62	hQri2/hNse4
Nse5	YML023c	Nse5	?
Nse6	Kre29	Nse6	?

* denotes Kleisin subunit

Table 1.1 Classification of SMC containing protein complexes in eukaryotes

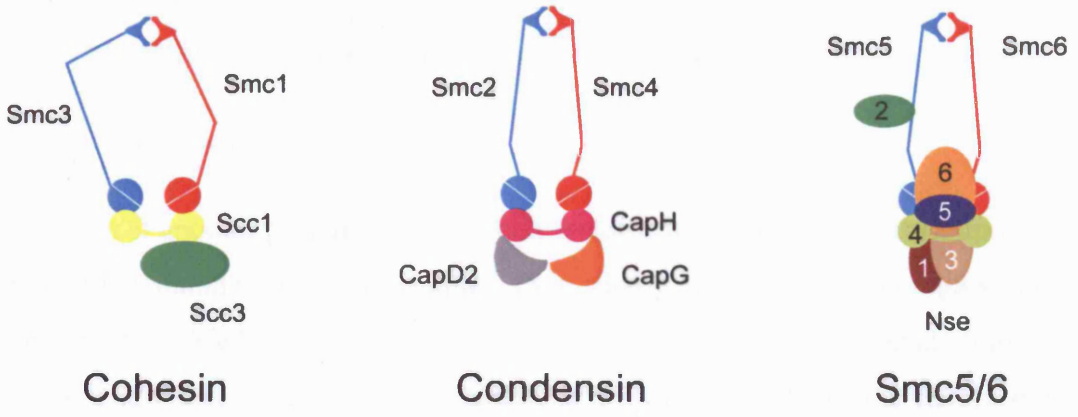

Figure 1.1 Schematic representing the architecture of SMC containing protein complexes in eukaryotes.

1.3 Mechanistic insights from ABC ATPases

1.3.1 The RAD50 protein

Yet another protein complex with architectural similarity to cohesin is the RAD50 containing protein complex (See figure 1.2A). This complex, also known as the MRN (Mre11/Rad50/Nbs1) or MRX (Mre11/Rad50/Xrs2) complex plays a key role in DNA repair reactions within the cell, and is involved in telomere maintenance, homologous recombination and non-homologous end joining (reviewed in Assenmacher and Hopfner, 2004). The Rad50 protein itself shares structural similarity to SMC proteins. Both electron micrographs and crystal structures of *P. furiosus* and human Rad50 reveal an elongated structure with globular domains at either end of the protein (See figure 1.2C) (Hopfner et al., 2000; 2001). The Rad50 protein contains orthologues in the three kingdoms of life (Hopfner et al., 2000), underlying its evolutionary importance in genome stability. Like other ABC type ATPases, Rad50 contains conserved residues required for ATP binding and hydrolysis, namely Walker A, Walker B and C-motif domains. The signature motif (also known as C-motif) is one of the most conserved features of ABC ATPases. Surprisingly, from the crystal structure of an ABC transporter (Hung et al., 1998), the signature motif was seen to be remote from the ATP binding site formed by the Walker A and B motifs. This paradox was explained by the crystal structures of both Rad50 (Hopfner et al., 2000) and MutS mismatch repair protein (Obmolova et al., 2000). In these dimeric structures, ATP is bound by the Walker A and Walker B from one ABC domain, while the C-motif makes specific contacts with the ATP γ-phosphate from the other ABC domain (See figure 1.2B). These crystal structures also revealed for the first time the ATP dependent dimerisation of the nucleotide binding domain (NBD) domains and this in turn was seen to promote the DNA binding of Rad50 in *in vitro* assays. This ATP-dependent dimerisation was shown to depend on the presence of a signature motif (Hopfner et al., 2000) and signature motif mutants were subsequently shown to be devoid of ATP binding activity (Moncalian et al., 2004). Furthermore, signature motif mutants in the *S. cerevisiae* Rad50 were not able to complement sensitivity to DNA damaging agent in a Rad50 deletion

background. The presence of a positively charged groove created by the ATP dependent dimerisation at the interface between two Rad50 catalytic domains has also been proposed based on the Rad50 crystal structure. This in turn has led to an attractive model of ATP dependent dimerisation and hence the creation of a DNA binding patch on the Rad50 catalytic domain. ATP hydrolysis in turn would lead to dissociation of the catalytic domains and thus release of DNA (Hopfner et al., 2000). The Mre11 component of the Rad50 complex possesses both endonuclease and exonuclease activities. (Paull and Gellert, 1998; Furuse et al., 1998) and binds to the Rad50 dimer via the coiled coils proximal to the ATPase heads of Rad50 (Hopfner et al., 2001). Rad50 DNA binding activities have been extensively studied to date. Earlier EM work on both human and *P. furiosus* Rad50 show DNA binding to occur via the globular catalytic domains of the protein. More recently, high resolution real time imaging of Rad50 protein in solution has provided illuminating new insights into its mechanism of action on DNA. Like cohesin (and also condensin, but to a lesser extent), the arms of Rad50 have been shown to be highly flexible (de Jager et al., 2001). Rad50/Mre11 protein complexes, when added to linear DNA, seem to have a preference for DNA ends. Atomic force microscopy (AFM) imaging of Rad50/Mre11 complexes revealed a striking change in the conformation of the complex upon DNA binding. In the absence of DNA, Rad50 self associates along with two Mre11 proteins to form a heterotetramer. This complex was seen as a variety of forms, but loosely resembles a ring with the hinge region in either an open or closed conformation (Moreno-Herrero et al., 2005). Upon DNA binding, the complex becomes more rigid, with the coiled coils adopting a parallel configuration. Heterotetramers are also seen to swap from intramolecular interaction at the hinge, to intermolecular interaction between hinges of different complexes, hence now becoming capable of tethering distal DNA molecules.

The hinge region itself is also different from the known crystal structure of the *T. maritama* hinge (Haering et al., 2002). Significantly, dimerisation occurs via the creation of a composite Zn^{2+} binding site via each of two conserved cysteine residues from two different Rad50 proteins. This is thought to lead to a switch from dimerisation within a Rad50 complex, to dimerisation in an open arm

conformation to facilitate long-range DNA bridging reactions (Hopfner et al., 2002).

Given the similarity between the SMC protein complexes, both at the sequence level and architecturally, it is reasonable to assume that they may share at least some similar mechanisms of action in terms of the ATP binding and hydrolysis cycle.

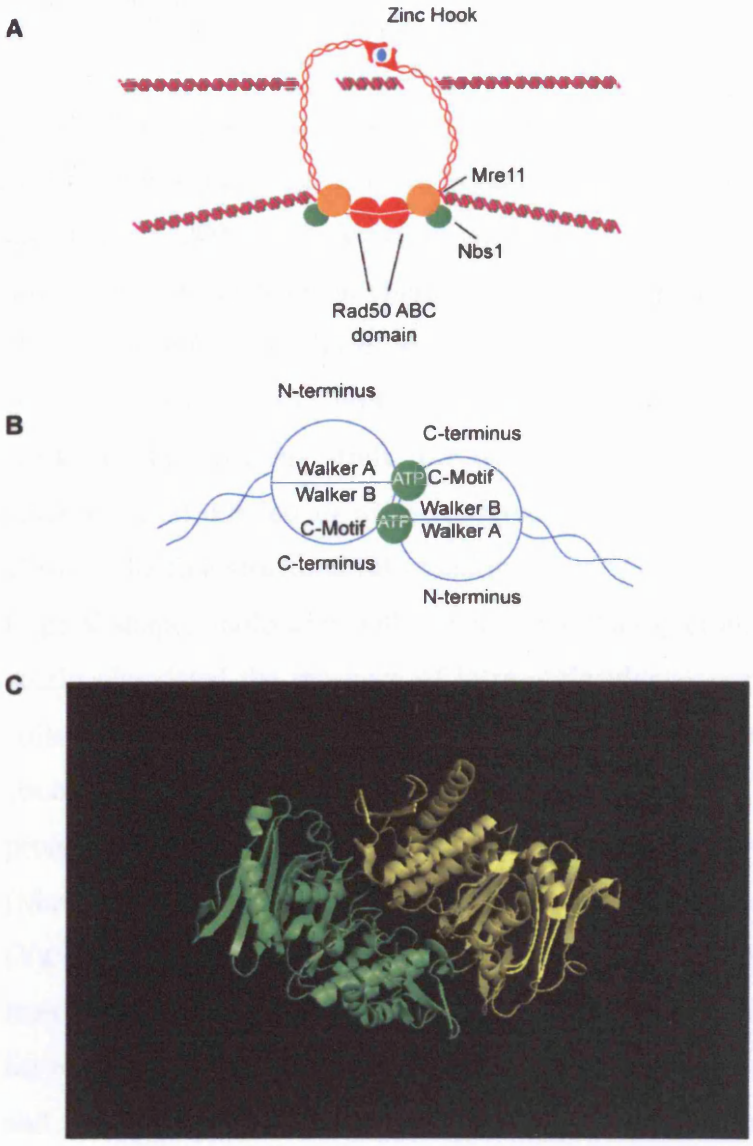

Figure 1.2 Structural organisation of the ABC ATPase Rad50

(**A**) Schematic model of Rad50/Mre11/Nbs1. Rad50 catalytic domains dimerise in an ATP dependent manner. The antiparallel coiled coils emanate from the catalytic domains and form a 'zinc hook' type hinge in the middle of the coils. Mre11 binds to Rad50 via the coiled-coils adjacent to the catalytic head domains. The exact location of Nbs1 has not been determined experimentally.
(**B**) Two ATP molecules bind to the Rad50 catalytic domain dimer using the contacts shown. The nucleotide binding site is composed of the Walker-A and Walker-B in one head and the C-motif from the adjacent catalytic domain. The γ-phosphate oxygens of ATP hydrogen bonds with the C-motif serine and glycine residues.
(**C**) A structure of the ATP bound Rad50 catalytic domain dimer. The catalytic domain has a dimension of approximately 70 x 40 x 25 Å and resembles a bowl shaped structure with a two-lobed fold in each of the catalytic domains. (Hopfner et al, 2000, figure prepared using PyMol software).

1.3.2 Bacterial SMC proteins

SMC containing protein complexes contribute to organisation and compaction of the genome in all organisms studied to date (reviewed in (Losada and Hirano, 2005). Prokaryotes contain a single SMC protein and extensive structural and biochemical characterisation of both *Escherichia coli* MukB and *Bacillus subtilis* SMC have been carried out to date. The first clue as to the possible roles of SMC proteins in any organism came from Hiraga and co-workers. In this early study, the use of temperature sensitive alleles and the deletion of MukB led to massive defects in nucleoid segregation (Niki et al., 1991). The first structural information on SMC proteins revealed the presence of large V shaped molecules with coiled-coils (Melby et al., 1998). This study also neatly elucidated the presence of intra-molecular as opposed to inter-molecular coiled coils in the SMC protein. Prokaryote SMC proteins, like their eukaryote counterparts, do not function alone, but rather interact with a subset of regulatory proteins. The *B. subtilis* SMC protein interacts with ScpA and ScpB (Mascarenhas et al., 2002), while *E. coli* MukB interacts with MukE and MukF (Yamazoe et al., 1999). Remarkably, the so-called 'Kleisin' family of SMC interacting proteins are also conserved in bacteria (Schleiffer et al., 2003). MukF for example, is predicted to form a similar helix-turn-helix structure at both its N- and C-terminus, similar to what is seen for the *S. cerevisiae* Kleisin, Scc1 (Fennell-Fezzie et al., 2005; Haering et al., 2004). Structural information does exist for the *T. maritama* SMC head (Lowe et al., 2001), and its crystal structure shows an ABC ATPase fold with the ability to aggregate DNA in an ATP dependent manner. The DNA binding activities of SMCs and how this is controlled by ATP binding and/or hydrolysis has been extensively characterised by Hirano and co-workers. The *B. subtilis* SMC protein has an intrinsic DNA binding ability, with a preference for ssDNA (Hirano and Hirano, 1998). This ability to bind DNA is independent of ATP in *in vitro* assays (Hirano and Hirano, 1998), and indeed a mutant in the C-Motif in the bacterial SMC does not inhibit DNA binding activities of the protein (Hirano et al., 2001). These results suggest that ATP hydrolysis is implicated in DNA compaction or aggregation activities of the SMC protein and is not required for the loading reaction onto DNA *per se*.

This seems to be indeed the case, because in spin down assays used to measure protein aggregation, the aggregation of protein is dependent specifically on the presence of ATP, but not necessarily on the ability to hydrolyse ATP, as the aggregation also occurs in the presence of the non-hydrolysable ATP analogue, ATPγS (Hirano and Hirano, 1998). Consistent with this notion, is the fact that a 'headless' SMC protein (and hence one lacking an ATPase domain) still retains its DNA binding activities comparably to the wild type SMC (Hirano and Hirano, 2002). These results are in direct contrast to the absolute requirement of ATP hydrolysis for cohesin complex loading onto DNA (Arumugam et al., 2003; Weitzer et al., 2003).

More important perhaps for the loading of bacterial SMC proteins onto DNA is the hinge domain. The crystal structure of the *T. maritama* SMC hinge has been solved and displays a 'doughnut' shaped structure which in principle could clamp a double helix (Haering et al., 2002). Indeed biochemical data reveal a basic patch in the hinge absolutely required for DNA binding by the SMC (Hirano and Hirano, 2006). Furthermore, hinge mediated dimerisation of SMC proteins was also a prerequisite for their DNA binding, suggesting perhaps the creation of a composite DNA binding patch formed by two hinge domains (Hirano and Hirano, 2002). Bacterial SMC proteins display a basal as well as a DNA stimulated ATPase activity (Hirano and Hirano, 1998), the latter recently being attributed to the presence of a conserved 'arginine finger' near the ATPase active site (Lammens et al., 2004). Good evidence now exists for a degree of 'communication' between the head and hinge, at least in that of the bacterial SMC. A comprehensive mutational analysis of residues in the hinge domain has uncovered an un-expected role for the hinge in regulating the mechano-chemical cycle of SMC. The introduction of mutations into the basic patch in the hinge required for DNA binding specifically abolishes the DNA stimulated ATPase activity of the protein, while the basal ATPase activity remains intact (Hirano and Hirano, 2006). This suggests that DNA binding at the hinge domain affects the ATPase activity of the head domains, possibly through either long distance activation through the coiled coils, or through a direct head-hinge interaction.

1.3.3 Membrane transporter ABC ATPases

The ABC (ATP binding cassette) protein superfamily spans a wide group of proteins involved in many diverse cellular processes. One member of this family, the ABC transporter family, is involved in the transport of a variety of substances across lipid membranes in both prokaryotes and eukaryotes. These proteins, also known as traffic ATPases, are amongst the largest gene family in bacteria numbering over 80 in *E. coli*. Some 48 membrane transporters have been linked to disease in humans (reviewed in Davidson, 2002; Dean et al., 2001).

A typical membrane transporter consists of a canonical ATP binding cassette containing the conserved residues seen in other ATP binding cassettes such as Walker A, Walker B and C-Motif domains (Locher et al., 2002). Predictably, these residues are highly conserved, and membrane transporters use power derived from ATP hydrolysis to transport their cargo in or out of a given cell. In addition to the nucleotide binding domain, membrane transporters also contain hydrophobic membrane spanning domains that convert the ATPase cycle to a power stroke to facilitate cargo transport. These membrane domains, in contrast to the NBD are more variant (Chen et al., 2003; Dawson and Locher, 2006), presumably to facilitate the transport of a variety of cargo. Membrane transporters carry a wide variety of cargos, including proteins, sugars, metal ions, minerals and certain classes of drugs and toxins. Their function is also of clinical importance, as mutations in these proteins have been shown to have a causative effect in many disease classes. This includes cystic fibrosis, multidrug resistance and adrenoleukodystrophy (Riordan et al., 1989; Gottesman et al., 1996; Mosser et al., 1993).

Membrane transporters can exist as a single polypeptide consisting of both the NBD and transmembrane domains, or these may be expressed as separate proteins. Crystal structures exist for separate NBD, which show a similar ATP dependent dimerisation arrangement as is the case for Rad50 (Smith et al., 2002; Yuan et al., 2001). Structures also exist for full-length proteins containing their membrane domains (Locher et al., 2002; Dawson and Locher, 2006). These together with ATP dependent conformational changes observed in the structure of MalK ATPase subunit of maltose transporter (Chen et al., 2003), have led to

models whereby ATP hydrolysis might cause opening of the transmembrane domains during repeated rounds of ATP binding and hydrolysis, thus enabling transport of a cargo across the membrane. Good evidence for this model came from electrophysiology experiments with the cystic fibrosis transmembrane conductance regulator (CFTR) protein, where it was shown that ATP binding results in the tight dimerisation of the NBD of the protein with a resulting opening of the distal transmembrane domains (Vergani et al., 2005).

Cohesin transport onto DNA also depends on ATP hydrolysis (Arumugam et al., 2003; Weitzer et al., 2003) but this reaction presumably is limited to a single transport event. The question of a conformational change in the coiled coils of cohesin (analogous to the alpha helical transmembrane domains) upon ATP hydrolysis has not been addressed to date. Indeed neither has the idea of whether ATP hydrolysis is required for unloading cohesin complexes from DNA.

1.4 The role of ATP binding and hydrolysis during the cohesin cycle

Cohesin complexes, unlike their bacterial SMC proteins, use energy derived from ATP hydrolysis to load onto DNA. Mutations in any of the conserved residues required for ATP binding or hydrolysis completely fail to complement the deletion of the wild type protein (Arumugam et al., 2003) or rescue the growth of temperature sensitive alleles of either Smc1 or Smc3 (Weitzer et al., 2003). Bacterial SMC proteins seem not to require ATP hydrolysis for the initial loading reaction (as discussed in section 1.3.2), but rather may use ATP hydrolysis for the mechanical knotting of protein as is the case for the condensin complex (see section 1.2.2). So why is their an apparent mechanistic difference between cohesin and condensin? This conundrum could be explained by the fact that cohesin loading is one in itself sufficient for it subsequently to be converted into a cohesive cohesin complex. In this case there is but a single ATPase requiring event, i.e. loading, assuming ATP hydrolysis is not required during cohesion establishment. Scc1 recruitment to cohesin complexes is also dependent on the binding, but not necessarily the hydrolysis, of ATP by Smc1. These results concluded that since the N-terminal Scc1 fragment

alone is incapable of binding Smc3, there is a step-wise binding of Scc1 to the cohesin complex. Scc1 first would bind via its C-terminus to Smc1 and this would allow the subsequent binding of Scc1 N-terminus to the Smc3 head. Mutant Smc1 and Smc3 proteins were also shown to be unable to promote the association of Scc1 with chromatin (Arumugam et al., 2003) Furthermore, the interaction between the Smc1 and Smc3 heads seems to be independent of ATP mediated contacts since ATPase mutant versions of an Smc1 head still retain the ability to bind full length Smc3 (Weitzer et al., 2003). This is of course fundamentally different to Rad50, where the interaction between the catalytic domains is absolutely dependent on ATP binding (see section 1.3.1).

Scc1 rather unexpectedly plays a very important role in stimulating the ATPase activity of Smc1 (Arumugam et al., 2006). Indeed it is apparent in this study that both Smc1 and Smc3 have only very low ATPase activity in the absence of Scc1. Smc1 and Smc3 when purified from yeast display a 6-8-fold increase in ATPase activity when supplemented with an equi-molar ratio of Scc1 C-terminus cleavage fragment. Furthermore, this stimulation of ATP hydrolysis by Scc1 can effect either Smc1 or Smc3. For example, both Smc1-E1158Q(Walker B)/Smc3 or Smc1/Smc3-E1155Q(Walker B) is stimulated to the same extent as wild type Smc1/Smc3 by Scc1 C-terminus. In these Walker B mutants, only ATP hydrolysis and not binding are perturbed. Hence, the ATPase heads of Smc1 and Smc3 can hydrolyse ATP independently of each other, providing that the integrity of ATP binding in the active site (as mediated using contacts from both heads) is intact. This result is hard to reconcile with the fact that this Walker B mutant completely fails to complement the wild type protein *in vivo*. In addition, the generation of a point mutant in Scc1 C-terminus that strongly affects the binding to Smc1, cannot be rescued by fusing the Scc1 C-terminus to Smc1 C-terminus (as is the case for wild type proteins). Hence, this mutation in Scc1 in addition to mediating the interaction with Smc1, is also likely to be important for modulating the ATPase cycle.

1.5 Chromosomal cohesion during the cell cycle

1.5.1 DNA binding of cohesin

As discussed in the previous section, ATP hydrolysis is required for cohesin's association with DNA. In addition to this, a conserved protein complex called Scc2/4 is also a prerequisite for this loading reaction. This protein was first identified in fission yeast (called Mis4) where it was shown to be required for the stable maintenance of a minichromosome (Takahashi et al., 1994). Later Scc2 and Scc4 proteins were identified in *S. cerevisiae*, and shown to be responsible for cohesin loading in late G1 (Ciosk et al., 2000; Toth et al., 1999). Scc2/4 seems to execute its primary function with respect to cohesin early in the cell cycle. For example, inactivation of temperature sensitive alleles of Scc2 (*scc2-4*) in G2/M retain robust cohesion (Ciosk et al., 2000) and Scc2 can be inactivated before release from a HU arrest without a very significant drop in cell viability (Lengronne et al., 2006). Hence it seemed that Scc2/4 is a 'loader' for cohesin complexes, and this is conserved in human cells (Watrin et al., 2006) as well as *Xenopus* egg extracts (Takahashi et al., 2004; Gillespie and Hirano, 2004), suggesting that this is an evolutionarily conserved mechanism. Rather unsatisfying however was the fact that cohesin and Scc2/4 occupied different binding sites on the chromosome as determined by chromosome spreading (Ciosk et al., 2000). This paradox was resolved by the observation that cohesin complexes initially dock at these Scc2/4 binding sites from which they seem to translocate to the more permanent places of residence on the chromosome (Lengronne et al., 2004). Mechanistically as to how cohesin complexes are modified by Scc2/4 has not to date been addressed. A very interesting speculation however has been put forward whereby Scc2/4 stimulates the ATPase activity of Smc1 and Smc3 to facilitate their loading (Arumugam et al., 2003). This hypothesis neatly explains how the loading reaction would be regulated so as to have one and only one ATPase reaction by a cohesin complex (a second ATPase reaction might unload cohesin complexes). Since after loading, cohesin complexes are quickly shuttled away from Scc2/4, this would provide a spatial regulation to inhibit further rounds of ATP hydrolysis, hence keeping cohesin complexes locked tightly shut onto chromatin.

Although this seemed a reasonable and elegant hypothesis to explain the loading reaction, it has been recently shown that hinge opening of cohesin complexes is also a prerequisite for the loading reaction (Gruber et al., 2006). In this study Nasmyth and colleagues demonstrated that keeping the Smc1 and Smc3 hinge domains tethered by means of a drug inducible dimerisation strategy, prevented cohesin recruitment to chromosomes. Hence any new models for cohesin binding must now accommodate ATP hydrolysis by the heads, a reaction by Scc2/4, and some mode of hinge opening as well as several other factors (discussed below).

A potential meiotic cohesin loader also exists in *C. elegans* called TIM-1 (Chan et al., 2003) where it is found to interact with cohesin. RNAi knockdown of TIM-1 is embryonic lethal, but the use of a temperature sensitive allele, *tim-1*, allowed the authors to show its involvement in synapse formation and sister chromatid cohesion in meiosis. Similar to results in budding yeast, TIM-1 is required for both Rec8 (the meiotic Scc1) and Scc3 binding to chromatin. Interestingly, and in contrast to budding yeast, TIM-1 is not required for Smc1 binding to DNA. This may suggest that at least in *C. elegans* embryos, Smc1/Smc3 heterodimers can bind DNA independently of the non-SMC subunits.

Cohesin binding to chromosomes seems also in some cases to require specific chromatin remodelling of target DNA (reviewed in (Riedel et al., 2004). This is hardly surprising keeping in mind the dimensions of a cohesin ring, some 35nm in diameter. This in principle could accommodate either two naked DNA molecules (each approximately 2 nm) or two 10 nm nucleosomal fibres. In human cells, Rad21 is seen to co-localise with a chromatin modifying complex, SNF2h, along many *alu* containing sequences on human chromosomes. These proteins are also seen to interact physically in pull down experiments with recombinant proteins. (Hakimi et al., 2002). Expression of an ATPase mutant version of SNF2h results in a reduction in the Rad21 binding to the *alu* sequence. This result suggests that chromatin remodelling is required for cohesin association with human chromosomes. It should be pointed out that the authors do not address a direct causative effect for a lack of this chromatin remodeller. An alternative explanation of the observed defects could be more general

pleiotropic effects the lack of such a chromatin remodeller might have on other aspects of the DNA landscape that might be required for cohesin localisation e.g. changes in transcription, which are known to be a major determinant of cohesin positioning in *S. cerevisiae* (Glynn et al., 2004; Lengronne et al., 2004). Chromatin remodelling seems also to be required for some aspects of cohesin binding to budding yeast chromosomes. Mutations or deletions in subunits of the chromatin remodelling complex called RSC have been shown to have modest cohesion defects (Huang et al., 2004; Baetz et al., 2004). The Sth1 of RSC subunit cycles on and off chromatin with kinetics preceding that of Scc1 but only does so on arm regions, with a constitutive localisation at centromeric regions. Furthermore a temperature sensitive allele of Sth1 shows a cohesion defect on arm but not centromeric regions when inactivated from G1. Similarly *RSC2Δ* cells show precocious arm splitting and reduced chromatin-bound levels of Scc1 (Huang et al., 2004). In fission yeast, cohesin loading at centromeres is dependent upon the presence of the HP1 homologue Swi6 which binds to heterochromatin via methylated lysine 9 on the histone H3 tail (Bernard et al., 2001; Nonaka et al., 2002). Swi6 itself is not essential in fission yeast but its deletion results in elevated instances of lagging chromosomes. Such a histone modification does not exist in *S. cerevisiae* nor indeed a HP1 homologue (Briggs et al., 2001).

The mechanism of regulation of Scc2/4 binding to chromosomes seems also not to be absolutely conserved between different species. In *S. cerevisiae* this complex is constitutively chromatin bound throughout the cell cycle (Ciosk et al., 2000). This is in contrast to the situation in human cells where Scc2/4 disappears from chromosomes at the metaphase to anaphase transition (Watrin et al., 2006). Similarly in *Xenopus* egg extracts, deposition of Scc2/4 on chromatin is dependent on origin licensing before S phase (Gillespie and Hirano, 2004; Takahashi et al., 2004). Hence for whatever reason, higher eukaryotes have an additional regulatory step that is not present in budding yeast.

In vitro binding studies have been performed for both human and yeast cohesin complexes with rather limited success (Losada and Hirano, 2001; Kagansky et al., 2004). In the case of human cohesin complexes (isolated from HeLa cells), the complex had the ability to interact with naked DNA in an ATP

independent manner. For yeast complexes (reconstituted from proteins expressed in insect cells), nucleosomal binding was observed, again independently of ATP. This binding however was somewhat unspecific as it could be observed for sites that are bound and unbound by cohesin *in vivo*. The source of these discrepancies between the known *in vivo* requirements for DNA binding could be explained by the absence of additional regulatory proteins that confer some specificity on the reaction. Yet an additional level of complication comes from reports that cohesin complexes may have multiple modes of interacting with DNA (Milutinovich et al., 2007; Schmitz et al., 2007). In the absence of a protein called Sororin, cohesin complexes seem much more dynamic and cycle on and off DNA more rapidly (Discussed below in section 1.5.3).

Scc2/4 proteins are of clinical significance since mutation in these proteins are reported to have causative effects in Cornelia de Lange syndrome (reviewed in (Strachan, 2005). This developmental disorder is characterised by cranio-facial abnormalities, growth and neurodevelopmental retardation. From two initial studies, mutations in the human *NIPBL* gene a homologue of the *Drosophila Nipped-B* and fungal *Scc2* were linked to the disease (Krantz et al., 2004; Tonkin et al., 2004). These mutations cluster in the C-terminal HEAT repeats of the gene products, Delangin-1 and -2. This disease is most probably a cohesin specific phenomenon, and not due to the roles of Scc2 in condensin or Smc5/6 regulation. This is explained by the fact that new clinical cases have been observed with mutations in the Smc1 and Smc3 subunits of the cohesin complex (Deardorff et al., 2007; Borck et al., 2007).

From the above it is clear that a conceptual mechanistic understanding of cohesin loading onto chromosomes remains very elusive. The field may have to await the development of an *in vitro* loading reaction with reconstituted cohesin complex, and their regulatory proteins such as Scc2 and Scc4. This of course would need to be coupled with a real time scanning force miscroscopy (SFM) imaging system as been described for Rad50 (see section 1.3.1) to see the dynamic reorganisation of cohesin complexes as they embrace DNA, or alternatively the use of single molecule FRET measurements.

1.5.2 Cohesion establishment in S phase

Cohesion establishment is probably the least well understood part of how cohesin complexes execute their essential function in cells. One of the first clues that cohesion establishment is somehow temporally linked to S phase was the observation that cohesin complexes could be loaded post replicatively but could not generate cohesion between sister chromatids (Uhlmann and Nasmyth, 1998). Further work in budding yeast identified the requirement for an essential establishment factor, Eco1/Ctf7; to build cohesive bridges between sister chromatids during S phase (Toth et al., 1999; Skibbens et al., 1999). Homologues of these proteins are also found in both human and *Drosophila* cells where they also have a role in the generation of cohesion (Hou and Zou, 2005; Williams et al., 2003). In yeast studies it was shown that Eco1 is neither required for the binding to, or maintenance of cohesin complexes on DNA. Subsequent to these studies a very large number of examples of cohesion defects in DNA replication protein mutants were observed. This included the partial rescue of *ctf7-108* by overexpression of yeast POL30 (PCNA) (Skibbens et al., 1999), the requirement for an alternative RFC complex Ctf8/Ctf18/Dcc1 for cohesion (Hanna et al., 2001; Mayer et al., 2001) and precocious sister separation in *CTF4*Δ cells – an interactor of the Pol α/primase (Hanna et al., 2001). It is also interesting to note that the *S. pombe* Eco1 homolog, Eso1, has a C-terminal domain similar to *S. cerevisiae* Eco1/Ctf7 but an animo terminal extension with homology to the *S. cerevisiae* Rad30 which is Polymerase η, a bypass polymerase (Tanaka et al., 2000). Cohesion defects to various degrees are also observed in the following examples: mutants in Pol2 the catalytic subunit of Pol ε, as well as TRF4Δ (encoding pol sigma) (Edwards et al., 2003), deletion of the DNA helicase Chl1 (Mayer et al., 2004; Skibbens, 2004; Petronczki et al., 2004) and in mutants of the Orc5 subunit of the origin recognition complex (Suter et al., 2004). In addition to this, an interaction between PCNA and Eco1 has been demonstrated in both budding yeast and human cells. In this study PCNA was shown to bind to the N-terminal 33 aa of Eco1 and either deletion of this PCNA interacting domain or the generation of a point mutation in ECO1 that prevents this interaction does not complement the deletion phenotype of ECO1, despite the protein retaining its acetyltransferase activity (Moldovan et al., 2006). This result

suggests that Eco1 must be associated with PCNA to fulfil its function in cohesion establishment. Eco1 has got an acetyltransferase activity but the roles of this activity in cohesion establishment are still very obscure. In *in vitro* studies Eco1 could autoacetylate, as well as modify cohesin components Scc1, Scc3 and Pds5. These modifications could not be seen *in vivo* however, and the mutation of the only Scc1 modification site did not have an effect *in vivo* (Ivanov et al., 2002). Given the very clear biochemical and genetic interaction between cohesin and replication proteins, it is conceivable to imagine that a polymerase switch mechanism might be in place to replicate through cohesin associated regions, particularly if these were present in such high numbers so as to cause a barrier to replication fork passage. Limited evidence does exist to support such a notion. A replication fork pause is known to occur at centromeres (Greenfeder and Newlon, 1992) which are very enriched in cohesin binding (Tanaka et al., 1999; Blat and Kleckner, 1999; Lengronne et al., 2004; Glynn et al., 2004). Many other unusual aspects of centromeric DNA, such as its heterochromatic nature, could of course explain this. In support of the idea of polymerase switching is the finding that reducing the gene dosage of Pol σ, encoded by the TRF4 and TRF5 genes, also results in a cohesion defect (Wang et al., 2000). However a functional link to support this circumstantial evidence is lacking but could be addressed by monitoring fork stalling by 2-D gels at cohesin associated regions (CARs) in the absence of bypass polymerases.

Despite this growing body of data, a descriptive model of how a replication fork converts a pre bound CAR into a cohesive site, tethering sister chromatids, remains absent. Two major schools of thought have emerged nonetheless. Cohesin rings are indeed very large with a 35nm diameter (Anderson et al., 2002; Haering et al., 2002). This in principle could allow the replication fork to replicate through the inner diameter of the cohesin ring, hence leaving sisters and only sisters trapped within the same ring. This model is compatible with most of the results observed so far, namely cohesin existing as a monomer (Haering et al., 2002; Weitzer et al., 2003), and cohesin having a topological association with DNA (Ivanov and Nasmyth, 2005). The main drawbacks to the model are the physical constraints of allowing a giant molecular machine like the replisome to traverse the ring (reviewed in Johnson and

O'Donnell, 2005) and the fact that yeast DNA replication likely occurs via a stationary replisome pumping DNA through (Kitamura et al., 2006) as is the case in bacteria (Lemon and Grossman, 2000). The second major model is a 'snapping' mechanism whereby two cohesin complexes somehow become catenated or bind each other directly during cohesion establishment (Milutinovich and Koshland, 2003). This model depends on the presence of dimeric cohesin complexes which have never been shown to exist (discussed above). More importantly, the model is rather puzzling with respect to how this snapping would occur at a mechanistic level, and what would prevent the snapping of cohesin complexes on the same sister. A variation of the first model is that cohesin does indeed exist as a ring around sisters, but that the complex is opened during establishment, perhaps being held proximal to the replisome by cohesion establishment factors like Eco1, before being locked again after fork passage.

1.5.3 Maintenance of cohesion

The cohesion generated during S phase must now persist until anaphase onset. Testament to the fact that the linkages generated during cohesion establishment are highly stable is that mammalian oocytes may exist in meiotic prophase for many decades before being allowed to continue cell division after fertilisation (reviewed in Petronczki et al., 2003). For some time it was assumed that a functional cohesin complex could exist stably bound to DNA after cohesion establishment. More recent evidence now shows that specific maintenance factors are required to regulate cohesin-chromatin interactions. One such regulator is a protein called sororin. Sororin/p35 was first identified in screens for APC^{Cdh1} substrates (Rankin et al., 2005). Sororin does not have an obvious homologue in non-vertebrates based on homology searches, but this is not to say an orthologue does not exist. This protein was shown to be associated with cohesin complexes in HeLa cells. As cells enter mitosis the protein is phosphorylated, which coincides with its dissociation from chromatin. Its depletion leads to chromosome congression defects as well as a substantially reduced pairing of sisters in mitosis (Rankin et al., 2005; Schmitz et al., 2007). In contrast, overexpression of sororin leads to tight pairing of sister chromatids in

mitosis (Rankin et al., 2005). So how then might sororin work at a mechanistic level? Clues come from the fact that sororin depletion does not seem to alter the level of cohesin on chromatin but rather alter the nature of its dynamics with chromatin. In sororin RNAi cells, cohesin complexes are less stably bound as determined by FRAP experiments (Schmitz et al., 2007). This situation is reminiscent of the case before DNA replication, where cohesin complexes have a dynamic interaction with DNA (Gerlich et al., 2006). Perhaps sororin works during S phase to somehow regulate the generation of more long-lived linkages between sister chromatids.

An additional apparent regulator of cohesion post replicatively in budding yeast is the SMC containing condensin complex. Temperature sensitive alleles in condensin subunits (*ycs4-2*) lead to a modest cohesion defect in mitosis when inactivated from either G1 onwards or in G2/M alone. This defect was observed on three arm loci on different chromosomes, but not at centromeres or telomeric regions. Remarkably, the observed defects seem to be reversible, as shifting down to the permissive temperature reverses the cohesion defect, at least at the *URA3* locus in the case of *ysc4-2* (Lam et al., 2006). A satisfying explanation as to how the condensin mediated linkages are resolved in a regulated fashion, as well as the fact that the defects are allele specific in condensin, cast some doubt over the validity of the results. An equally plausible interpretation could be that the observed defects are in fact a read out of chromosome decondensation. In this case, GFP tagged loci could become separated by an appreciable distance so as to be resolved under the microscope. The reversibility observed could be simply attributed to recondensation of the separated loci (Lavoie et al., 2002).

A final regulator of chromosomal cohesion in G2/M cells, again in *S. cerevisiae*, is the origin recognition complex (ORC). This hetero-hexamer binds to the ARS consensus sequence (ACS) in *S. cerevisiae*, and serves as an initiator for DNA replication (reviewed in Bell, 2002). Orc's involvement in cohesion came to light due to the observation that depletion of the Orc2 subunit of ORC leads to precocious separation of a variety of loci, including arm, centromeric and telomeric regions. This, like that of condensin, was locus specific and did not occur at *URA3*. Similarly to condensin, re-addition of Orc2 rescues the separation of the locus (Shimada and Gasser, 2007).

1.5.4 Removal of cohesin

Cohesin removal and the subsequent segregation of the sister chromatids into the dividing daughter cells is an irreversible process. Hence it is not surprising to learn that cells have evolved multifaceted mechanisms to ensure the faithful partitioning of the genome at anaphase. One of the early players identified as an integral player in the metaphase to anaphase transition was Securin. This protein was identified in screens in both fission yeast (called Cut2) and budding yeast (Pds1) (Funabiki et al., 1996; Yamamoto et al., 1996). Subsequent work showed that securin is destroyed at the hands of the Anaphase Promoting Complex (APC) (Cohen-Fix et al., 1996). But securin is not part of the molecular glue that holds sister chromatids together, and neither is it essential in budding yeast (Ciosk et al., 1998). Another part of the puzzle came with the discovery of cohesin (Michaelis et al., 1997; Guacci et al., 1997b), discussed in section 1.2.1). Mutations in these proteins lead to premature separation of sister chromatids, and the wild type proteins were seen normally to dissociate from chromatin at around the metaphase to anaphase transition (Toth et al., 1999). Hence cohesins were also somehow required to keep DNA molecules tightly cohered in G2. Soon after this it was discovered that mutation in a protein, Esp1 in budding yeast, prevented this anaphase removal of cohesins (Ciosk et al., 1998). A mechanistic understanding as to how Separase (Esp1 in budding yeast) came to be able to remove cohesins came with the discovery that the cleavage of the Scc1 subunit of cohesin, in an Esp1 dependent manner, was enough to trigger anaphase in budding yeast (Uhlmann et al., 1999). In this work it was shown that the expression of a non-cleavable Scc1 could bind chromatin in G1 (in the presence of Esp1 activity). Importantly, it could also be demonstrated that this non-cleavable Scc1 variant prevented sister separation. It was later shown that Esp1 is a member of the CD clan of cysteine proteases that includes the caspases (Uhlmann et al., 2000). Mutation of either of the residues in the catalytic dyad in the protease active site (histidine 1505 or cysteine 1531) abolished the protease activity of Esp1. Furthermore, the cleavage of Scc1 that was engineered to contain recognition sequences for the Tobacco etch virus (TEV) protease also

triggered nuclear segregation. This showed unequivocally that Scc1 cleavage is required and sufficient for chromosome segregation. Separase cleaves Scc1 at either of two cleavage sites, either after arginine 180 or arginine 268, the latter being used preferentially (Uhlmann et al., 1999). After cleavage, Scc1 C-terminus now contains an N-terminal arginine residue, which is known to be a destabilising residue for the N-end rule (Varshavsky, 1996). The over-expression of a stable variant of this cleavage fragment (Met 269-566) is toxic to cells. Similarly, deletion of Ubr1, a ubiquitin protein ligase that targets Scc1 for proteolysis at the hands of the proteasome, results in increased rates of chromosome loss comparable to the strain over-expressing the cleavage fragment (Rao et al., 2001). So why is overexpression of a stabilised cleavage fragment toxic? It has been shown that overproduction of this fragment has the ability to cause a moderate cohesion defect in G2/M cells as assessed by a GFP dot separation assay (Weitzer et al., 2003). It could be argued that this is a dominant negative effect and that the cleavage fragment simply competes with endogenous Scc1 for binding to Smc1, hence leading to the generation of open rings. Against this idea is the finding that the fragment can also disrupt head-head interaction (assessed biochemically by immunoprecipitation) in G1 cells when Scc1 is largely absent (Weitzer et al., 2003).

Importantly, the mechanism of cohesin cleavage is conserved in meiosis in both budding (Buonomo et al., 2000) and fission yeast (Kitajima et al., 2003a) where Rec8 is cleaved, as well as in mitosis (Hauf et al., 2001) and probably meiosis (Terret et al., 2003) of higher eukaryotes.

In budding yeast, phosphorylation of the Scc1 subunit of cohesion in mitosis by the polo like kinase, Cdc5 has been shown to enhance its cleavage by separase both *in vitro* and *in vivo* (Alexandru et al., 2001; Hornig and Uhlmann, 2004).

In budding yeast mitosis all cohesins are removed at the metaphase to anaphase transition in a separase dependent manner. Cohesins subsequently are re-loaded in late G1 when Scc1 has been re-synthesised (Toth et al., 1999). In mammalian cells in contrast only a very small fraction of Scc1 is cleaved at anaphase onset (Waizenegger et al., 2000; Hauf et al., 2001). Instead, the vast majority of cohesin complexes dissociate from chromosomes in early mitosis in a

manner independent of separase, but dependent on the polo like kinase (Plk) and Aurora B (See figure 1.3) (Sumara et al., 2002; Losada et al., 2002). However it remained to be determined exactly how these phosphorylation reactions contributed to cohesin dissociation from chromatin. Knowing already that cohesin subunits could be phosphorylated by Plk *in vitro* and in *vivo*, and that this reduces cohesin affinity for chromatin, Hauf *et al* then showed that the production of a non-phosphorylatable version of the SA2 subunit of cohesin was refractory to the early mitotic dissociation of cohesins from chromosomes (Hauf et al., 2005). Under such circumstances mammalian chromosomes arrested in mitosis did not adopt the classical 'X' shape with well-resolved arms, but rather a tight pairing along their entire length. This suggested that SA2 was the crucial and perhaps only target of these mitotic kinases.

So how does the so-called prophase pathway remove cohesin complexes from chromatin? A reasonable speculation at this point was to assume that phosphorylation of cohesin subunits, particularly SA2 by mitotic kinases, reduced their relative affinity for chromatin so much so as to cause their dissociation. However, it now seems that SA2 phosphorylation is not the most downstream event in the prophase pathway. Depletion of a protein called Wapl confers on cells a resistance to the prophase removal of cohesins. When the protein is depleted in either HeLa cells or *Xenopus* extracts, mitotic chromosomes are poorly resolved along their arms and retain higher overall levels of cohesin on chromatin (Kueng et al., 2006; Gandhi et al., 2006). Indeed the protein was first identified in *D. melanogaster* based on similar phenotypes (Verni et al., 2000). Similarly, overexpression of Wapl results in precocious sister separation. Interestingly, in Wapl depleted cells, mitotic kinases were shown to be active and SA2 is phosphorylated comparably to wild type cells. Hence, Wapl can be thought of as some sort of ring opener, and is certainly in a good position to modulate the unloading of the cohesin ring, as it binds to the complex via the Scc1 and SA2 subunits (Kueng et al., 2006).

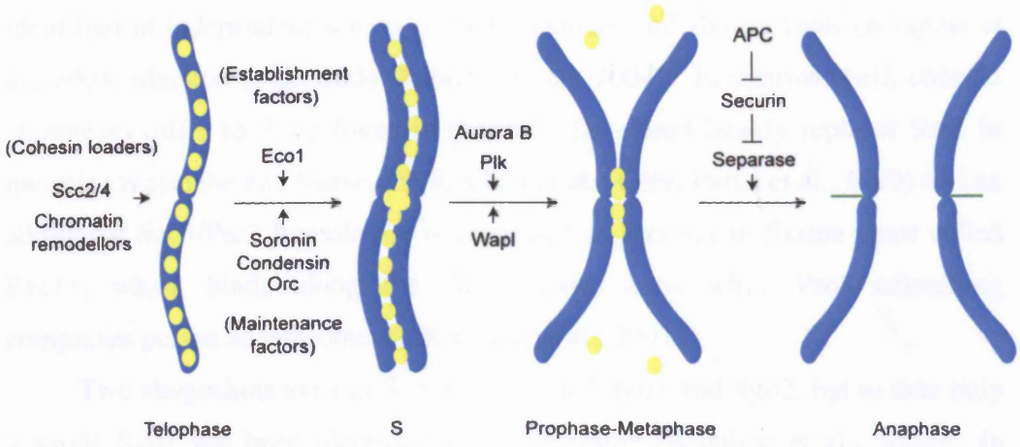

Figure 1.3 Summary of the key regulators of the cohesin cycle in higher eukaryotes

Yellow circles represent cohesin complexes, chromosomes represented in blue

1.6 Cohesion during meiosis and the role of shugoshin

Meiosis consists of a specialised form of nuclear division where two rounds of cell division follow from a single round of DNA replication. This in turn leads to the formation of haploid germ cells as part of the process of sexual reproduction. During the first meiotic division (reductional division), sister chromatids from each homologue recombine with each other and become covalently attached via chiasmata. In this first nuclear division, cohesin must be destroyed along the chromosome arms to allow homologues to segregate. In the second meiotic division (equational division), cohesin is cleaved at centromeres, hence allowing sister chromatids to segregate. The former step therefore requires that cohesin cleavage is restricted to arms only i.e. that centromeres remain attached to ensure error free segregation in meiosis II. This process requires specific protection of centromeric cohesion in meiosis I, a process now known to

require the action of a conserved family of proteins called shugoshins (Reviewed in Petronczki et al., 2003; Watanabe, 2005).

Drosophila Mei-S332 is a candidate protector protein that resides at meiotic centromeres and is required for cohesin's ability to persist at the centromere after anaphase I (Kerrebrock et al., 1995). Shugoshins in other organisms were first identified in independent screens in both budding and fission yeast (Kitajima et al., 2004; Marston et al., 2004; Rabitsch et al., 2004). In meiosis itself, cohesin complexes differ to those found in mitotic cells. Rec8 largely replaces Scc1 in meiosis (Watanabe and Nurse, 1999; Klein et al., 1999; Parisi et al., 1999) and an additional Scc3/Psc3 homologue is expressed in meiosis in fission yeast called Rec11, which binds along the chromosome arms while Psc3 containing complexes persist at centromeres (Kitajima et al., 2003b).

Two shugoshins exist in *S. pombe*, termed Sgo1 and Sgo2, but to date only a single Sgo1 has been identified in *S. cerevisiae* (Kitajima et al., 2004). In fission yeast both Sgo1 in meiosis I, and Sgo2 in mitosis localise to centromeres. Deletion of Sgo1 leads to premature Rec8 dissociation from centromeric regions before the second meiotic division, hence leading to random segregation at meiosis II with elevated non-disjunction (Kitajima et al., 2004; Rabitsch et al., 2004). Rec8 is also prematurely lost from centromeres in a *SGO1*Δ background after anaphase I in *S. cerevisiae* (Marston et al., 2004). Sgo1's function in fission yeast seems to be limited to meiosis as *SGO1*Δ cells do not exhibit any obvious mitotic defects (Kitajima et al., 2004). In budding yeast, *SGO1* deletion show meiotic defects comparable to those seen in *S. pombe*, namely premature loss of Rec8 from centromeres from anaphase I and random and premature segregation events in meiosis II (Marston et al., 2004; Katis et al., 2004). Interestingly, Sgo1 also has a role in budding yeast mitosis (Marston et al., 2004; Kitajima et al., 2004; Katis et al., 2004), and its deletion results in precocious separation of sister chromatids before anaphase onset. Sgo1 is removed from kinetochores at anaphase onset, probably due to degradation (Marston et al., 2004; Katis et al., 2004). Fission yeast Sgo1 localisation in meiosis and Sgo2 localisation in mitosis depends upon the Bub1 kinase, without affecting the stability of either protein (Kitajima et al., 2004). The fact that Sgo1 in budding yeast plays important roles

in both meiosis and mitosis may reflect the fact that only a single shugoshin exists in *S. cerevisiae*.

Since cohesin in higher eukaryotes is removed in a two step manner (see section 1.5.4) in mitosis leading to resolution of sister DNA molecules, it was not surprising to learn that shugoshin proteins were key players in this process also. It has now been demonstrated that shugoshin protects centromeric cohesion in mitosis from the so-called prophase pathway of cohesin removal. In human cells, Sgo1 also localises to kinetochores from the time that cells enter mitosis, and dissociates in late anaphase (McGuinness et al., 2005; Kitajima et al., 2005). Depletion of Sgo1 leads to a variety of phenotypes, namely congression defects and the precocious loss of centromeric cohesion due to premature Scc1 dissociation (Kitajima et al., 2005; McGuinness et al., 2005; Salic et al., 2004; Tang et al., 2004). Human Sgo1 localisation to kinetochores also depends on Bub1 (Tang et al., 2004; Kitajima et al., 2005) as is the case for yeast Sgo1 as discussed above. Remarkably, the expression of a non-phosphorylatable version of the cohesin subunit SA2 rescues the precocious centromeric separation seen in Sgo1 depleted cells (McGuinness et al., 2005). This strongly suggests that loss of cohesin from centromeres in Sgo1 depleted cells is due to hyperphosphorylation of SA2 by a kinase that is normally inhibited either directly or indirectly by Sgo1.

Mechanistically this seems indeed to be the case. Sgo1 has been shown to be able to recruit the phosphatase PP2A to centromeres in budding and fission yeast as well as in HeLa cells, indicating that this is an evolutionary conserved process (Riedel et al., 2006; Kitajima et al., 2006). Sgo1 interacts with PP2A physically, and PP2A is recruited to kinetochores in a Sgo1-dependent manner. PP2A likely performs its essential protector function at the kinetochore through direct inhibition or reversal of SA2 phosphorylation in mammalian cells and Rec8 dephosphorylation in fission yeast meiosis (Kitajima et al., 2006). Sgo1 itself protects a core 50 kb pericentromere domain from Rec8 removal before anaphase II in budding yeast (Kiburz et al., 2005). Of future interest will be the understanding of the function of Sgo1 in budding yeast mitosis, an organism that does not have a prophase pathway. It could be speculated however, that Sgo1 function here is limited to its role in kinetochore-microtubule interaction and the spindle assembly checkpoint (Salic et al., 2004; Indjeian et al., 2005).

1.7 DNA damage induced cohesion

In addition to cohesin's role in generating sister chromatid cohesion (discussed in section 1.1 and 1.2.1), there has long existed circumstantial evidence that cohesin might have an additional role in the repair of DNA damage. Indeed the Scc1 subunit of cohesin in *S. pombe*, Rad21, was characterised based on the sensitivity of this mutant to both UV and ionizing radiation, long before its essential role in chromosomal cohesion was established (Birkenbihl and Subramani, 1992). Later work in *S. cerevisiae* demonstrated that the repair of double strand breaks in G2 cells was seriously compromised when cohesin function was disrupted. Furthermore, cohesin likely does not initiate repair by signalling or activation of the checkpoint, as Scc1 depletion does not lead to a delay in cell cycle progression (Sjogren and Nasmyth, 2001). This result is in agreement with findings in chicken DT-40 cells where cohesin seems to function in post-replicative repair. In Scc1 depleted cells both increased chromosome breaks in response to ionizing radiation, and a reduced level of sister chromatid exchange are observed (Sonoda et al., 2001). More direct evidence for cohesin's role in DNA damage repair comes from the observation that cohesin components are recruited to laser beam induced DNA damage foci in mammalian cells along with other classical DNA damage proteins such as Mre11, Rad50 and Ku proteins (Kim et al., 2002). The underlying mechanism however as to how this recruitment was regulated and its functional significance was unknown at this point. Subsequently it was demonstrated in *S. cerevisiae* that cohesin is recruited to a HO induced double strand break in a very tightly regulated manner. Cohesin binding to the DSB, like cohesin loaded in late G1 as part of the normal cell cycle, requires the loader complex Scc2/Scc4 (Strom et al., 2004; Unal et al., 2004). Importantly, suppressing cohesin loading in G2 after induction of a HO induced DSB prevented its efficient repair as judged by pulse field gel electrophoresis. This extends on the previous findings (Sjogren and Nasmyth, 2001) and shows that *de novo* cohesin loading is also required for efficient DSB repair, and that cohesin loaded prior to the break as part of the normal cell cycle is alone not sufficient for repair (Strom et al., 2004; Unal et al., 2004). The

cohesin domain formed around the DSB spans approximately 50-100 kb, depending on the site of the break (endogenous MAT locus versus an ectopic site). Remarkably, the cohesin domain established around a DSB is competent in cohering sister chromatids even when induced post replicatively. Under these conditions of DSB induction by IR, approximately 1-4 DSBs are formed per chromosome (Strom et al., 2004). Consistent with this observation is the finding that the recruitment of non-cleavable Scc1 to IR induced breaks prevents the subsequent separation of sister chromatids (Strom and Sjogren, 2005). This again suggests that cohesin recruited to sites of damage in G2 forms cohesive structures, and in addition, it is removed by separase as is the case with other cohesin complexes at anaphase onset. Not surprisingly, cohesin recruitment to sites of DNA damage is also regulated by components of the DNA repair pathway. Specifically, cohesin recruitment is dependent upon the Mre11 component of the Rad50/Mre11/Xrs2 complex. Mec1 and Tel1 also act redundantly, and a double deletion fails in cohesin recruitment (Unal et al., 2004). Previous work in budding yeast has shown γ-H2AX to be recruited around a HO break, and that deletion of both Mec1 and Tel1 prevented this recruitment (Shroff et al., 2004). Likewise, cohesin recruitment to a DSB also depends on the presence of this phosphorylated H2AX at the break, and fails in strains where the H2AX phospho sites have been mutated (Unal et al., 2004). While Mre11 is essential for cohesin recruitment to the DSB, its deletion only marginally reduces γ-H2AX recruitment (Unal et al., 2004) . This suggests that a function of Mre11 independent of γ-H2AX formation is responsible for the formation of a cohesin domain at DSBs. In mammalian cells cohesin components are seen to interact by IP with both Rad50 and ATM (Kim et al., 2002). Indeed Smc1 itself has been shown to be a direct target of ATM/Tel1 in mammalian cells, and is phosphorylated on two sites, Ser 957 and Ser 966 in response to UV, IR and HU imposed genotoxic stress (Kim et al., 2002; Yazdi et al., 2002). Moreover, the expression of a non-phosphorylatable version of Smc1 leads to an override of the S phase checkpoint and decreased cell survival after IR treatment (Yazdi et al., 2002; Kim et al., 2002; Kitagawa et al., 2004). Does DNA damage induced cohesion contribute to chromosomal cohesion in unchallenged cells in the context of the normal cell cycle? Some evidence does exist to suggest that this might be

the case. Firstly, DNA double strand break formation is a legacy of every S phase, regardless of the presence of genotoxic agents (Lisby et al., 2001; Zou and Rothstein, 1997), and hence it is conceivable that cohesin would be recruited to these break sites. Consistently, cohesion defects are seen in deletions of Mre11/Rad50/Xrs2 and are not additive in an *mcd1-1* background (Warren et al., 2004).

A future interesting point to be addressed is the understanding of the hierarchical recruitment of cohesin to DNA double strand breaks. Cohesin and Smc5/6 recruitment both depend upon Mre11 (Unal et al., 2004; Lindroos et al., 2006), and there is now some evidence from human cells that Smc5/6 is in turn required for cohesin recruitment (Potts et al., 2006). Mre11 is likely to be one of the most upstream elements of the cascade, as both itself and the Tel1 kinase are amongst the earliest proteins recruited to damage foci, at least in budding yeast (Lisby et al., 2004).

1.8 FRET as a tool to monitor protein-protein interactions

1.8.1 The principle of FRET

Traditional methods to probe protein-protein interactions such as immunoprecipitation, yeast two-hybrid and cross-linking experiments while proving invaluable in identifying components of protein complexes *in vivo* (Mendelsohn and Brent, 1999), remain limited on a number of fronts. These techniques do not provide any information on the spatial separation of proteins as part of the same complex, their interaction in specific subcellular compartments or their behaviour in time and in space.

Fluorescence resonance energy transfer (FRET) is a process whereby energy is transferred non-radiatively (i.e. without the involvement of a photon) from an excited molecular fluorophore (the donor) to another fluorophore (the acceptor) (Lakowicz, 1999). The concept was formulated by Förster in 1948 and remained only theoretical until Stryer showed it could be used as a molecular ruler in 1978 (Stryer, 1978). The transfer of energy between fluorochromes depends upon a number of criteria. These include (1) spectral overlap between the emission spectra of the donor and the excitation spectra of the acceptor

(Figure 1.4A). Overlap is an absolute requirement for the phenomenon of FRET, but an appropriate level, depending on the specific application is required on a case-by-case basis. For example, a high degree of overlap will result in efficient energy transfer between a suitably close FRET pair, but will require determination of the amount of cross talk between the channels (discussed below) (Gordon et al., 1998). Cross talk in emission detection refers to the detection of the donor fluorescence through the acceptor emission filter and *vice versa.* Excitation bleedthrough on the other hand is the excitation of the acceptor at the donor excitation wavelength and *vice versa* (Lakowicz, 1999; Gordon et al., 1998; Berney and Danuser, 2003). (2) A second important determinant of FRET is orientation of the dipole moment of the acceptor and donor molecules at an angle other than 90° to each other (Figure 1.4B). When a fluorophore is excited by an external magnetic field such as light, this induces an oscillating electromagnetic field or dipole in this molecule. This in turn can influence the electromagnetic field of adjacent fluorophores that has spectral overlap. The dipole moment is a mathematical term that refers to both the magnitude and orientation of a dipole/magnetic field within a molecule. If the two dipole moments of adjacent fluorophores are perpendicular to each other, they will not be able to influence each other, and no FRET will occur (Lakowicz, 1999; Vogel et al., 2006). An orientation factor, K^2, denotes the angular relationship between the fluorophores and is generally assigned a value of 2/3 due to the rotational freedom of the fluorophores (Lakowicz, 1999). However this value can range from 0 (when the dipoles are perpendicular) to 4 (when the diploes are colinear and parallel) (Lakowicz, 1999). (3) Another determinant of FRET is the proximity of the fluorophores relative to one another. FRET generally occurs when the donor and acceptor molecules are less than 100Å of one another. The efficiency of transfer (defined as the number of transfer events divided by the number of photons absorbed by the donor) is dependent on the inverse sixth power of the inter fluorophore distance (Lakowicz, 1999). The so-called Förster distance/radius is the distance at which the energy transfer is 50%. Hence it is the case that there is not a linear relationship between distance and the efficiency of FRET (see figure 1.4C). The transfer efficiency, E, is given by:

$$E = \frac{R_0^6}{R_0^6 + r^6}$$

Where R_0 = the Förster Distance (typically 20-60 Å)
and r = the distance between fluorophores (Lakowicz, 1999).

The choice of a suitable FRET pair depends upon many criteria. Earlier FRET work used primarily synthetic dyes such as Cy3 and Cy5 which were used mostly in *in vitro* settings. However since the mid 1990s the cloning of the Green Fluorescent Protein (GFP) (Chalfie et al., 1994) and the production of red and blue shifted variants thereof (Heim and Tsien, 1996) have provided new opportunities in FRET. Specifically, the production of genetically encoded GFP fusion proteins enables the examination of protein-protein interactions *in vivo*. Yeast is particularly amenable to this technology since the ability to tag the endogenous gene by homologous recombination (Knop et al., 1999; Prein et al., 2000) eliminates problems such as over-expression artefacts or mixed populations which can be encountered with cell lines of higher eularyotes. However, owing to their small size, cell biology in general is more challenging. The applications of FRET are almost limitless. In recent years this technology has been used to look at the cleavage of caspase substrates after the induction of apoptosis, probing antibody antigen interactions and Ca2+ signalling (reviewed in Truong and Ikura, 2001). Single molecule FRET also represents a very powerful tool that can be used to detect conformational changes within a protein as it interacts with a substrate or DNA molecules (Ha, 2001).

When energy transfer occurs between a suitable FRET pair two phenomena are observed. Firstly, the donor emission is decreased and secondly, the acceptor emission will be sensitized. These two criteria are the basis for FRET and their interpretation is the basis for measuring and quantifying FRET which is discussed in the next section below.

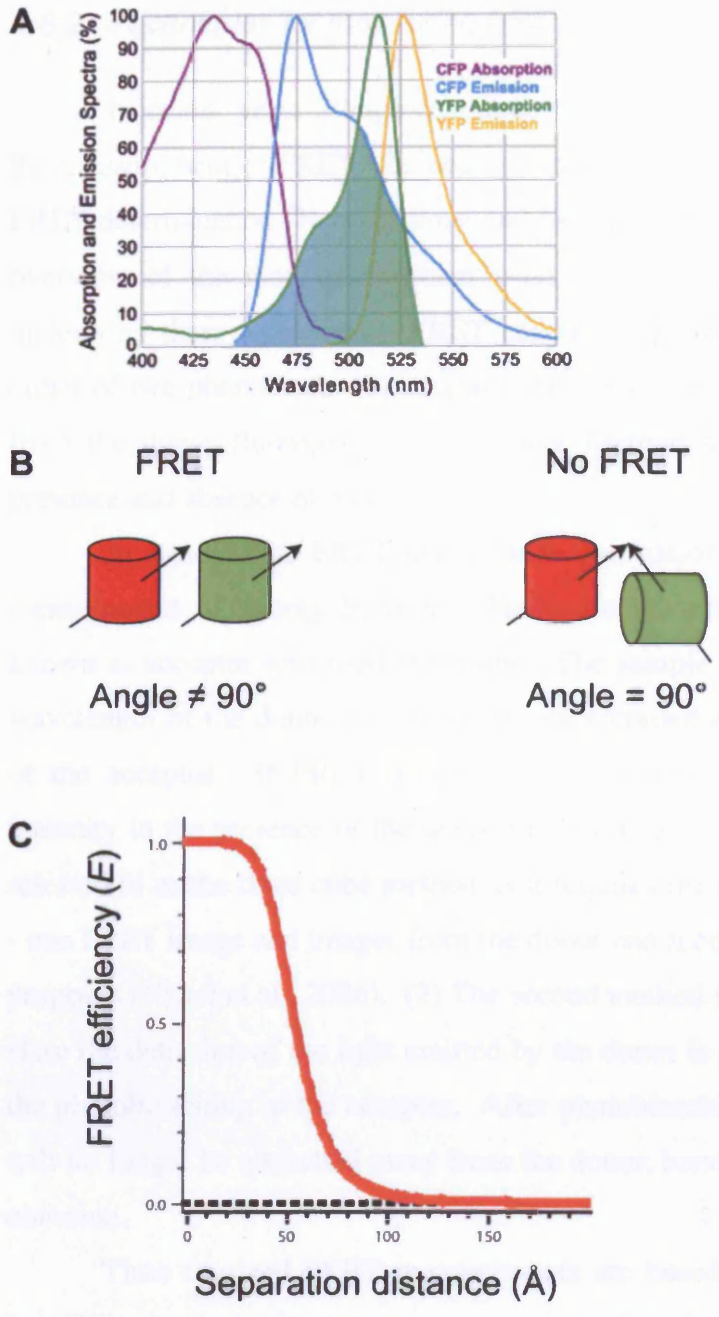

Figure 1.4 Requirements for FRET

(A) Emission and absorption spectra of both CFP and YFP. The overlap between the emission spectra of CFP (the donor) and the excitation spectra of YFP (the acceptor) is highlighted in green

(B) The dipole moment (black arrow) of the FRET pair must be non-perpendicular to each other if energy transfer is to occur. At values other than 90 FRET will occur at a range of different efficiencies

(C) The relationship between the FRET efficiency, *E*, and the separation distance of the fluorophores Cerulean and Venus. Note the non-linear nature of the relationship between these two parameters. Figure adapted from (Vogel et al., 2006)

1.8.2 Techniques for measuring FRET

In recent years a huge catalogue of techniques have been developed for the measurement of FRET. Indeed one review article cites 22 different ways of FRET determination (Jares-Erijman and Jovin, 2003). Here is presented a simple overview of the more mainstream ways to measure FRET and the concepts underlying these techniques. FRET can be determined by the measurement of either of two phenomena: (1) acceptor sensitised emission due to energy transfer from the donor fluorophore or (2) donor lifetime based measurements in the presence and absence of an acceptor.

In steady state FRET applications two major methods are used for the measurement of energy transfer. These are (1) emission measurement, also known as acceptor sensitised technique. The sample is excited at the excitation wavelength of the donor and emissions are recorded at the emission wavelength of the acceptor. If FRET occurs, the acceptor will have greater fluorescent intensity in the presence of the donor than in its absence. This technique is also referred to as the three cube method as it requires the acquisition of three images - one FRET image and images from the donor and acceptor channel for correction purposes (Vogel et al., 2006). (2) The second method is acceptor photobleaching. Here the detection of the light emitted by the donor is performed before and after the photobleaching of the acceptor. After photobleaching of the acceptor, energy will no longer be quenched away from the donor, hence resulting in its increased emission.

Time resolved FRET measurements are based on these same principles but differ from steady state measurement in that they monitor lifetimes of the fluorophores. The most commonly used technique to measure this is called FLIM or fluorescence lifetime imaging microscopy. In this technique the donor's decay kinetics are measured in the presence and absence of an acceptor after excitation at the donor excitation wavelength. If FRET is occurring, the donor will have a shorter lifetime (due to acceptor quenching) in the presence of this acceptor.

A final technique used to measure FRET is that of fluorescence polarisation anisotropy. The basis for this is the existence within a fluorophore of a transition moment that lies along a specific direction within the fluorophore structure. In fluorophores in solution where they are free to diffuse, these

moments are randomly oriented. When such a sample is excited with linearly polarised light, only those fluorophores with the same orientation of their absorption transition moments will be excited (Lakowicz, 1999). In a biological setting in the absence of FRET, the molecule excited with polarised light will also be the molecule emitting fluorescence, hence there will be a substantial correlation between the orientation of these molecules. Anisotropy (r) refers to the extent of polarisation of the emission. When FRET occurs the molecules excited will emit fluorescence, but also emissions will come from acceptor molecules due to energy transfer. In the case of the latter there will be no correlation between the orientations of these molecules, thus with an overall decrease in anisotropy (Lakowicz, 1999; Vogel et al., 2006). Polarised fluorescent microscopy has recently been used to determine the subunit orientation of septins before and after the onset of cytokinesis (Vrabioiu and Mitchison, 2006).

1.8.3 Limitations of FRET

Observing protein-protein interactions at a whole cell level by any technique has drawbacks and FRET is no exception. Problems here include the presence of different populations of interacting proteins within the cell, conformational changes that become lost in averaging in whole cell FRET measurements, and the potential of the conjugated fluorophore to perturb protein function.

Whilst FLIM-FRET is superior to intensity based methods in that lifetime measurement are independent of fluorescent intensities, it is not suitable for all applications. For example samples with either low quantum yields or susceptibility to rapid photobleaching cannot be used with this technique. The longer time frames used for FLIM also may result in photodamage to the sample. However, as with any other technique to measure FRET, the presence of mixed populations of interacting proteins will result in a mixed population of decay kinetics (Lakowicz, 1999; Peter and Ameer-Beg, 2004).

Intensity based measurements also suffer from a number of drawbacks, paramount amongst these are the need to as accurately as possible assign a

spectral bleedthrough value to donor and acceptor; and fluctuations in the relative levels of the FRET pair. As discussed above, since we tag the endogenous gene this becomes the only source of the protein in the cell. We also know that the relative concentration of cohesin subunits is stoichiometric in the cell. With respect to bleedthrough values, it has been previously shown that these are independent of intensity values (Muller et al., 2005). Furthermore, since both the spillover factors and the $FRET_R$ are calculated on the same specimen, and so too the numerator and denominator, they therefore become self-normalising for fluctuations in intensity and/or concentration (Gordon et al., 1998; Muller et al., 2005).

Acceptor photobleaching, like FLIM, calls for the near complete elimination of the acceptor by photobleaching which may involve the exposure of the sample to potentially damaging light for long periods. This is particularly true if DsRed is used as an acceptor which requires anything up to 30 minutes of laser exposure to be reduced by 90% (Erickson et al., 2003).

On technical terms, the implementation of a dedicated microscope system for FRET requires the purchase of such things as sensitive cameras with low electrical noise and fast read out speeds, specific band pass filter sets and suitable dichroic mirrors (reviewed in Hailey et al., 2002).

2 Chapter 2: The dissection of cohesin architecture *in vivo* using FRET

Cohesin architecture to date has been assessed entirely based on *in vitro* studies. The ring shaped model of cohesin is based on electron micrographs of purified cohesin complexes from a variety of organisms. These EM studies coupled with a subunit-subunit interaction analysis of proteins expressed in *S. cerevisiae* have led to a model of cohesin as an enormous proteinacious ring (Haering et al., 2002; Gruber et al., 2003; Anderson et al., 2002).

Informative as these studies may be, their *in vitro* nature may not truly reflect events occurring in live cells. Electron microscopy for example has given notoriously varied interpretations of the oligomerisation state of MCM proteins (Yu et al., 2002). Caveats from insect cell studies may include such things as lack of post-translational modification contributing to protein-protein interactions, unphysiologically high concentration of proteins leading to false positive interactions, and lack of accessory proteins, which may support protein-protein interactions *in vivo*. Given the lack of any clear attempts to clarify the architecture and behaviour of cohesin in unperturbed live cells, we set about examining cohesins *in vivo* using Fluorescence Resonance Energy Transfer (FRET). In this chapter we present a comprehensive analysis of interactions between components of the cohesin complex.

2.1 Evaluation of FRET for determining protein-protein interactions in *S. cerevisiae*

To analyse FRET between cohesin subunits *in vivo*, we utilised a recently developed simple and robust method based on the FRET ratio (Muller et al., 2005). In this approach, fluorescent intensities of CFP and YFP are measured with an epifluorescent microscope, and FRET is seen after excitation of the CFP fluorophore as increased emission in the YFP channel. Even without FRET, fluorescence is detected after CFP illumination in the YFP channel (and *vice*

versa) due to spectral spillover between the channels. Therefore, spillover factors are first determined using strains expressing YFP or CFP fluorophores only. $FRET_R$ is then determined as the ratio of the observed FRET intensity over the expected spillover in each experimental strain (see Materials and methods). This analysis was performed in strains Y1967 (*MATa/α SMC1-CFP/SMC1-CFP / ΔADE3/ΔADE3*) and Y1972 (*MATa/α SMC1-YFP/SMC1-YFP ΔADE3 ΔADE3/*), yielding CFP spillover factor and YFP spillover factors of 0.34±0.04 (n=48) and 0.09±0.04 (n=46) respectively. These measurements were repeated throughout the course of our experiments and did not change significantly.

Using techniques such as acceptor photobleaching for FRET quantification depends upon the presence of equal amounts of donor and acceptor molecules. For example, in cells with very high concentration of acceptor (in this case YFP) any given donor (CFP) will have a higher chance of randomly being within the FRET range of 10 nm, hence giving an artificially higher FRET value (reviewed in (Vogel et al., 2006). $FRET_R$ however, gives a measure for FRET that is independent of fluorophore concentration, but sensitivity of the measurements is greatest for equimolar concentration of the two fluorophores and this is because of a higher signal to spillover ratio. We therefore compared the concentration of the cohesin subunits within budding yeast by measuring fluorescent intensities of CFP fusions expressed at their genomic loci. For these, and all following experiments, we used homozygous diploid yeast strains, which yield increased fluorescent intensities over haploid strains. *ADE3* was deleted and the growth medium supplemented with adenine to reduce background fluorescence from intermediates of the adenine biosynthesis pathway. Fluorescence intensities were measured in an area of fixed size within the nucleus of all strains containing the cohesin subunit-fluorophore fusions. This showed that in budded G2 cells all cohesin subunits were present in nuclei at roughly the same concentration (Figure 2.1A). From these measurements we calculated protein copy number per cohesin subunit based on estimates for Scc1, based on quantitative western blotting, of approximately 6000 copies per cell (Weitzer et al., 2003).

As a positive control for FRET we attached a tandem fusion of CFP with YFP, separated by a short glycine-alanine linker, to the C-termini of both Scc3 and Pds5. $FRET_R$ for these strains was 2.15±0.2 (n=32) and 2.12±0.24 (n=34)

(Figure 2.1B). This provides an upper limit for $FRET_R$ expected from closely juxtaposed CFP and YFP fluorophores. If there is no FRET between CFP and YFP, the signal intensity in the FRET channel is expected to be equal to the spillover from both fluorophores, resulting in a $FRET_R$=1. This was observed for example when the C-terminal Scc3-CFP tag was combined with Pds5-YFP, $FRET_R$=1.07±0.09 (n=52), or vice versa Scc3-YFP with Pds5-CFP $FRET_R$=0.99±0.14 (n=31) (Figure 2.1B).

2.2 Localisation of cohesin in live budding yeast

While observing fluorophore-tagged cohesin subunits, we noticed that in cells with small to medium-sized buds cohesin was enriched in a distinct focus within the nucleus (Figure 2.2A). At higher resolution the focus appeared to take the shape of a ring, and dual colour imaging including the spindle pole body (SPB) component Spc29 showed that the focus assembled around this organelle (Figure 2.2B). These foci likely represent cohesin enriched at centromeres that cluster around the SPB (Guacci et al., 1997a; Blat and Kleckner, 1999).

While centromeres remain attached to the SPB throughout the cell cycle, the timing of foci appearance correlated well with cohesin binding to chromosomes, from the G1/S transition when buds emerge until in mitosis. In early anaphase nuclei, when cohesin dissociates from chromosomes after Scc1 cleavage, the foci disappeared. Between anaphase and G1 most subunits appeared diffuse throughout the nucleus. As an exception, Scc3-CFP was enriched along the nuclear membrane during this time (Figure 2.2A). We do not know the reason or possible consequence of this localisation. Because of the greater signal intensities most fluorescence and FRET measurements in G2 cells were made within nuclear foci. Measurements within the diffuse nuclear region that were performed in parallel gave similar results (Figure 2.13).

2.3 The constitutive close interactions of the SMC heads

Crystal structures for many ABC ATPases such as Rad50 (Hopfner et al., 2000), the MalK ATPase subunit of the maltose transporter from *E. coli* (Chen et

al., 2003), and the SMC protein from bacteria (Lowe et al., 2001; Lammens et al., 2004), show an arrangement with two ATP molecules binding between the ATPase domains of these proteins. This arrangement, known as a nucleotide sandwich dimer, is also present in membrane transporter proteins (Dawson and Locher, 2006). Models have now emerged based on these crystal structures whereby ATP binding induces dimerisation, and ATP hydrolysis leads to dissociation of these domains. Indeed a crystal structure for the yeast Smc1 head does exist (see introduction). Limited evidence exists to support the notion of Scc1 acting as a bridge between the Smc1 and Smc3 heads (Gruber et al., 2003).

To examine this seemingly paradoxical evidence, we looked at the interaction between the Smc1 and Smc3 heads in cycling cells. Smc1 was tagged at its C-terminus by YFP and Smc3 with CFP. $FRET_R$ was determined in this strain in a cycling cell population and found to be 2.06±0.14 (n = 38) (Figure 2.3A). This value is close to the theoretical upper limit of FRET observed for the CFP-YFP fusions, indicating a very close proximity of the Smc heads. Swapping the tags (i.e. Smc1-CFP, Smc3-YFP) yielded consistent results ($FRET_R$ = 2.12±0.19, n = 47). We next sought to determine if the interaction between the Smc heads is cell cycle regulated or whether it depends on Scc1. In G1 cells for example, Scc1 is largely absent, having been destroyed in the previous mitosis. To address this question we monitored FRET between Smc1-CFP and Smc3-YFP after release of small unbudded G1 cells, obtained by centrifugal elutriation, into the cell cycle. At the early time points (30 mins, 60 mins) the fluorescent signals are seen diffuse throughout the nucleus, probably because of a lack of Scc1 and thus the inability to bind chromatin. $FRET_R$ however, remained relatively unchanged between G1 (T = 30mins, FRETR = 2.03±0.44) and G2/M (T = 120 mins, FRET = 1.97±0.18) (Figure 2.3B). Hence major spatial rearrangements of the Smc heads are unlikely to occur with Scc1 binding and/or cell cycle progression.

Despite the high FRET observed between Smc1 and Smc3 in the previous experiment, it is hard to physically estimate the distance between the Smc heads. Because FRET was similarly high in G1, when Scc1 is absent, it is likely that it represents direct dimerisation of the ATPase heads. To confirm more directly that the observed $FRET_R$ represents direct, Scc1-independent association of the

Smc heads, we repeated the measurements in cells in the presence of, or depleted for Scc1. If Scc1 were a bridge between the SMC heads, and since the heads can also interact in the absence of Scc1, then Scc1 depletion should result in a larger population of direct Smc1-Smc3 head interactions in the cell. This would be predicted to drive $FRET_R$ upwards. To test this prediction the Scc1 promoter was replaced with the *GAL1* inducible promoter. Scc1 was also tagged with three HA epitopes to monitor its expression. Cells were grown in YP medium containing raffinose and galactose. The culture was then split and one half was transferred to media containing only raffinose to repress Scc1 expression. Both cultures were imaged 2 hours later. As expected, in the absence of Scc1 cohesin failed to associate with chromosomes, and nuclear foci were not observed (data not shown). FRET between Smc1-CFP and Smc3-YFP was similar with or without Scc1 (with Scc1: $FRET_R$=1.77±0.12, n=53, without Scc1 $FRET_R$= 1.85±0.27, n=47) (Figure 2.3C). These results suggest that the two Smc heads dimerise, probably in an ATP bound state, in the absence of Scc1, and that they retain close association after Scc1 joins the complex and cohesin is loaded onto chromosomes. We next analysed whether we could detect Smc head disengagement when Scc1 is cleaved and the cohesin ring dissociates from chromosomes in anaphase. For this we measured FRET in early anaphase cells displaying dumbbell-shaped nuclei selected from the 120 min timepoint of the experiment shown in Figure 2.3B. Foci of cohesin had dispersed, as expected, but we did not find evidence for a greater distance between the Smc heads ($FRET_R$=1.92±0.26, n=63). FRET in our experiments is a population average of all cohesin molecules present in the observation area. Transient, asynchronous dissociation of the Smc heads during cohesin loading or unloading from chromosomes may not be detectable with our measurements. Alternatively, ATP binding and hydrolysis during loading, and Scc1 cleavage during anaphase may lead to conformational changes in the cohesin complex that do not alter the distance between the fluorophores attached to the Smc1 and Smc3 C-termini, and hence are not detectable under our experimental settings.

2.4 Scc1 C-terminus induces chromatin dissociation of the cohesin complex

We next asked whether the Smc1 and Smc3 heads can be seen to open or come apart, as might be expected at some point for either ring opening in the loading reaction, or cleavage and removal of the ring at anaphase onset. To do this we induced conditions in our cells that would be predicted to result in head-head destabilisation and/or disengagement by over-expressing the Scc1 C-terminal cleavage fragment that is normally produced in anaphase. It has been shown previously that over-expression of this fragment results in a robust loss of cohesion and destabilization of the interaction between the Smc1 and Smc3 heads (Weitzer et al., 2003). We introduced into our FRET strains a C-terminally FLAG tagged Scc1 (met269-566) under the control of the *GAL1* inducible promoter. Cells were grown at 25°C in YP medium supplemented with raffinose. The culture was then split, and to one half was added nocodazole and to the other half nocodazole and galactose to induce expression of Scc1 met 269-566-FLAG for 2 hours. Western blot analysis against the FLAG epitope showed expression at the two hour time point (Figure 2.4B). FRET measurements for cells not expressing the cleavage fragment was 1.92±0.18 (n = 58) (Figure 2.4A). Upon over-expression of the Scc1 cleavage fragment, nuclear foci disappeared, consistent with chromatin dissociation of cohesins (Figure2.4A). Nonetheless, $FRET_R$ between the Smc1 and Smc3 heads remained robust at 1.99±0.22, n = 71) (Figure 2.4A). These results suggest that despite the fact that the cleavage fragment disrupts the interaction between the Smc heads and result in their unloading from chromatin, their spatial proximity remains unchanged. How can we reconcile these results with the fact that under the above experimental conditions, cohesin rings were probably unloaded by opening of the Smc heads? Under our experimental settings, each fluorescent image is captured with a 400ms exposure time. Even slower events on the second or even minute timescale would be difficult to detect if the alternate conformation affects below say 10-20% of the molecules at any time. Hence population molecular events occurring asynchronously over and above this time frame are not detectable using our assay. Secondly, the very high local concentration of SMC heads, promoted by

the Smc hinge, may well support their juxtaposed association even if it were the case that their relative affinity for one another was substantially reduced.

2.5 Scc1 adopts a conformation at the SMC heads different to current models

We next used FRET to study the interaction of Scc1 with the Smc heads. From a crystal structure Scc1's C-terminal winged Helix domain (WHD) binds to the terminal two β-sheets on the Smc1 head (Haering et al., 2004). This structural information on the position of the Smc1 head and Scc1 C-terminus allowed us to ascertain whether our interpretation of constitutive head-head interactions would hold up under more quantitative conditions. This now provided us with an index to further examine the notion of head-head interactions. We constructed strains harbouring fluorophores at the Scc1 N- or C-termini, in combination with fluorophores at the Smc heads. In the following, we use YFP-Scc1 to indicate YFP fused to the Scc1 N-terminus, and Scc1-YFP for the fluorophore at the C-terminus. Many current models of the cohesin complex draw Scc1's N- and C-termini in considerable distance from each other, bridging a gap between the Smc1 and Smc3 heads. (Shintomi and Hirano, 2007; Losada, 2007).

The Scc1 C-terminus is thought to contact only Smc1 while the N-terminus associates with Smc3 (Haering et al., 2002). If this arrangement were correct, we would expect strong FRET between fluorophores at the Scc1 C-terminus and Smc1, but weak or no FRET with Smc3. Inversely we would expect FRET between fluorophores at the Scc1 N-terminus and Smc3, but not with Smc1. In contrast to these expectations we observed equally strong FRET between the Scc1 C-terminus and both Smc1 and Smc3. $FRET_R$ between Scc1-YFP and either Smc1-CFP or Smc3-CFP was 1.87±0.25 (n=52) and 1.86±0.16 (n=45), respectively (Figure 2.5A). This suggests that the Scc1 C-terminus is placed close and equidistant from both Smc1 and Smc3 heads. We confirmed this observation after exchanging the fluorophore tags; $FRET_R$ between Scc1-CFP and either Smc1-YFP or Smc3-YFP was 1.88±0.17 (n=42) and 1.93±0.15 (n=42), respectively. These results are inconsistent with models in which Scc1 bridges a

gap between the Smc heads. Instead they support our finding that the two Smc heads are closely juxtaposed, and suggest that the Scc1 C-terminus is placed between the two heads, in a perpendicular fashion (Figure 2.5B). The arrangement of the Scc1 C-terminus in its crystal structure with an Smc1 head is consistent with our FRET results, if we consider that Smc3 adopts the position of the second Smc1 head in the homodimer structure.

We next analysed the positioning of the Scc1 N-terminus relative to the Smc heads. $FRET_R$ of CFP-Scc1 with Smc1-YFP or Smc3-YFP was 1.23±0.13 (n=49) and 1.58±0.13 (n=48) respectively (Figure 2.5A). This suggests that the Scc1 N-terminus is positioned closer to the Smc3 head, but that it retains proximity also with Smc1. The association of the Scc1 N-terminus with Smc3 is thought to be less stable than that of the C-terminus with Smc1. We therefore analysed whether we could see any evidence for a change or regulation of this interaction during the cell cycle. Plotting $FRET_R$ as a function of cell cycle progression showed that the interaction remained constant (Figure 2.6A). $FRET_R$ also remained largely unchanged in cells arrested in G2/M with nocodazole or early S phase with hydroxyurea (Figure 2.6B). From these results we suggest that the two Smc heads remain in contact for most of the cell cycle, and Scc1 binds the two heads in an orientation that is largely perpendicular to the axis that connects the two heads (Figure 2.5B).

2.6 Scc3 maps to the SMC heads of the cohesin complex

Next we turned our attention to the Scc3 component of the cohesin complex. Scc3 is known to bind to Scc1's C-terminus, and binds to the holo cohesin complex in an Scc1 dependent manner (Haering et al., 2002). To map Scc3 with respect to the other subunits *in vivo*, we carried out FRET experiments with fluorophores attached to either terminus of the subunit. We found Scc3-YFP to FRET well with both Smc3- and Smc1-CFP (1.37±0.14, n = 55 and 1.35±0.16, n = 55) (Figure 2.7A). Scc3's N-terminus also FRETs with both Smc1 and Smc3 (YFP-Scc3/Smc1-CFP $FRET_R$ =1.21±0.21, n = 32 YFP-Scc3/Smc3-CFP $FRET_R$ = 1.27±0.14, n = 37), but to a lesser extent than with the C-terminus of Scc3. Scc3 C-terminus also maps more proximally to the C-terminus of Scc1 (Scc3-

YFP/Scc1-CFP, $FRET_R$ = 1.4±0.14, n = 44) than it does to Scc1's N-terminus (Scc3-YFP/CFP-Scc1, $FRET_R$ = 1.2±0.13, n = 42), consistent with the characterised biochemical interaction. Scc3's N-terminus in contrast maps approximately equidistantly between C-terminus Scc1 (YFP-Scc3/Scc1-CFP, $FRET_R$ = 1.25±0.13, n = 47) and N-terminus Scc1 (YFP-Scc3/CFP-Scc1, 1.22±0.17, n =45) (Figure 2.7A).

2.7 Pds5 as a matchmaker between the SMC head and the SMC hinge

2.7.1 Pds5 interacts with the cohesin complex in an Scc1 dependent manner

In budding yeast there exists an interdependency of chromatin binding between Scc1 and Pds5 as demonstrated by chromatin immunoprecipitation. Previous data from both budding and fission yeast show Pds5 staining on chromosomes to weaken or dissociate at the time of anaphase onset (Panizza et al., 2000; Tanaka et al., 2001). In light of this we now asked whether Scc1 was required for Pds5 association with the cohesin complex *per se*. We again used a strain in which expression of Scc1 was under control of the *GAL1* promoter. Scc1 was either expressed, or repressed for 2.5 hours, before cell extracts were prepared and complex formation between Pds5 and Smc1 analysed by co-immunoprecipitation against myc tagged Pds5. In the presence of Scc1, we could recover both Scc1 and Smc1 in the Pds5-myc immunoprecipitate (Figure 2.8B). As with human cohesin (Sumara et al., 2000) this interaction was reduced in the presence of high salt concentrations (Figure 2.8A), but was robust when buffer containing 50 mM KCl was used for extract preparation. In the absence of Scc1 however, the interaction between Pds5 and Smc1 was now abolished (Figure 2.8B). The reciprocal experiment pulling down Pk tagged Smc1 yielded similar results (Figure 2.8C). This suggests that Scc1 is required for Pds5 association with cohesin, possibly reflecting an interaction between the subunits as suggested by the FRET results. Many interpretations could follow logically from these results (Figure 2.8D). Perhaps Scc1 binding to the cohesin complex at the heads

induces a conformational change down the coiled coils to facilitate Pds5 binding at the hinge. Alternatively Pds5 could mediate the interaction of Scc1 and the Smc hinge from opposite sides of the ring, acting as a molecular matchmaker between the distal sides of the cohesin ring.

2.7.2 Construction of a fluorophore conjugated Smc1 hinge

We next asked if Pds5 would map to any component around the heads of the cohesin complex, or indeed interact with the Smc hinge. To address the latter we now attempted to construct a fluorophore conjugated Smc1 hinge. This construct would need to be the sole source of Smc1 in the cell to avoid problems with sub-populations of complexes if wild type Smc1 were present in addition to the hinge fusion. To best choose a position in the Smc1 hinge which would likely not perturb protein function, we reasoned that the insertion of the fluorophore in a predicted loop at an exposed surface may be the best option. Hence, we modelled the *S. cerevisiae* Smc1 hinge against the *T. maritama* Smc hinge, for which there is a known crystal structure (Haering et al., 2002) (Figure 2.9A). In addition, we used a secondary structure prediction programme to identify potential loops (Shepherd et al., 1999). Based on this analysis we identified two potential sites in the Smc1 hinge – proline 539 or proline 600 (Figure 2.9B). An insertion at the former residue did not yield a functional protein (data not shown). A fluorophore could however be inserted at proline 600.

This construct was constructed briefly as follows. The *Smc1* open reading frame until proline 600 was cloned using PCR as an Xma I/Sal I fragment into YIplac128, and fused to a Sal I/Sph I fragment encoding the remainder of Smc1. Inserted into the Sal I site was PCR-amplified YFP (or CFP) flanked by linker peptides of the sequence VDGSTG on both sites. Next a 472 bp *Smc1* promoter PCR fragment was added upstream using Nde I/Xma I sites, and finally an additional 470 bp sequence upstream of the *Smc1* promoter fragment was amplified but cloned behind the *Smc1* open reading frame using Sph I and Nla III. This construct was linearised by Sph I restriction for integration at the *Smc1* locus.

2.7.3 *Pds5 maps to the Smc1 hinge*

Having now created a fluorophore conjugated Smc1 hinge, we used it to screen for potential interactors. We could not detect any robust interaction between the YFP-hinge and core components around the head e.g. Smc1-CFP (1.05±0.19, n = 55) or Scc3-CFP (1.06±0.13, n = 53). We did observe a very low $FRET_R$ between CFP-Pds5 and Scc1-YFP ($FRET_R$ = 1.08±0.16, n = 47) and between Pds5-YFP and CFP-Scc1 ($FRET_R$ = 1.1±0.13, n = 42) (Figure 2.10). A *t*-test to evaluate the significance of these values suggested that they are greater than those obtained for the Pds5-YFP/Smc1-CFP pair ($p<0.01$). Nevertheless, the very weak FRET should be regarded equivocal. To our surprise we found a clear FRET signal between both N- and C-terminally tagged Pds5 and the Smc1 hinge-YFP insertion ($FRET_R$=1.15±0.23, n=48 and $FRET_R$=1.21±0.19, n=40, respectively, which is greater than the Pds5-YFP/Smc1-CFP pair at $p<0.0001$). This suggests that Pds5 is in contact with the Smc1 hinge. Despite the fact that this result is low, it was consistently reproducible. These results suggest that Pds5 makes contact with the Smc1 hinge, probably constitutively throughout the cell cycle (Figure 2.10).

2.8 A head-hinge interaction in the cohesin complex

Atomic force microscopy (AFM) images of *S. pombe* Psm1/Psm3 heterodimers show a very flexible coiled coil with the apparent ability to undergo 'head-hinge' interactions (Sakai et al., 2003). Head-hinge interactions have also been recently been proposed to be the initial step for loading of budding yeast cohesin complexes onto DNA (Gruber et al., 2006). Good evidence now also exists from the bacterial SMC protein that there is communication between the SMC head and hinge. Given the above, we wondered if we could find any biochemical evidence for such an interaction. We over-expressed in yeast an Smc1 head construct consisting of the N- and C-terminal head domains connected by a short peptide linker (Weitzer et al., 2003) as well as the two Smc1 and Smc3 halves of the hinge flanked by 50 amino acids on either side. Immunoprecipitation against an affinity epitope on the Smc1 half-hinge demonstrated stable complex formation with the Smc3 hinge (Figure 2.11A).

Moreover, this Smc hinge complex efficiently co-immunoprecipitated the Smc1 head, suggesting a direct head-hinge interaction. The quantities of overexpressed hinge and heads precipitated in this experiment exceeded the level of the endogenous cohesin complex, and we could not detect other cohesin subunits in the immunoprecipitate. For example, immunoprecipitation of either Pds5 or Scc1 does not pull down tagged hinge components (Figure 2.11C). Therefore the interaction between the Smc head and hinge observed in this experiment is most likely direct. We further investigated if ATP binding or hydrolysis by the Smc1 head was required for this interaction with the hinge. To address this question we repeated the immunoprecipitation reaction with Smc1 head constructs with mutations in the Walker A or C-motif which are predicted to prevent ATP binding and hydrolysis respectively. These ATPase mutant Smc1 heads still bound to the Smc3 hinge comparably to wild type Smc1 indicating that ATP is not required for this interaction (Figure 2.11B). This evidence for a direct Smc1 head-hinge association is in contrast to our failure to detect physical proximity between the two by FRET *in vivo* (Figure 2.7B). A possible solution to this apparent paradox is that our biochemical results reveal an interaction that occurs only transiently *in vivo*, either because of a conformational equilibrium biased towards complexes with separated heads and hinge (for example imposed by the presence of coiled coils), or because the interaction underlies additional regulation and occurs only as a transient intermediate e. g. during cohesin loading onto chromosomes. As discussed previously our FRET on populations of molecules within the cell precluded us from detecting such intermediates. In an attempt to look at 'pre-loaded' cohesin complexes, we tried to perform FRET experiment in Scc2/Scc4 mutant backgrounds. However, increased background fluorescence at the higher restrictive temperature required to inactivate the loader alleles, as well as the presence of dead autoflouorescent cells even at permissive temperature, prevented us from analysing these strains.

2.9 Cohesins show no evidence of dimerisation *in vivo*

Multiple models have been put forward as to how cohesin might link two replication products after DNA synthesis (Milutinovich and Koshland, 2003; Nasmyth and Haering, 2005). One important question in this respect is whether

one cohesin ring encircles and holds together both sister chromatids, or whether individual cohesin complexes bind each sister chromatid and linkages are established by interactions between more than one cohesin complex. Dimerisation of the Rad50 protein occurs via its Zinc hook structure to facilitate intermolecular cross-linking of DNA molecules for DNA repair reactions to occur (Hopfner et al., 2002). *In vitro* characterisation of cohesin isolated from yeast chromosomes has so far not found evidence for higher order interactions between more than one cohesin complex (Weitzer et al., 2003; Ivanov and Nasmyth, 2005; Haering et al., 2002). Nonetheless, dimerisation of cohesin complexes at S phase via a 'snapping' mechanism is still a popular alternative to that of the ring model. The existence of such interactions *in vivo* is difficult to exclude, and perhaps the regime used to generate yeast extracts may perturb potential interaction between different cohesin complexes. We therefore utilised our FRET assay to search for interactions between more than one cohesin complex. We first analysed two copies of Smc1, that were tagged in a diploid yeast strain at their C-termini with CFP and YFP, respectively. The existence of cohesin dimers in 'head to head' orientation should result in FRET between the two tagged Smc1 termini. However, no FRET was detected ($FRET_R$=1.05±0.24, n=51) (Figure 2.12). A similar experiment with the two copies of Smc3 tagged again did not yield evidence for an interaction ($FRET_R$=1.03±0.13, n=34) (Figure 2.12). A corollary of this experiment is that the FRET observed between fluorescently tagged Smc1 and Smc3 is due to interaction between these heads as part of the same complex, and not for example, between adjacent cohesin complexes in CAR due to molecular crowding or higher order interactions between cohesin complexes. The above experiments would not however detect dimeric cohesin if they existed in a 'hinge to hinge' orientation (as is the case for RAD50). To test this idea we constructed both YFP and CFP insertions into each copy of the Smc1 hinge in a diploid yeast strain. Again this yielded a baseline $FRET_R$. ($FRET_R$=1.0±0.22, n=40) (Figure 2.12). While these results cannot exclude association between more than one cohesin complex at sites different from the ones here tested (e.g. the coiled coils), our observations pose limitations on how such interactions could occur *in vivo*.

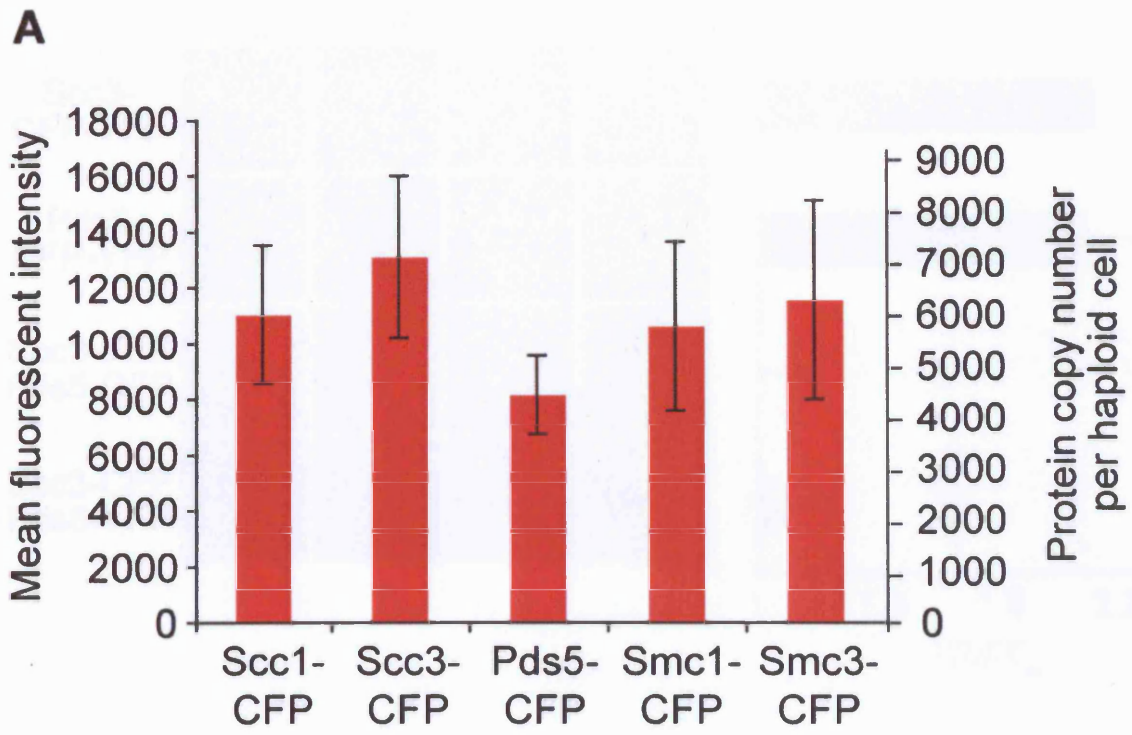

Figure 2.1 continued…

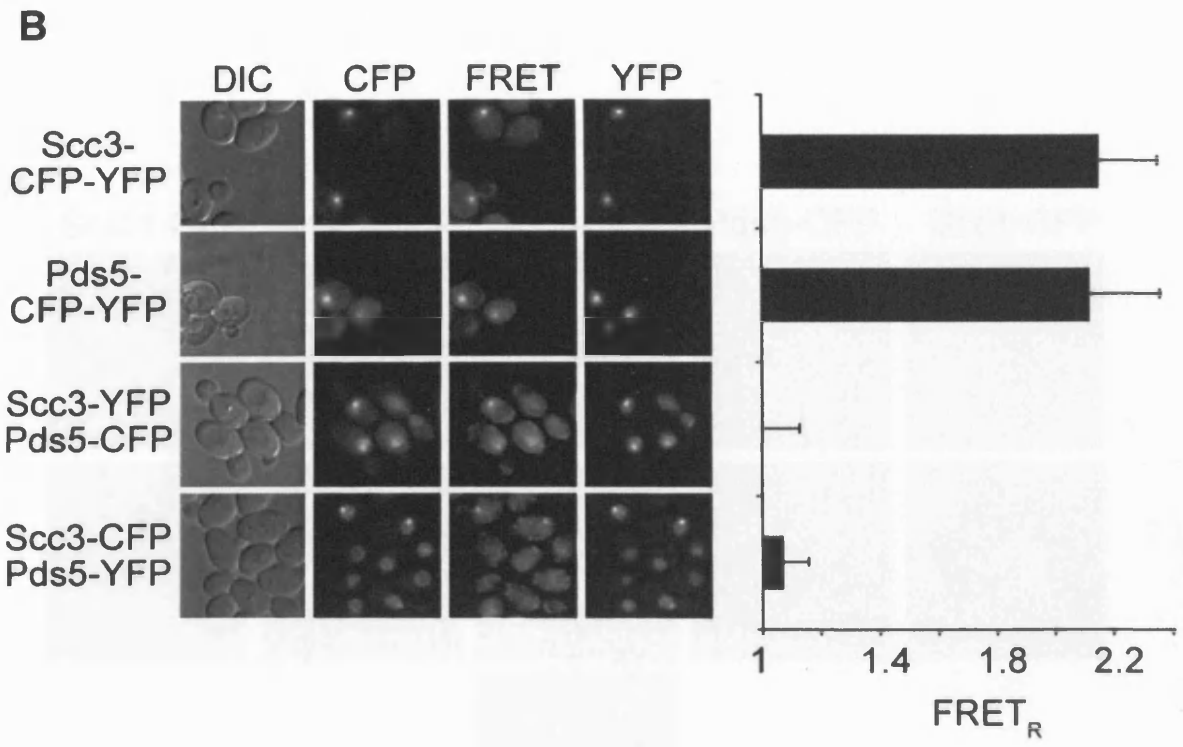

Figure 2.1 Establishment of FRET to analyse proximity between cohesin subunits in budding yeast

(**A**) *In vivo* concentrations of five budding yeast cohesin subunits. Nuclear fluorescence intensities were measured in yeast strains Y3087 (*MAT*a/α *SCC1-CFP*), Y2490 (*MAT*a/α *SCC3-CFP*), Y2489 (*MAT*a/α *PDS5-CFP*), Y1967 (*MAT*a/α *SMC1-CFP*) and Y1971 (*MAT*a/α *SMC3-CFP*). Error bars represent standard deviation (n≥50 for each strain).

(**B**) Positive and negative FRET controls. Strains Y2588 (*MAT*a/ α *SCC3-YFP-CFP*) and Y2587 (*MAT*a/ α *PDS5-YFP-CFP*) were subject to FRET analysis. Fluorescence in the YFP, FRET, and CFP channels is shown, as well as the $FRET_R$ values derived as described in Materials and methods. Strains containing fluorophore pairs at the Scc3 and Pds5 C-termini, Y2575 (*MAT*a/α *SCC3-YFP PDS5-CFP*) and Y2574 (*MAT*a/ α *SCC3-CFP PDS5-YFP*), showed fluorescence intensities in the FRET channel as expected from spectral spillover alone.

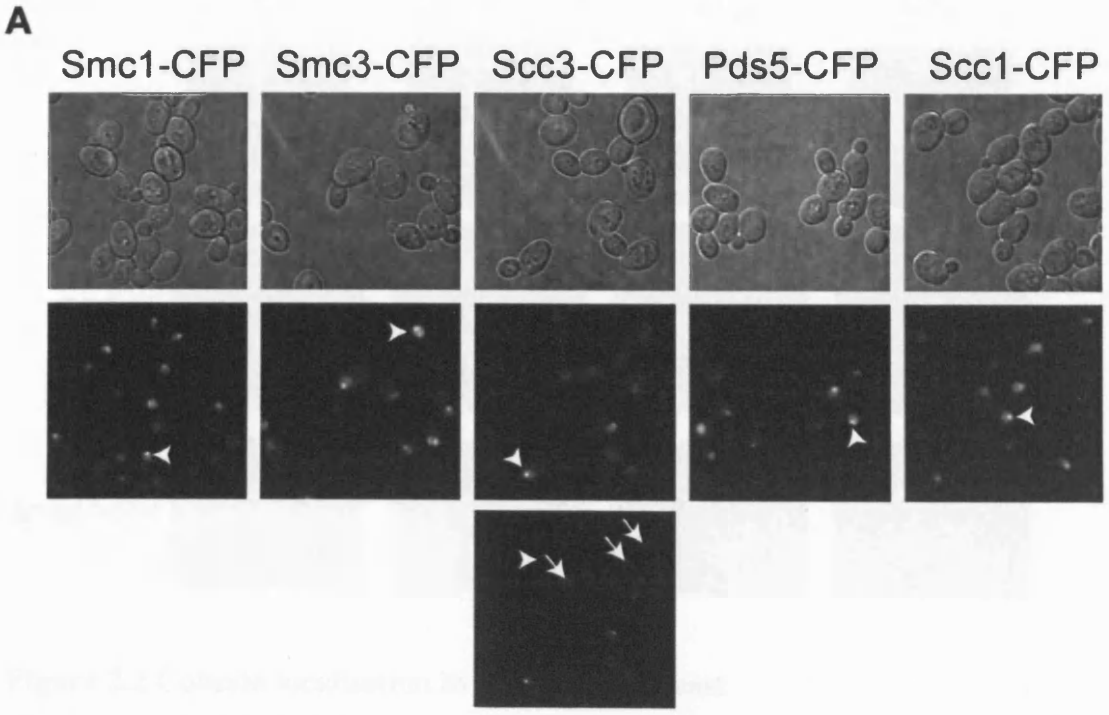

Figure 2.2 continued…

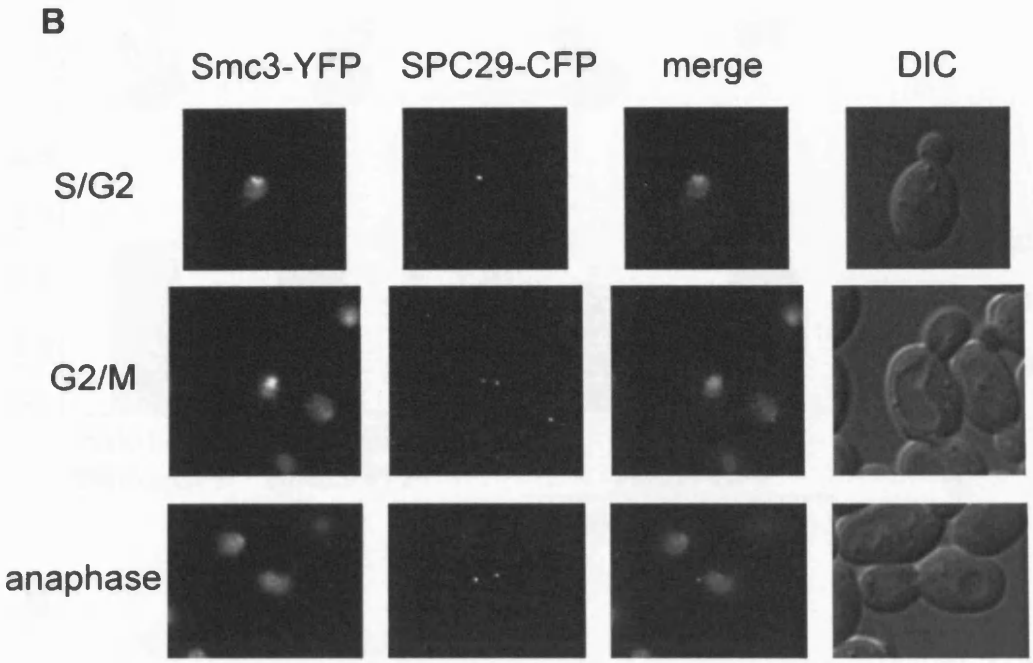

Figure 2.2 Cohesin localisation in live budding yeast

(**A**) Strains Y1967 (*MAT*a/α *SMC1-CFP),* Y1971 (*MAT*a/α *SMC3-CFP*), Y2490 (*MAT*a/α *SCC3-CFP*), Y2489 (*MAT*a/α *PDS5-CFP)* and Y3087 (*MAT*a/α *SCC1-CFP)* were grown overnight on YPD plates at 30°C and imaged as described in the materials and methods. Arrowheads depict nuclear foci in cells with small to medium sized buds, see for all cohesin components. Arrows show additional Scc3 localisation at the nuclear periphery in anaphase and G1 cells.
(**B**) Cohesin foci cluster around the spindle pole bodies and disappear in early anaphase. Strain BESY131 (*MAT*a/α *SMC3-YFP SPC29-CFP*) was grown overnight at 30°C and imaged as described in the materials and methods.

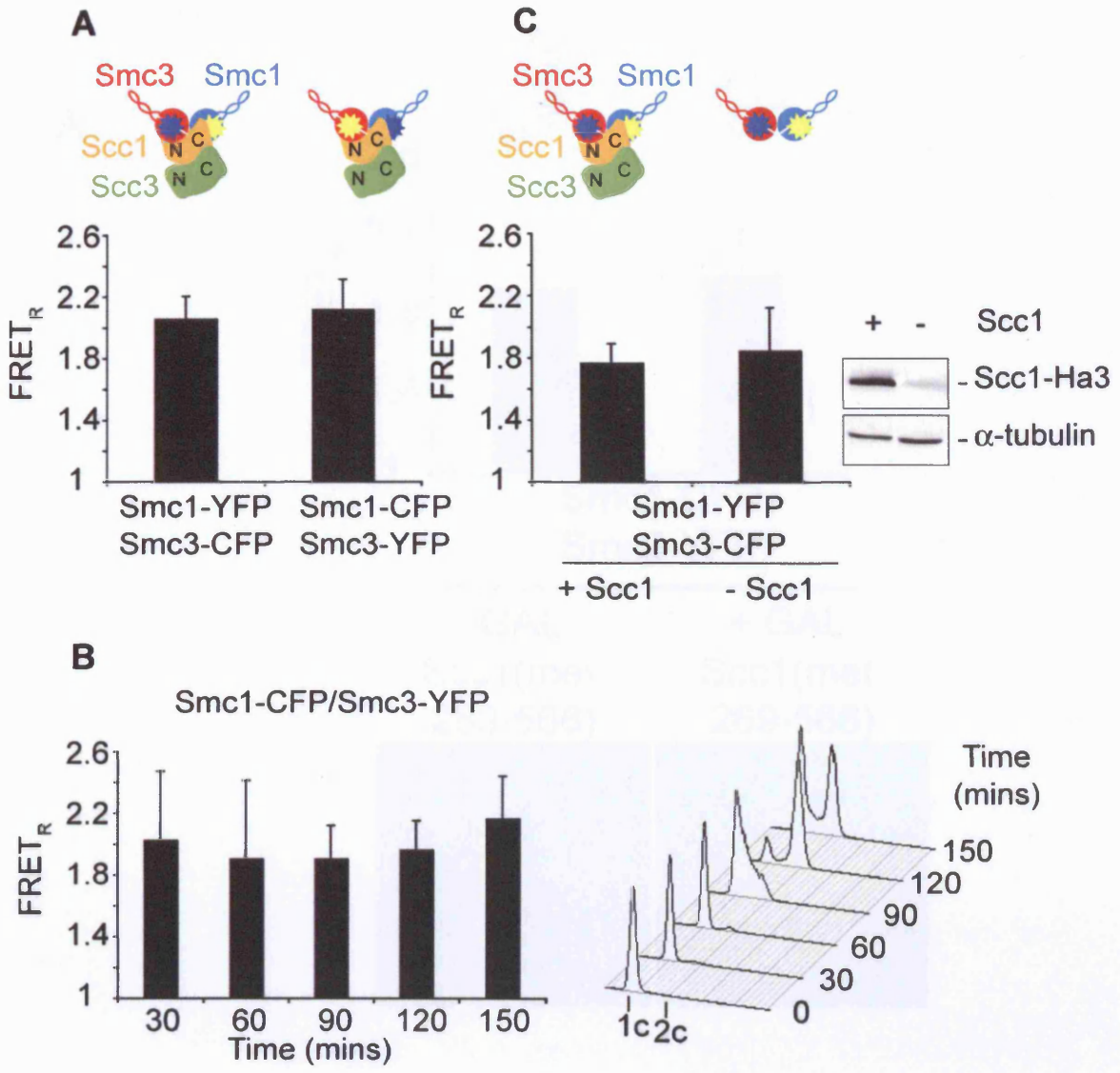

Figure 2.3 Constitutive close interaction of the SMC heads of the cohesin complex

(**A**) Close proximity of fluorophore pairs attached to the Smc1 and Smc3 heads. FRET was analysed in exponentially growing cells of strains Y1966 (*MAT*a/α *Smc1-YFP Smc3-CFP*) and Y1972 (*MAT*a/α *Smc1-CFP Smc3-YFP*).
(**B**) Constitutive Smc1/Smc3 head proximity throughout the cell cycle. Small unbudded G1 cells of strain Y1972 were isolated by centrifugal elutriation and released to progress through a synchronous cell cycle. Samples for FRET analysis were processed every 30 min. Cell cycle progression was monitored by FACS analysis of DNA content.
(**C**) Scc1-independent association of the Smc1/Smc3 heads. Strain Y2864 (*MAT*a/α *Smc1-YFP Smc3-CFP GAL1-SCC1-Ha3*) was grown in galactose-containing medium and half of the culture shifted to medium lacking galactose to repress Scc1 expression. After 2 hours Scc1 levels and FRET were analysed.

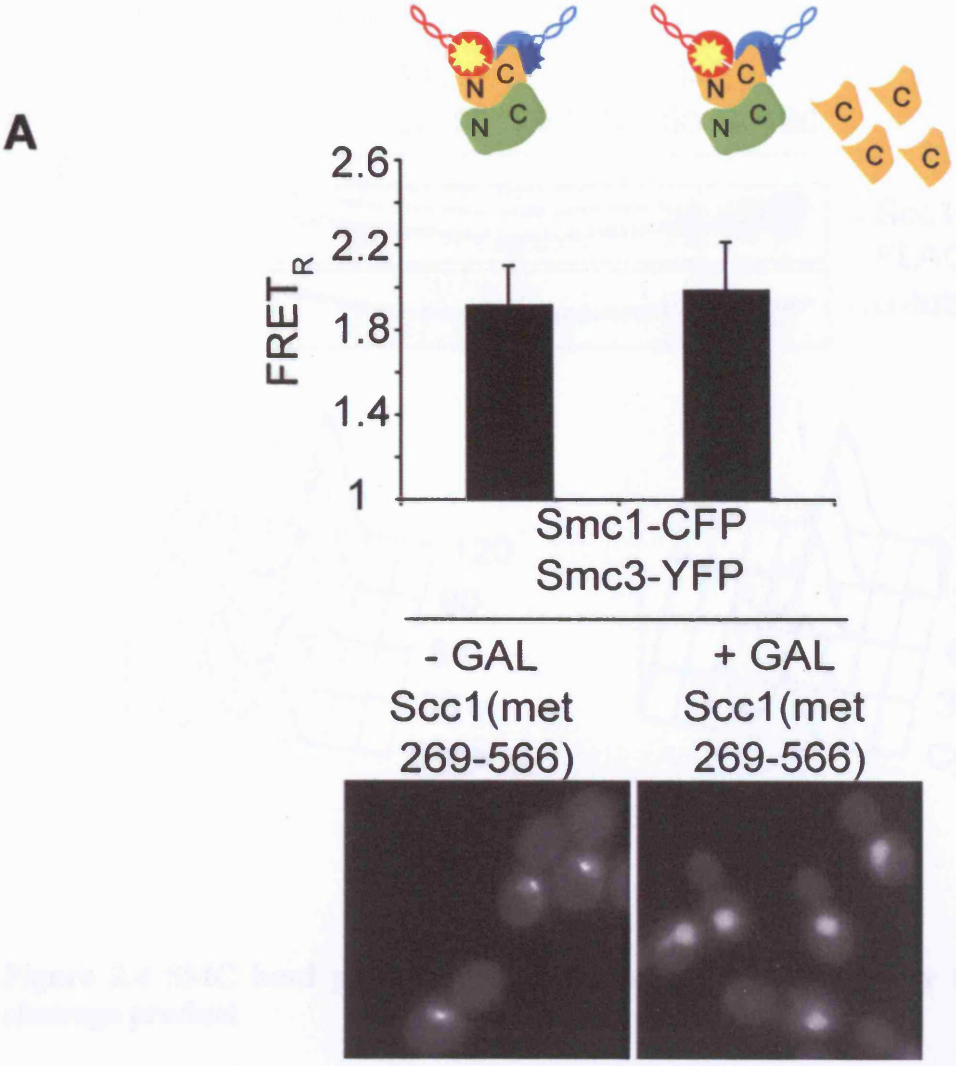
A
N
C
N
C
N
C
N
C
C
C
C
C
2.6
2.2
1.8
1.4
1
FRET$_R$
Smc1-CFP
Smc3-YFP
- GAL
Scc1(met
269-566)
+ GAL
Scc1(met
269-566)

Figure 2.4 continued...

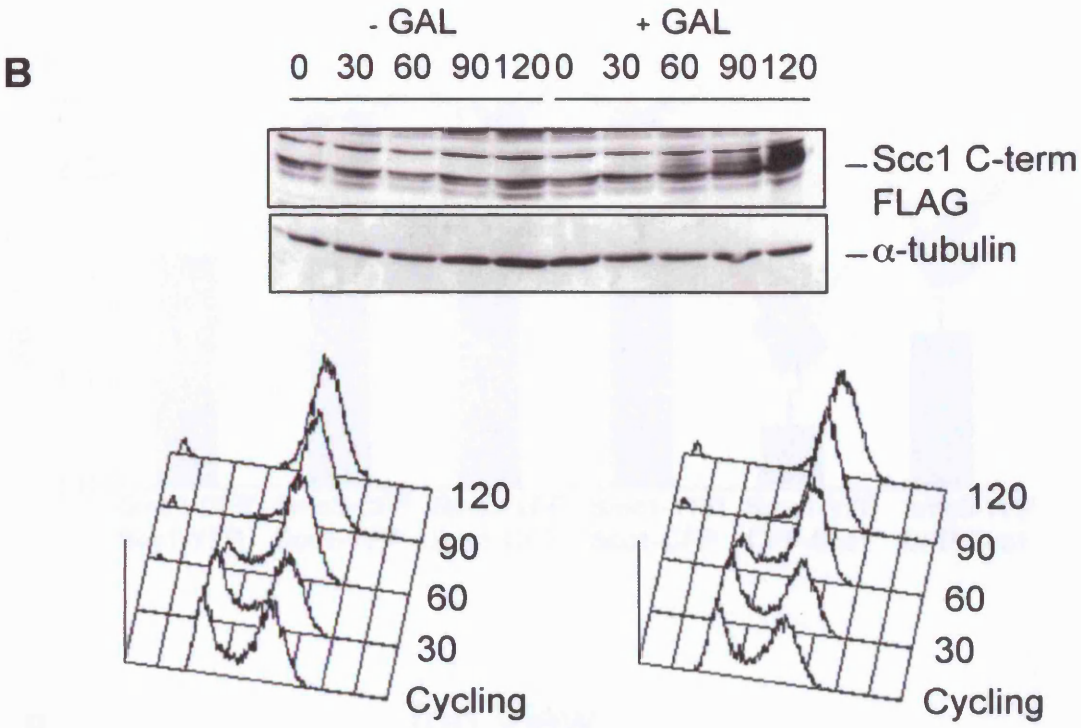

Figure 2.4 SMC head proximity after chromatin dissociation by the Scc1 cleavage product

(**A**) Cells of strain Y3254 (*MATa/α SMC1-CFP/SMC1-CFP SMC3-YFP/SMC3-YFP GAL1-SCC1(met269-566)/GAL1-SCC1(met269-566)*) were grown in YP raffinose medium, and arrested in G2/M by nocodazole treatment. Expression of the Scc1 C-terminal fragment was induced by galactose addition for 2 hours. FRET was analysed in these and control cells that were left without galactose. Images show redistribution of cohesion (Smc1-CFP) from nuclear foci after expression of the Scc1 cleavage fragment.
(**B**) Cell cycle arrest was monitored by FACS analysis, and expression of the Scc1 cleavage fragment confirmed by Western blotting against he FLAG epitope.

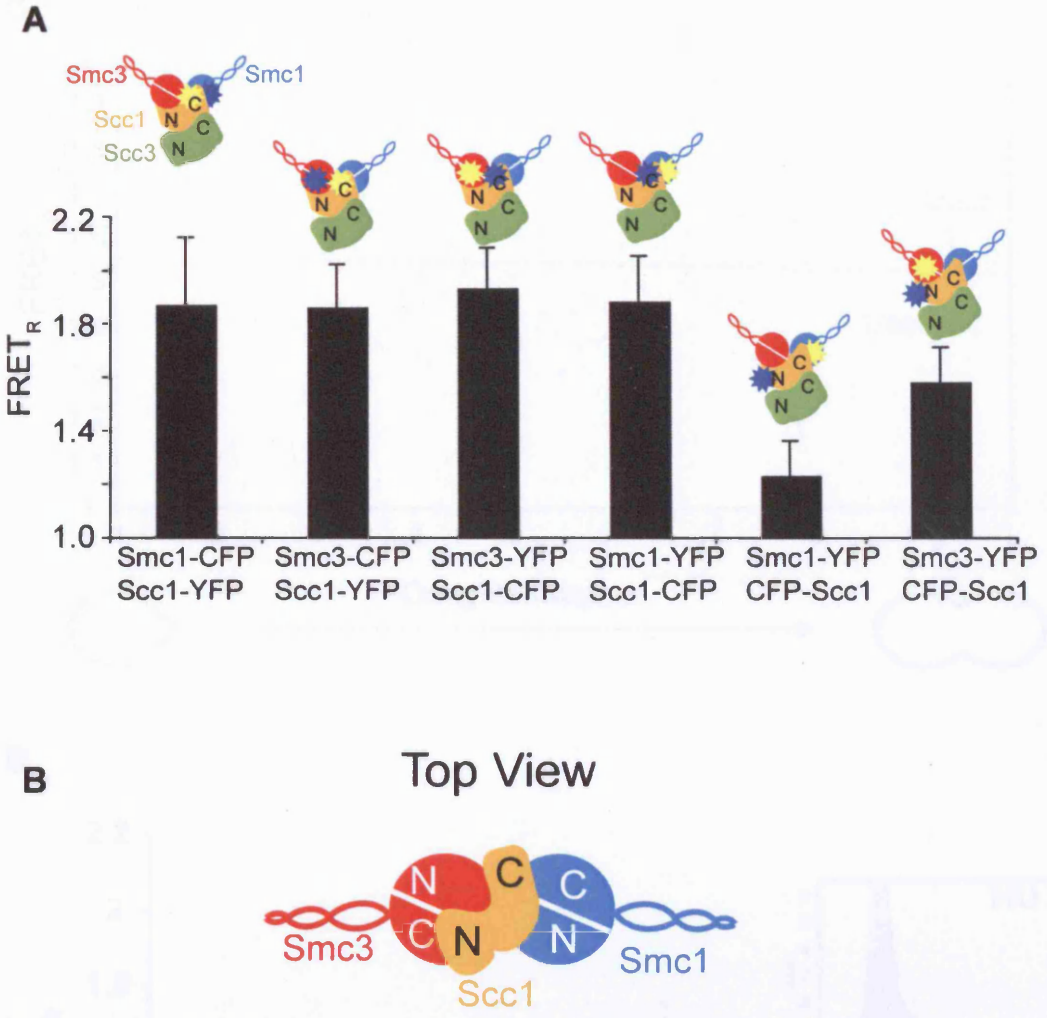

Figure 2.5 Scc1 lies perpendicular to the SMC heads of the cohesin complex

(**A**) FRET measurements in strains Y2480 (*MATa/α SCC1-YFP Smc1-CFP*), Y2481 (*MATa/α SCC1-YFP Smc3-CFP*), Y2482 (*MATa/α SCC1-CFP Smc3-YFP*), Y2483 (*MATa/α SCC1-CFP Smc1-YFP*), Y2593 (*MATa/α CFP-SCC1 Smc1-YFP*) and Y2594 (*MATa/α CFP-SCC1 Smc3-YFP*) show that the Scc1 C-terminus is placed close and equidistant to both Smc1 and Smc3 heads.
(**B**) A schematic representation of the geometry of Scc1 relative to the Smc1 and Smc3 heads.

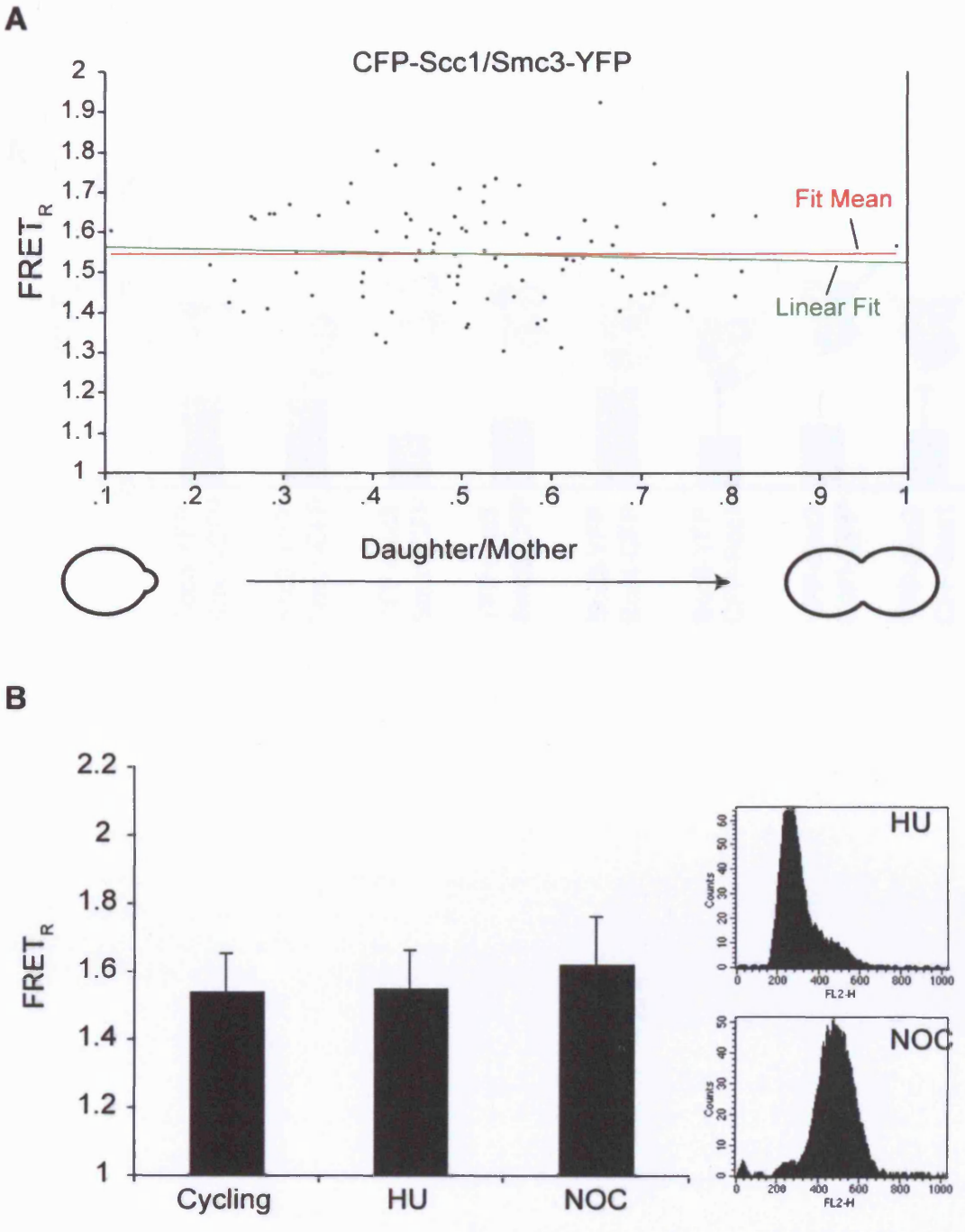

Figure 2.6 Cell cycle analysis of the interaction between N-terminal Scc1 and the Smc3 head

(**A**) FRET values in an exponentially growing culture of Y2594 (*MAT*a/α CFP-SCC1 SMC3-YFP) was determined for cells concomitant with their bud size ratio as an indicator of cell cycle progression.
(**B**) FRET experiment were carried out in Y2594 arrested in HU and NOC

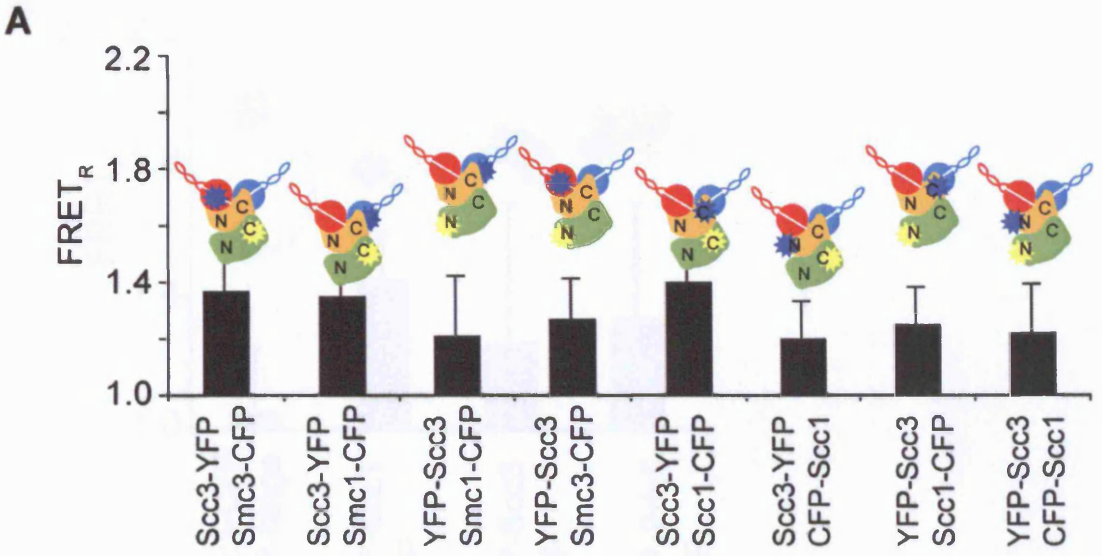
A
2.2
1.8
1.4
1.0
FRET$_R$
Scc3-YFP Smc3-CFP
Scc3-YFP Smc1-CFP
YFP-Scc3 Smc1-CFP
YFP-Scc3 Smc3-CFP
Scc3-YFP Scc1-CFP
Scc3-YFP CFP-Scc1
YFP-Scc3 Scc1-CFP
YFP-Scc3 CFP-Scc1

Figure 2.7 continued…

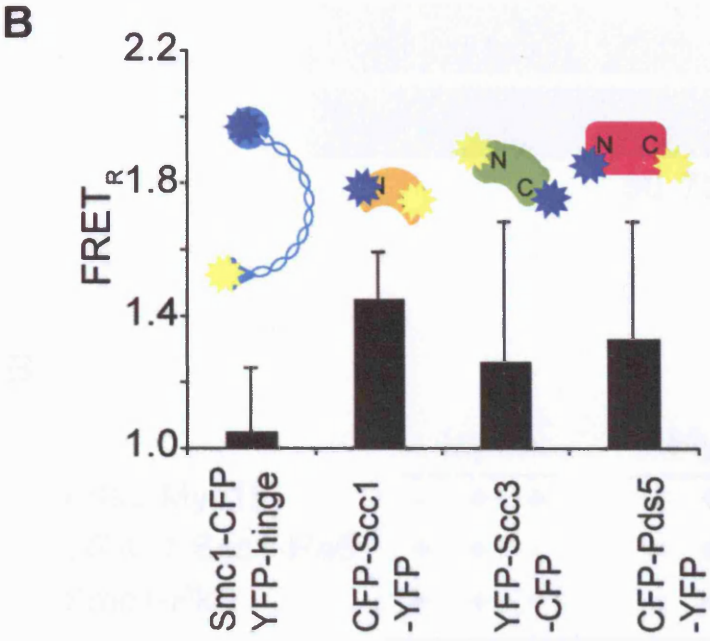

Figure 2.7 Scc3 interacts with the SMC heads of the cohesin complex

(**A**) Mapping of Scc3 to the cohesin complex. FRET was analysed, from left to right, in strains Y2589 (*MATa/α SCC3-YFP SMC3-CFP*), Y2533 (*MATa/α SCC3-YFP SMC3-CFP*), Y2721 (*MATa/α YFP-SCC3 SMC1-CFP*), Y2704 (*MATa/α YFP-SCC3 SMC3-CFP*), Y2534 (*MATa/α SCC1-CFP SCC3-YFP*), Y2591 (*MATa/α SCC3-YFP CFP-SCC1*), Y2722 (*MATa/α YFP-SCC3 SCC1-CFP*) and Y2723 (*MATa/α YFP-SCC3 CFP-SCC1*).

(**B**) Analysis of interactions within cohesin subunits. FRET experiments were performed with strains Y2598 (*MATa/α Smc1-YFP-hinge-CFP*), Y2592 (*MATa/α CFP-SCC1-YFP*), Y2872 (*MATa/α YFP-SCC3-CFP*) and Y2865 (*MATa/α CFP-PDS5-YFP*).

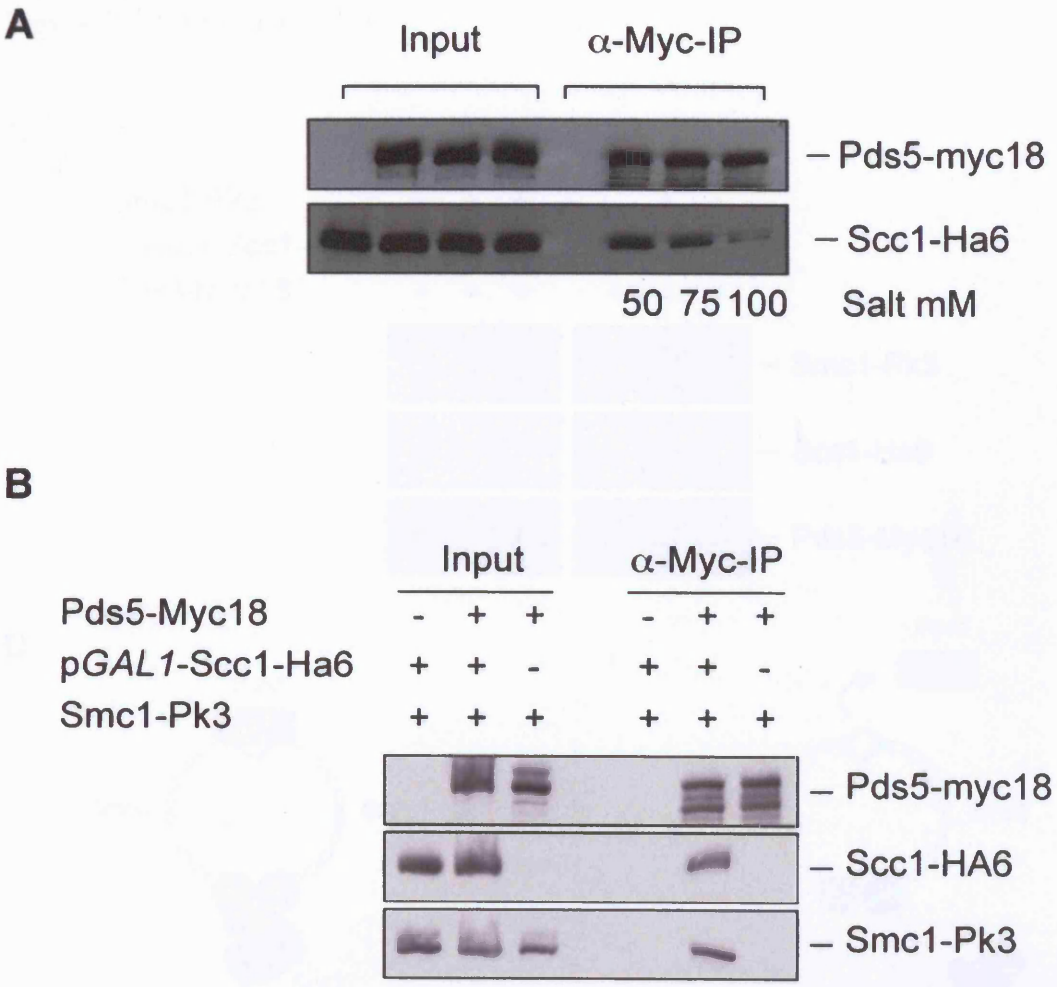
A
Input
α-Myc-IP
– Pds5-myc18
– Scc1-Ha6
50 75 100
Salt mM
B
Input
α-Myc-IP
Pds5-Myc18
pGAL1-Scc1-Ha6
Smc1-Pk3
– Pds5-myc18
– Scc1-HA6
– Smc1-Pk3

Figure 2.8 continued…

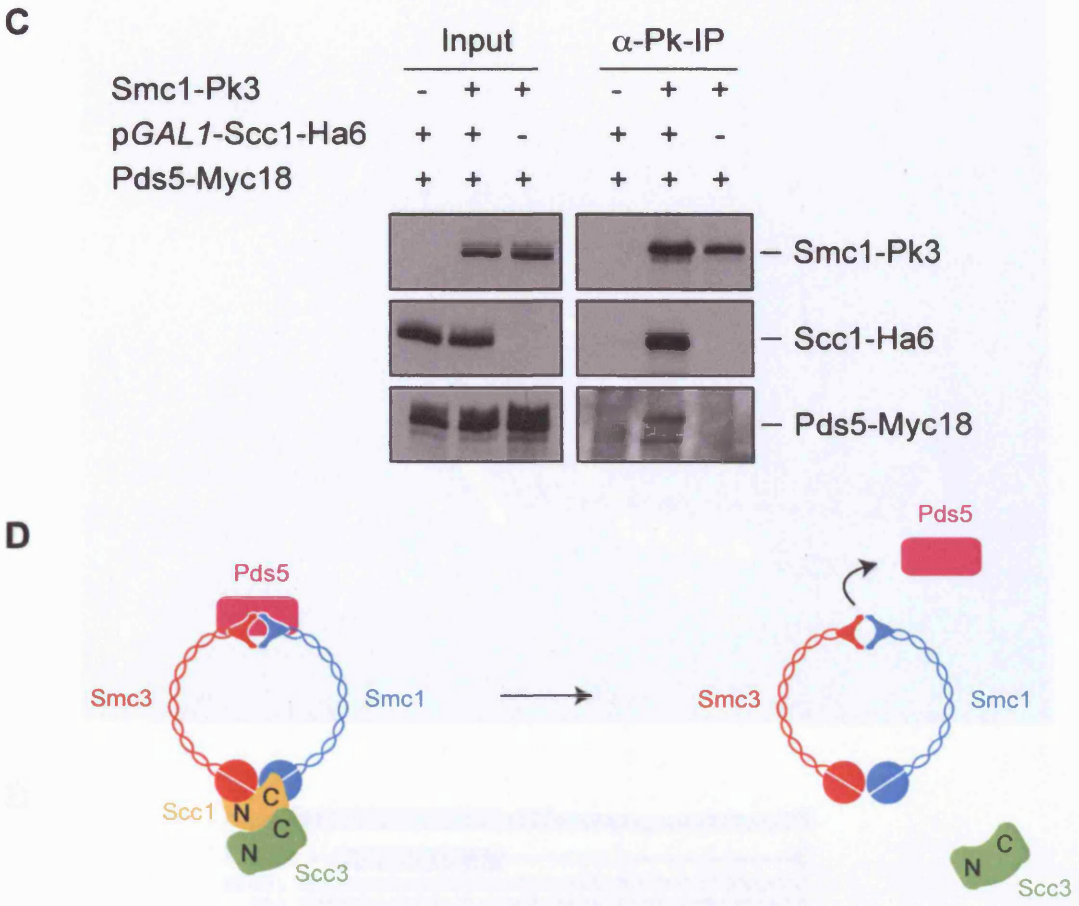

Figure 2.8 Scc1 dependent binding of Pds5 to the cohesin complex

(**A**) Pds5 interacts with the cohesin complex in salt sensitive manner. Pds5 immunoprecipitates were performed in low salt buffers. Extracts were prepared in starins Y2791 (*MATa SCC1-Ha6 SMC1-Pk3*) and Y3207 (as Y2791, but *PDS5-myc18*). After IP reactions, beads were washed in buffers containing increasing salt concentrations.
(**B**) Extracts were prepared from haploid strains Y3223 (*MATa Smc1-Pk3 GAL1-SCC1-Ha6*) and Y3210 (as Y3223, but *PDS5-myc18*) in the presence or absence of Scc1, and co-immunoprecipitation of Smc1 with Pds5 was analysed by immunoblotting.
(**C**) Reciprocal experiment of (A) above. Extracts were prepared from Y3231 (*MATa GAL1-SCC1-Ha6 PDS5-myc18*) and Y3210 in the presence or absence of Scc1.
(**D**) Schematic representing a possible interaction of Pds5 with the cohesin complex.

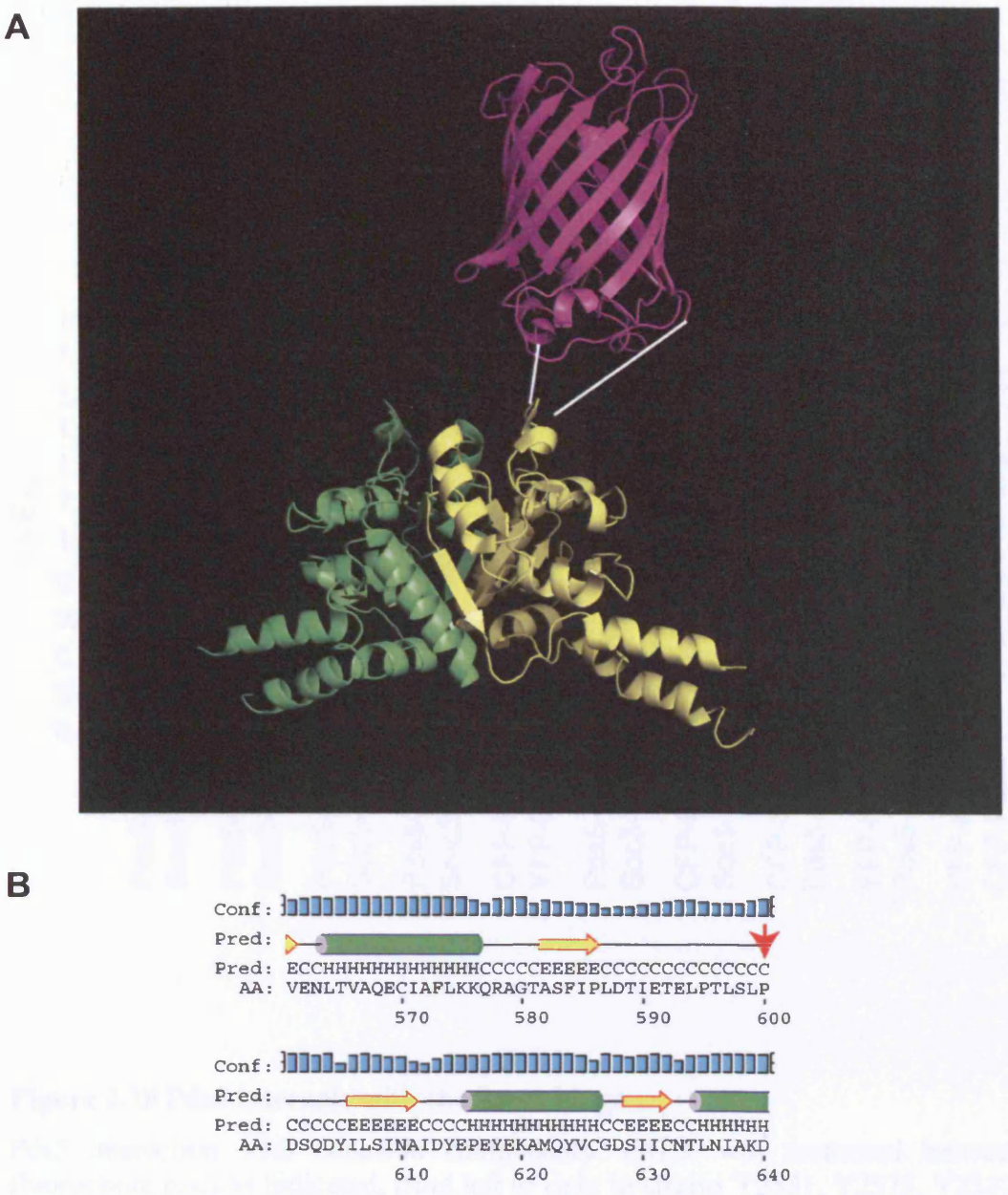

Figure 2.9 A fluorophore conjugated Smc1 hinge

(**A**) Representation of the Smc1-CFP or YFP hinge. The purple protein is the crystal structure of the Green Fluorescent protein from *A. Victoria* (Ormo et al., 1996). Below this is the crystal structure of the *T. maritama* SMC hinge (Haering et al, 2002). The position of the insertion is at Proline 600 in *S. cerevisiae* SMC1, which corresponds to residue 587 (Glutamic acid) in *T. Maritama*. Figure was prepared using PyMol software

(**B**) Secondary structure predictions on the Smc1 hinge. H indicates α-helix, E = β-turn and C = loop. Secondary structure predictions were performed using BTPRED (Shepherd et al., 1999).

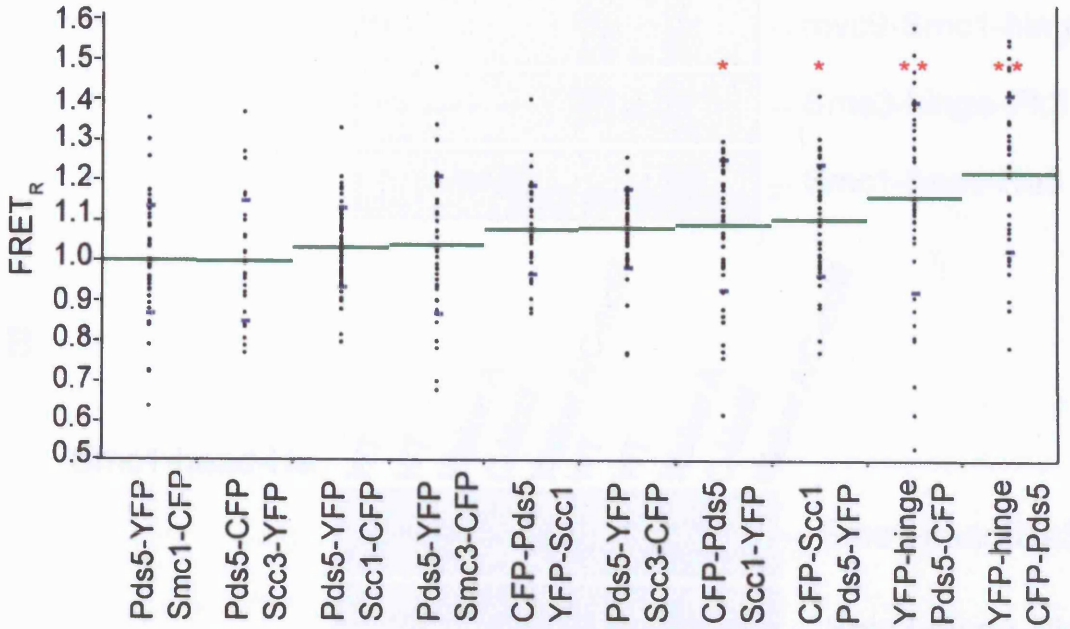

Figure 2.10 Pds5 interacts with the Smc1 hinge

Pds5 interaction with cohesion components. FRET was measured between fluorophore pairs as indicated, from left to right in strains Y2531, Y2575, Y2532, Y2530, Y3264, Y2574, Y3275, Y2590, Y2706 and Y2705. Individual measurements are indicated as points, with the mean as green and standard deviation as blue lines. $FRET_R$ was significantly different from the Pds5-YFP/Smc1-CFP pair at * $p<0.01$ and ** $p<0.0001$, respectively, by Student's *t*-test.

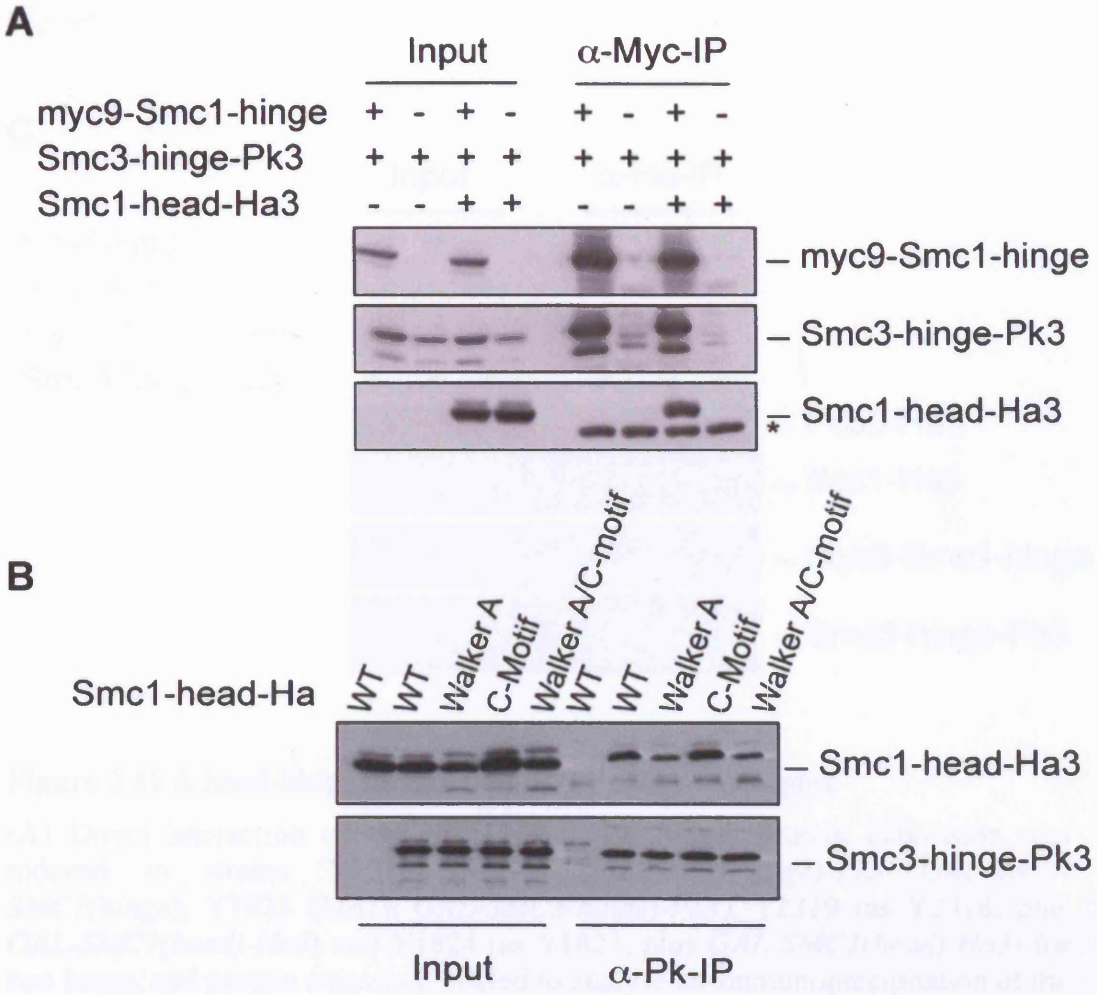
A
Input
α-Myc-IP
myc9-Smc1-hinge + - + - + - + -
Smc3-hinge-Pk3 + + + + + + + +
Smc1-head-Ha3 - - + + - - + +
– myc9-Smc1-hinge
– Smc3-hinge-Pk3
– Smc1-head-Ha3
*
B
Smc1-head-Ha
WT
WT
Walker A
C-Motif
Walker A/C-motif
WT
WT
Walker A
C-Motif
Walker A/C-motif
– Smc1-head-Ha3
– Smc3-hinge-Pk3
Input
α-Pk-IP

Figure 2.11 continued…

Figure 2.11 A head-hinge interaction in the cohesin complex

(**A**) Direct interaction of the Smc1 head and hinge. Protein expression was induced in strains Y2318 (*MAT*a *GAL-SMC3(hinge)-Pk3 GAL-myc9-SMC1(hinge)*, Y1823 (*MAT*a *GAL-SMC3(hinge)-Pk3), Y2319* (as Y2318, plus *GAL-SMC1(head)-Ha3*) and Y1824 (as Y1823, plus *GAL-SMC1(head)-Ha3*) for two hours, and protein extracts prepared to analyse co-immunoprecipitation of the Smc1 head and hinge. Asterisk indicates the IgG heavy chain.
(**B**) The head-hinge interaction is independent of ATP binding or hydrolysis by Smc1. Protein expression and extracts were prepared as in (A) above in strains Y982 (*MATa GAL-SMC1(head)-Ha3*), Y1824 (*MATa GAL-SMC1(head)-Ha3 GAL-SMC3(hinge)-Pk3*), Y1834 (as Y1824 except *SMC1-WALKER A (head)*), Y1836 (as 1824 except *SMC1 C-MOTIF A (head)*), and Y1837 (as 1824 except *SMC1 WALKER-A/C-MOTIF (head)*).
(**C**) Pds5 or Scc1 does not bind to an over-expressed Smc1-Smc3 hinge. Extracts were prepares as in (A) above in strains Y2318, Y2935 (as Y2318 except Pds5-Ha3) and Y2936 (as Y2318 except Scc1-Ha3). Immunoprecipitates of either Pds5 or Scc1 were analysed for the presence of hinge components.

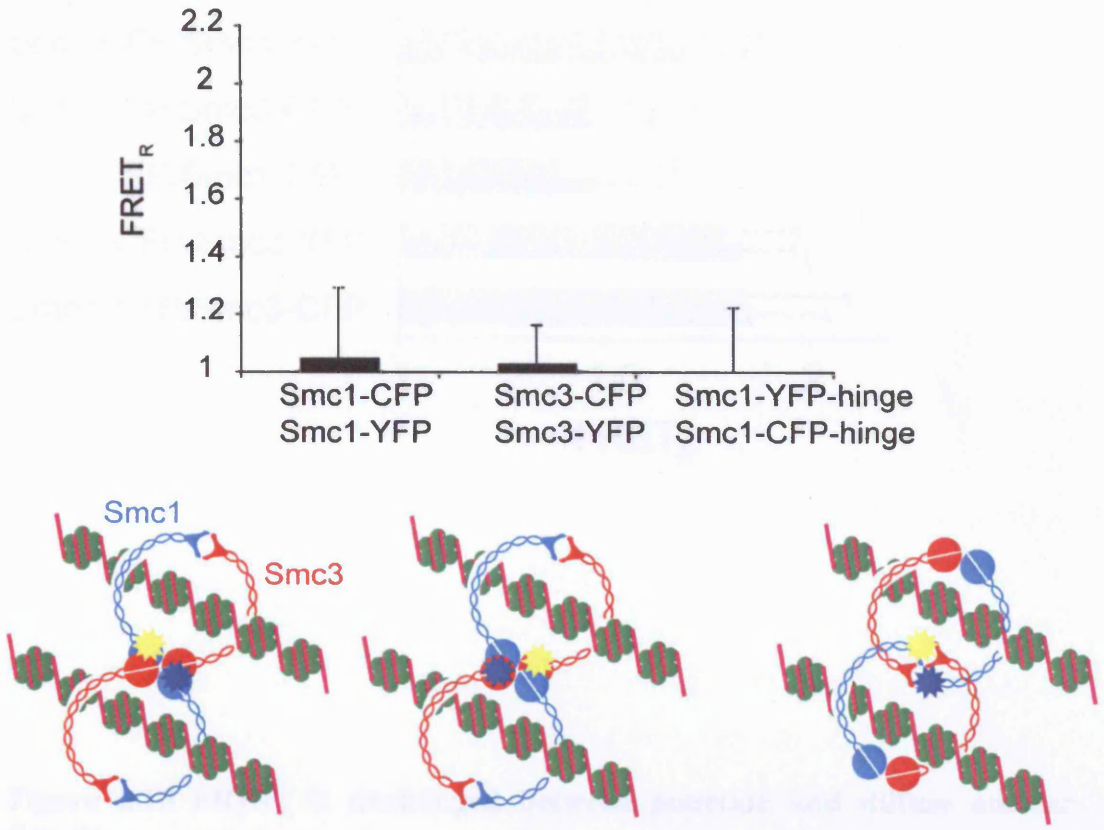

Figure 2.12 Search for evidence of cohesin multimerisation *in vivo*

FRET measurements to analyse proximity of more than one Smc1 head, Smc3 head or Smc1 hinge, were conducted in strains Y3082 (*MAT*a/α *SMC1-CFP/SMC1-YFP*), Y3083 (*MAT*a/α *SMC3-CFP/SMC3-YFP*) and Y3228 (*MAT*a/α *SMC1-hingeCFP/SMC1-hingeYFP*).

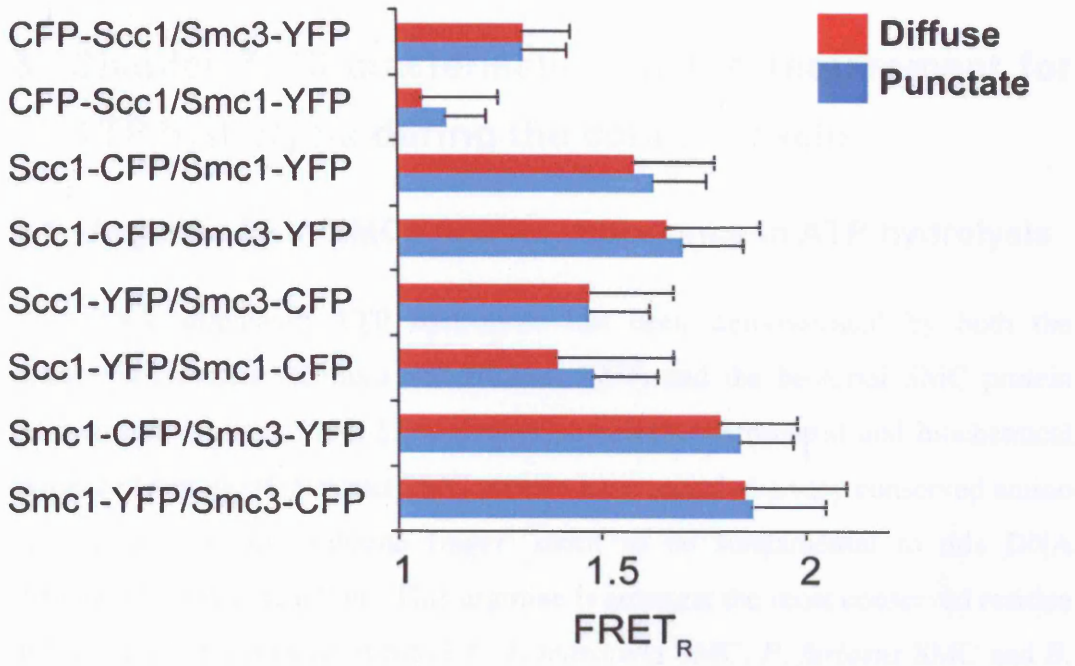

Figure 2.13 FRET$_R$ is unchanged between punctate and diffuse nuclear signals

FRET measurements were taken for both the punctate and diffuse nuclear localisations of cohesins (see figure 2.2). These measurements were performed in strains Y2594, Y2593, Y2483, Y2482, Y2481, Y2480, Y1972 and Y1966 from top to bottom shown in the graph. FRET$_R$ values remain approximatey constant between these two measurements.

3 Chapter 3: Characterisation of the requirement for ATP hydrolysis during the cohesin cycle

3.1 Arginine 58 in SMCs and its importance in ATP hydrolysis

DNA stimulated ATP hydrolysis has been demonstrated by both the condensin complex (Kimura and Hirano, 1997) and the bacterial SMC protein (Hirano and Hirano, 1998; Lammens et al., 2004). Structural and biochemical evidence from the *P. furiosus* SMC protein have revealed a very conserved amino acid as part of an 'arginine finger' motif to be fundamental to this DNA stimulated ATPase reaction. This arginine is amongst the most conserved residue in SMC proteins, present in Smc1-6, *T. maritama* SMC, *P. furiosus* SMC and *B. subtilis* SMC protein (Figure 3.1A). From the structure of the *P. furiosus* SMC protein this domain undergoes conformational change upon nucleotide binding, such that the arginine finger binds the ATP α phosphate in the nucleotide bound state. This motif is also present in GTPase activating proteins (GAPs) as well as AAA+ ATPases many of which are involved in DNA replication (Scheffzek et al., 1997). Despite this high degree of conservation, the role of this residue in eukaryotic SMC proteins has to date not been studied. From the crystal structure and *in vitro* ATPase assays the arginine finger reaches down into the active site to convey DNA stimulated ATP hydrolysis by prokaryote SMC complexes (Figure 3.1B).

3.2 Construction of ATPase mutants of Smc1 and Smc3

To gain more insight into the roles of these arginine fingers in Smc1 and Smc3 function we first asked if Smc1 or Smc3 with these residues mutated to alanine were functional. To do this we used overlap extension PCR to generate *SMC1 R58A* and *SMC3 R58A*. These ORFs were then cloned under the control of the *GAL1* inducible promoter. These constructs were then transformed into temperature sensitive yeast strains of Smc1 and Smc3 (*smc1-259* and *smc3-42* respectively). After checking expression of the constructs, these strains were then

streaked on YP plates supplemented with 2% raffinose and 2% galactose at 25°C and 37°C. As observed previously neither *smc1-259* nor *smc3-42* can form colonies at 37°C. Over-expression of Smc1R and Smc3R rescued the growth of *smc1-259* and *smc3-42* at 37°C (Figure 3.2A). Hence it appears that mutation of these residues in Smc1 or Smc3 alone did not significantly perturb protein function. We next asked if loss of both of these arginine fingers would lead to a phenotype. To do this we first replaced the endogenous *SMC1* gene with *SMC1R* and *SMC3* with *SMC3R* as the sole source of Smc1 or Smc3 in the cell. Again these strains showed no obvious visible phenotype (data not shown). Crossing of *smc1R* with *smc3R* did yield spores harbouring both mutant alleles (Figure 3.2B). These strains did now show a slightly abnormal phenotype based on colony morphology and had an increased doubling time relative to wild type cells (data not shown). We next asked if chromatin levels of cohesin were comparable in these mutant strains relative to wild type. To do this we tagged Scc1 with three Pk epitopes. Biochemical fractionation of soluble and chromatin bound proteins from wild type and Smc1R/Smc3R revealed a marked reduction of Scc1 on chromatin in the mutant strain in a cycling cell population (Figure 3.2C). This indicates that arginine fingers are somehow required for the complete loading of cohesin complexes onto chromatin.

3.3 Smc1R/Smc3R mutants show reduced kinetics of binding to chromatin

To assess if the binding kinetics of mutant cohesin complexes could load onto chromatin comparably to wild type complexes, we again performed biochemical fractionation experiments. Wild type and mutant cells were arrested in G1 with α-factor and allowed to enter the cell cycle, and subsequently blocked in mitosis with nocodazole. Scc1 is absent in G1 cells, having been cleaved by separase in the previous mitosis (Uhlmann et al., 1999). In the mutant cells we do however, see some Scc1 in G1 arrested cells. This is perhaps due to the incomplete destruction of Scc1 in this mutant, as separase preferentially cleaves chromatin bound cohesin which is known to be phosphorylated (Alexandru et al., 2001, Hornig and Uhlmann, 2004). From figure 3.3 it can be seen that mutant

cohesin complexes show very reduced kinetics of binding to chromatin compared to wild type complexes. At the time of S phase, approximately half of cellular wild-type cohesin, but significantly less of Smc1R/Smc3R cohesin was chromatin bound. This indicated that arginine fingers and their likely role in ATP hydrolysis are important to facilitate timely loading of cohesin onto DNA.

3.4 Smc1R/Smc3R show cohesion defects in a single cell cycle

To measure sister chromatid cohesion in this mutant, we analyzed the GFP-marked *URA3* locus with an array of Tet operators in strains co-expressing a GFP-Tet repressor fusion. Wild type and mutant strains were arrested in G1 with the mating pheremone α-factor at 25°C. Cells were then released into media containing glucose to repress Cdc20 expression. Samples were taken every 15 minutes post release and GFP dot separation at *URA3* was scored. Between 2% and 3% of wild-type cells showed premature loss of cohesion in the Cdc20 block. Under the same conditions 10% to 12% of the mutant strains displayed cohesion defects (Figure 3.4). The increase in GFP dot separation in the mutant coincided with passage through S-phase. Hence in a single cell cycle, arginine fingers in Smc1 and Smc3 contribute to the generation of robust cohesion between sister chromatids, at least at the *URA3* locus.

3.5 Cohesion defects can be rescued by extending the window for cohesin loading

The previous results are consistent with either of two possible scenarios. If ATP hydrolysis is simply required for the loading reaction, allowing more time for cohesin loading before cohesion establishment should at least partly alleviate the observed cohesion defects. Alternatively during cohesion establishment, cohesin complexes could be stripped from DNA, as is the case with most DNA binding proteins (Gruss et al., 1993), and be reloaded again behind the replication fork (reviewed in Gerbi and Bielinsky, 2002). This reloading reaction would likely require an ATP hydrolysis reaction by cohesin, as is required for all known

association of cohesin complexes with DNA (Weitzer et al., 2003; Arumugam et al., 2003). To differentiate between these possibilities we again arrested cells in G1. The culture was then split and one half was released into a Cdc20 arrest. The other half was released for two hours into an early S phase arrest with HU before being released into a Cdc20 block. Chromatin fractionation revealed that this imposed delay allowed for more cohesion loading to occur (Figure 3.5A). GFP dot separation was then scored. In the mutant as before 12% of GFP dots were separated at the *URA3* locus compared to approximately 2% in wild-type cells. In the mutant delayed in S phase, GFP dot separation was now significantly reduced in the Cdc20 block at 3% to 4% (Figure 3.5B). These results suggest that by allowing more time to load more cohesin complexes before cohesion establishment in S phase rescues cohesion defects in the ATPase mutant alleles. This is consistent with the fact that cohesin complexes are unlikely to be removed from DNA and reloaded in an ATP hydrolysis dependent manner with fork passage in S phase.

3.6 Double mutants show elevated rates of minichromosome loss

Since the replacement of Smc1 and Smc3 with arginine finger mutant alleles of Smc1 and Smc3 have no observed growth defects individually, we now asked if these strains were genomically unstable in any way. To do this, we crossed the arginine finger ATPase mutant strain into a minichromosome containing strain background (Hieter et al., 1985). This was done both for the single mutants in Smc1 and Smc3 as well as for the double Smc1R/Smc3R mutant. Cells harbouring either Smc1R or Smc3R displayed only modestly increased frequency of chromosome loss (1.2% and 0.25% respectively). In contrast, cells carrying both mutant alleles displayed very elevated rates of minichromosome loss (57%) (Figure 3.6). This result is in direct contrast to mutations within the Walker A, Walker B or C-motif that when introduced into either Smc1 or Smc3 alone, render the protein dysfunctional (Weitzer et al., 2003; Arumugam et al., 2003). Thus it seems to be the case that these residues do not

co-operate in the ATP hydrolysis reaction, so that the presence of a single arginine finger within a cohesin complex is sufficient to execute their function.

We have also tried to determine the effects of elongating the window for cohesin loading by genetic means. The S phase cyclins Clb5 and Clb5 govern the transition from G1 to S, and their deletion results in a delay in the onset of DNA replication (Schwob and Nasmyth, 1993). We could combine deletion of either Clb5 or Clb6 with the double ATPase mutant, but not both in this background (data not shown), hence precluding us from investigating this concept further.

3.7 Smc1R/Smc3R shows normal cohesin positioning

Cohesin loading in budding yeast occurs in late G1 in an Scc2/4 dependent manner. Mechanistically as to how Scc2/4 achieves this loading reaction remains to be determined. One attractive possibility is that Scc2/4 stimulates the ATPase activity of Smc1 and Smc3 hence facilitating their loading (Ciosk et al., 2000, Arumugam et al., 2003). From high resolution mapping studies in budding yeast, cohesin complexes are first seen to dock at Scc2/4 sites from which they translocate to convergent intergenic sites (Lengronne et al., 2004). This would in theory provide a temporal and spatial regulation to ensure that a single round of ATP hydrolysis would lead only to cohesin loading. Since the cohesin complexes after loading moves away from Scc2/4 sites, this would prevent further rounds of ATP hydrolysis, thus ensuring cohesin complexes remain tightly locked on chromatin. Many proteins involved in DNA metabolism such as DNA helicases, topoisomerases, recombinases and replicases use power derived from ATP hydrolysis to translocate along, or pump through DNA (reviewed in Cozzarelli et al., 2006). Our putative ATPase mutants now enabled us to ask if ATP hydrolysis was similarly required for cohesin translocation along chromosomes. To this end we synchronised our *smc1R/smc3R* strain in G1 with α factor. Cells were released into medium containing nocodazole and samples for ChIP were taken one and two hours post release. Samples were prepared and the cohesin binding pattern for chromosome six was analyzed using Scc1-Pk. The pattern of cohesin binding between mutant and wild type cells was indistinguishable. This indicates that cohesin most likely does not use power derived from ATP

hydrolysis to translocate along DNA, and for example does not get stuck at Scc2/4 sites in an intermediate of the loading reaction.

We now asked if perhaps ATP hydrolysis works in concert with Scc2/4 dependent new cohesin loading during S phase to establish cohesion. This might be the case for example if Scc2/4 were to act as a positive regulator of the ATPase reaction of Smc1 and Smc3 as has been previously postulated (discussed above). Under such a scenario Scc2/4 could promote a second round of ATP hydrolysis during cohesion establishment. To do this we attempted to cross our Smc1R/Smc3R strain into an *scc2-4* background. This combination however was synthetic lethal (Figure 3.8). This may simply reflect the fact that the combination of these mutant alleles may give rise to a situation where not enough cohesin complexes are loaded on chromatin to support viability, even at the permissive temperature.

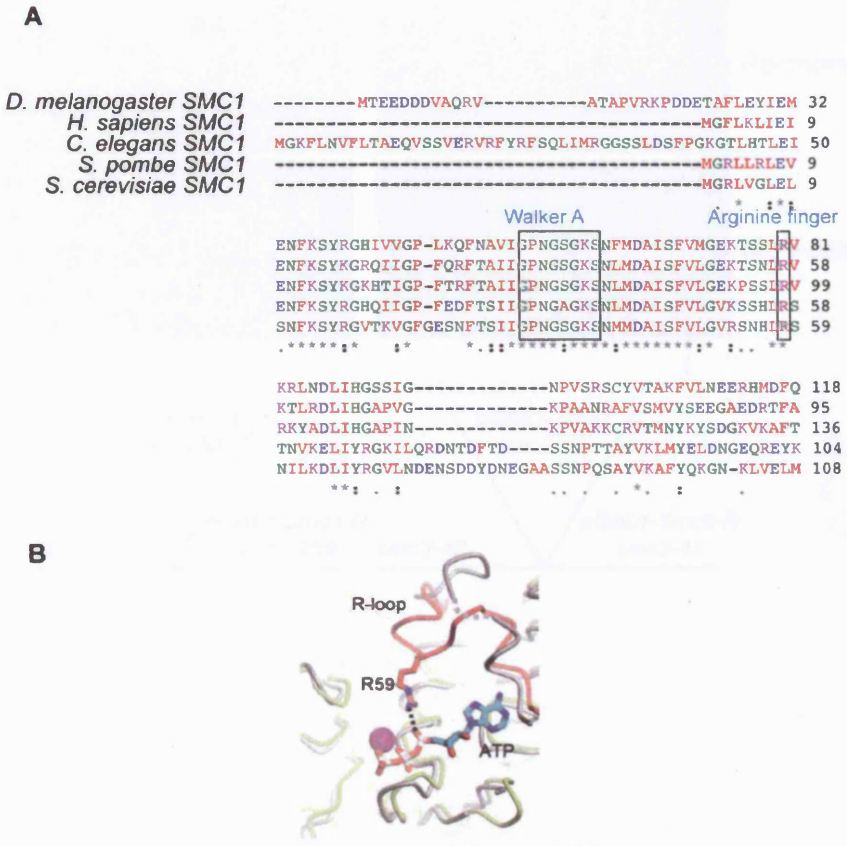

Figure 3.1 Arginine fingers in SMC proteins

(**A**) Amino acid alignment of Smc1 N-terminus from *D. melanogaster. H. sapiens, C. elegans, S. pombe and S. cerevisiae.* Arginine 58/9 is highly conserved in Smc1 as shown and also in Smc3 (data not shown). The conserved Walker A consensus sequence is also highlighted for comparison. Asterisk indicates conserved amino acids. Figure was prepared using ClustalW (Higgins et al., 1996).

(**B**) Crystal structure of the *P. furiosus* SMC head domain (Lammens et al., 2004). Note the ATP induced conformational change of the R-loop. The Arginine loop (red) changes from being distal from the active site in the nucleotide free state (grey lines), to a conformation where R59 H-bonds with the ATP α-phosphate in the ATP bound form (yellow lines).

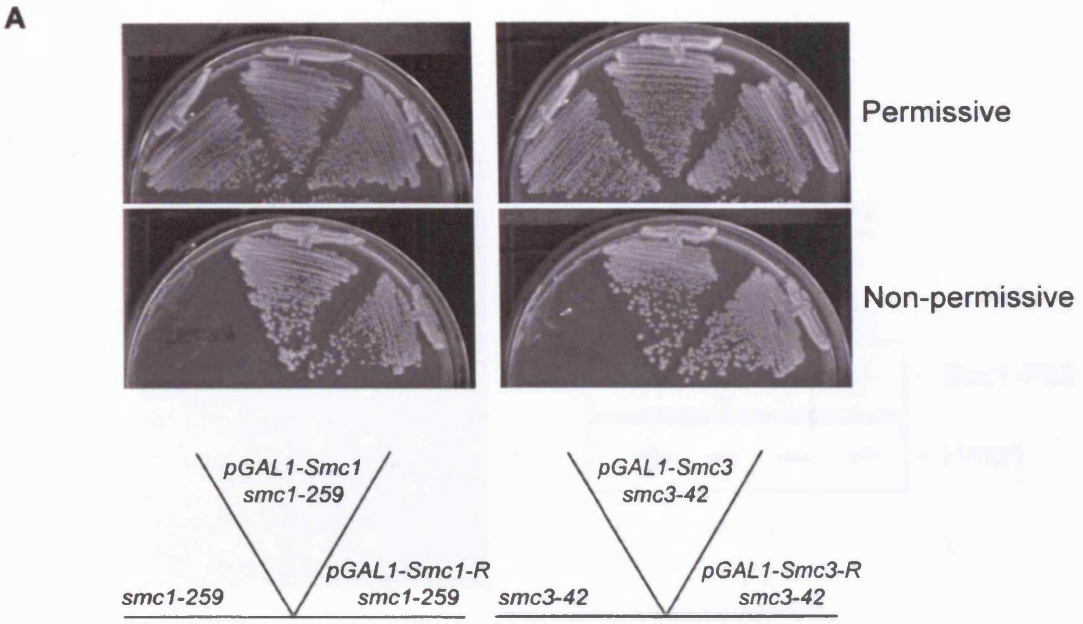
A
Permissive
Non-permissive
pGAL1-Smc1
smc1-259
pGAL1-Smc1-R
smc1-259
smc1-259
pGAL1-Smc3
smc3-42
pGAL1-Smc3-R
smc3-42
smc3-42

Figure 3.2 continued…

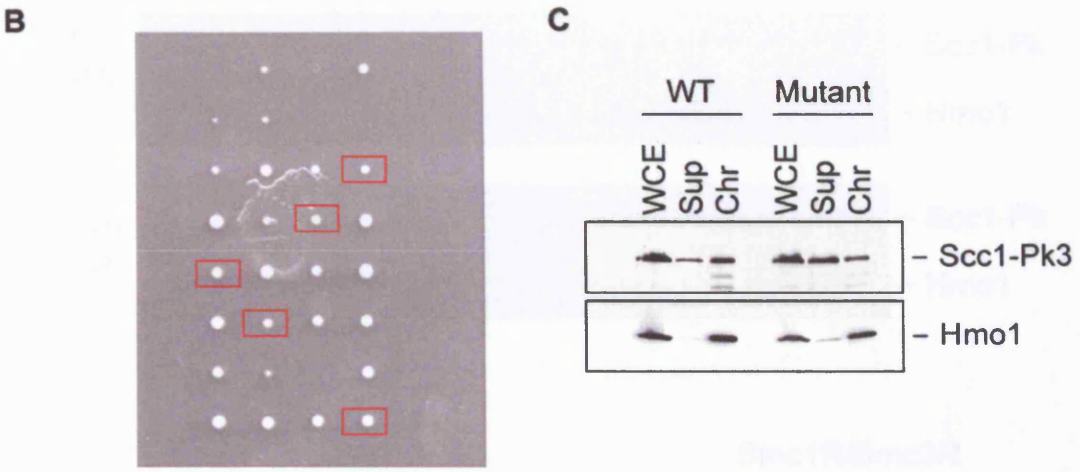

Figure 3.2 Arginine finger mutants in Smc1 or Smc3 complement the wild type protein

(**A**) Strains of Y6753 (*MATa smc1-259 TetOs::URA3 TetR-GFP::HIS3*), Y754 (as K6753 except *GAL-SMC1-Ha6::LEU2), Y2078* (as K6753 except *GAL-smc1R58A-Ha6::LEU2*), Y2043 (*MATa smc3-42 TetOs::URA3 TetR-GFP::HIS3*), Y2079 (as Y2043 except GAL-Ha9-SMC3) and Y2078 (as Y2043 except GAL-Ha9-*smc3R58A*) were streaked on YP-Raff/Gal plates at either 25°C or 37°C.

(**B**) Crossing of strains bearing single arginine finger mutants Y2185 (*MATα smc1R58A*) with Y2186 (*MATa smc3R58A*) yields spores bearing both mutant alleles (red boxes).

(**C**) Biochemical fractionation of Y2330 (*MATa smc1R58A smc3R58A SCC1-Pk3*) in a cycling population shows reduced chromatin levels of cohesin. WCE = whole cell extract, Sup = supernatent, Chr = chromatin. Hmo1 is used as a chromatin control.

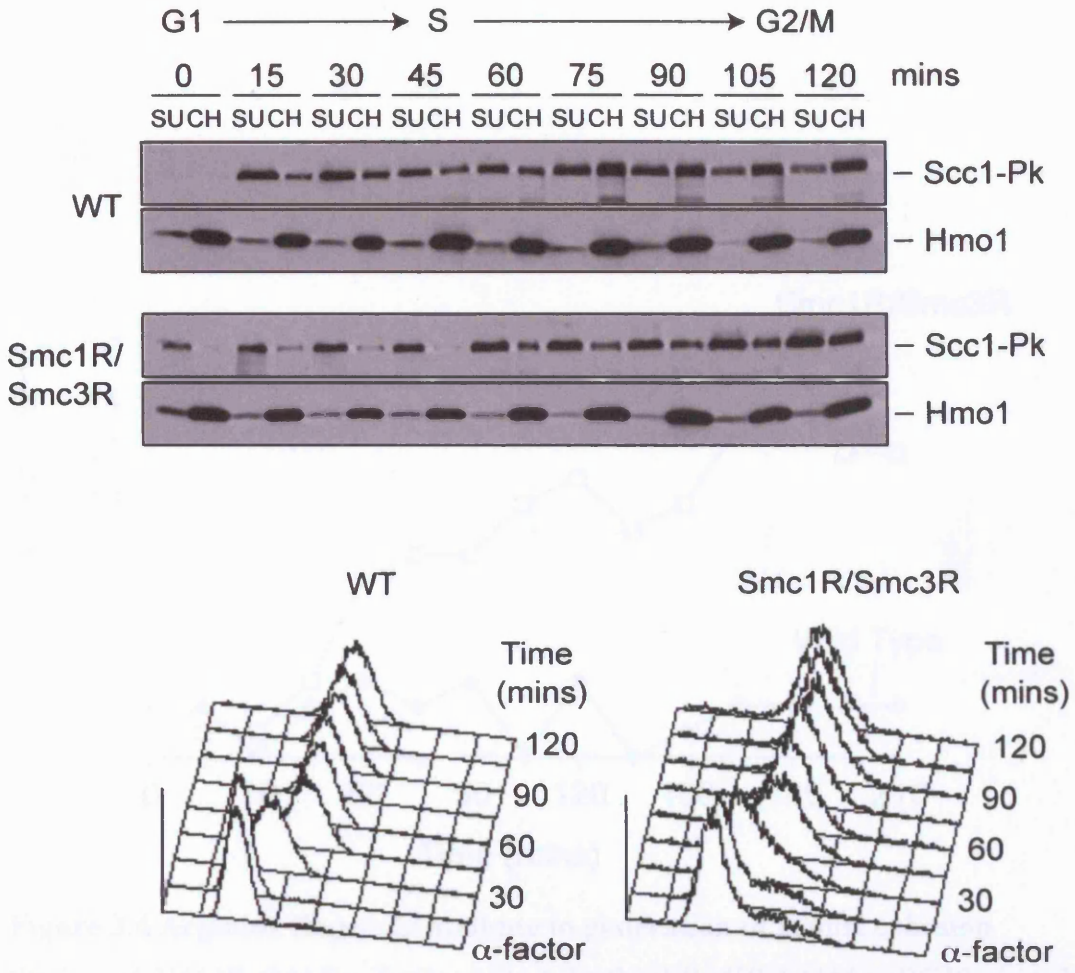

Figure 3.3 Cohesin's arginine fingers are important for binding to DNA

Strains of Y2329 (*MAT*a *Scc1-Pk3*) and Y2330 (as Y2329 except but *smc1R58A smc3R58A*) were arrested in G1 with α-factor at 25°C before being released into a G2/M block with nocodazole. Chromatin fractionation was performed at the indicated time points. Cell cycle progression was followed by FACS analysis of DNA content. SU = Supernatent, CH = chromatin.

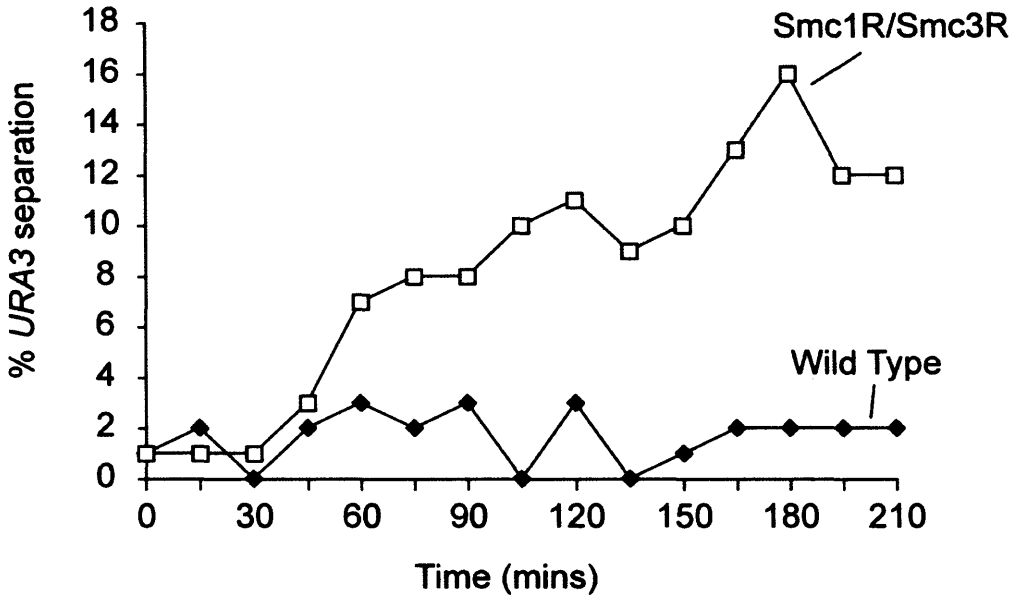

Figure 3.4 Arginine fingers contribute to generation of robust cohesion

Strains of Y1119 (MATa *TetOs::URA3 TetR-GFP::HIS3 GAL-CDC20::LEU2*) and Y2655 (as Y1119 except *smc1R58A smc3R58A*) were synchronised in G1 at 25°C with α-factor before being released into a Cdc20 block and GFP dot separation was analysed. Cell cycle progression was monitered by FACS analysis (not shown).

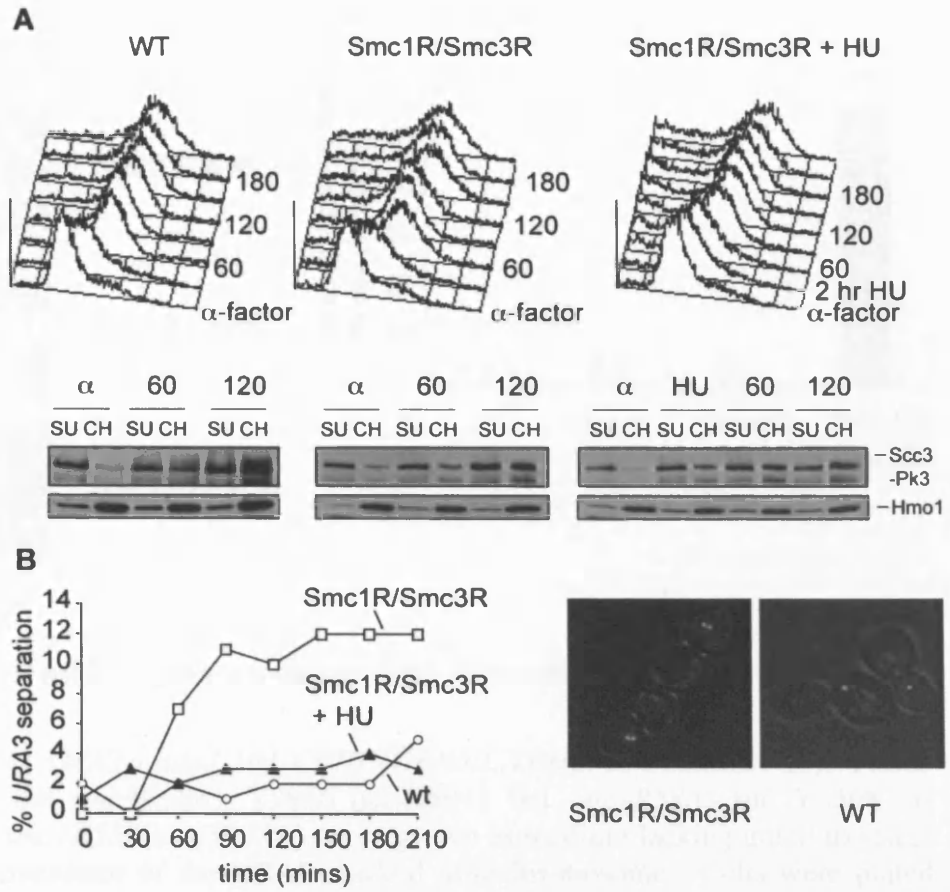

Figure 3.5 The cohesion defect due to arginine finger mutation is rescued by increasing the time for cohesin loading in G1

(**A**) Strains Y2738 *(MAT*a *GAL-CDC20 TetR-GFP::HIS3 TetOs::URA3 Scc3-Pk3*) and Y2739 (as Y2738 but *smc1R58A smc3R58A*) were released from synchronisation with α-factor into a metaphase block by Cdc20 depletion. Half of the culture was halted for 2 hours in an HU imposed arrest before being allowed to complete S-phase (time points of this culture are after release from HU). Chromatin fractionation shows enrichment of cohesin on chromatin in the mutant before release from the HU arrest. SU = Supernatent, CH = chromatin.
(**B**) The GFP-marked *URA3* locus was visualised to assess sister chromatid cohesion. Photographs show cells at 210 min.

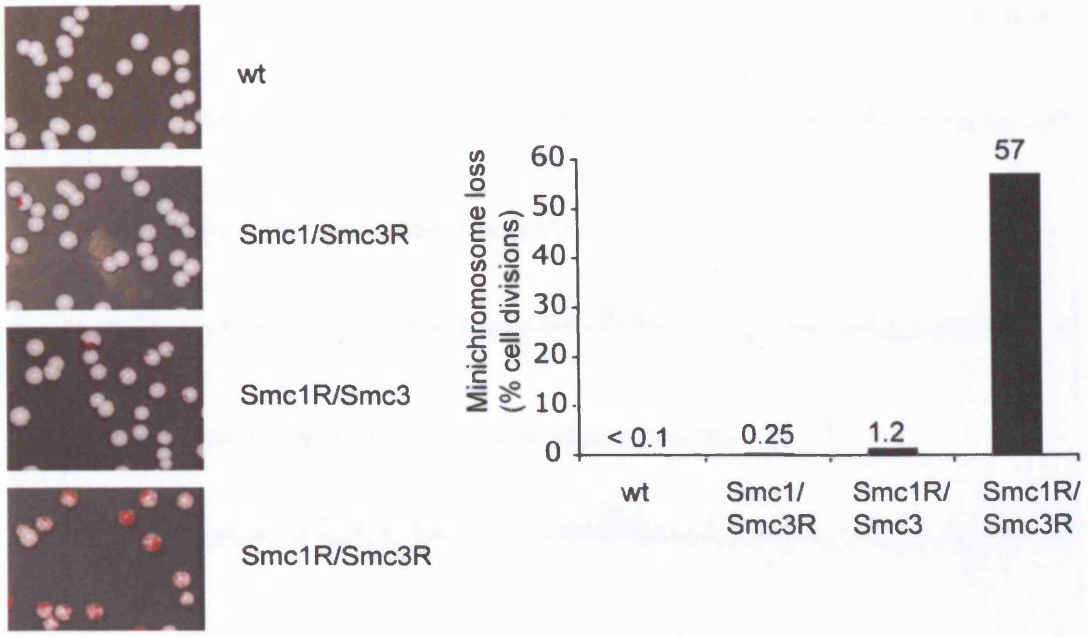

Figure 3.6 Double arginine mutants show elevated rates of minichromosome loss

Strain K5041 (*MATa ade2-101 CFIII (CEN3.L.YPH278) URA3SUP11*), Y2885 (as K5041 but *smc3R58A*), Y2886 (as K5041 but *smc1R58A*) and Y2368 (as K5041 but *smc1R58A smc3R58A*), were grown in medium lacking uracil to select for the maintenance of the URA3-marked minichromosome. Cells were plated on rich media to allow for spontaneous loss of the *SUP11* suppressor of the *ade2-101* mutation. Chromosome loss in the first division after plating was scored by the presence of equal or greater than half sectored colonies. The frequency of first cell division loss events was scored in >1500 colonies per strain.

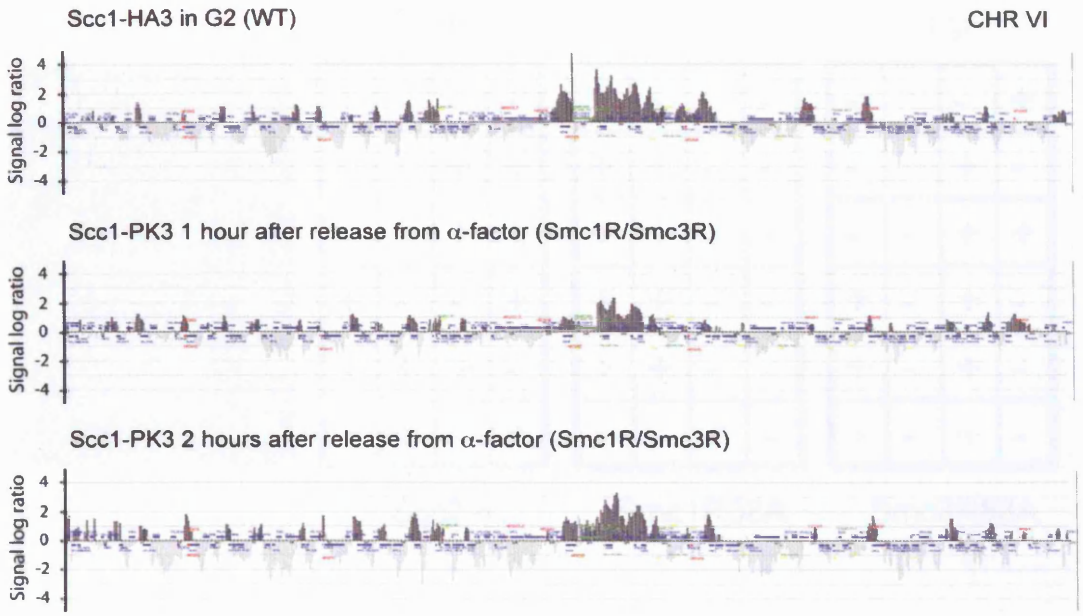

Figure 3.7 Arginine finger mutant cohesin binds to chromosome VI in a pattern similar to wild type cohesin

Cells of strain Y2330 (*MATa smc1R58A smc3R58A SCC1-Pk3*) was arrested in G1 with α-factor and released into medium containing nocodazole. Samples for chromatin immunoprecipitation were taken one and two hours after release. For comparison chromatin immunoprecipitation of SCC1-Ha3 in nocodazole arrested strain Y1569 (*MATa SCC1-Ha3*) is shown. The arginine fingers are not required for cohesin to reach its final association pattern along chromosome VI. Cell cycle progression was monitored by FACS analysis of DNA content (data not shown).

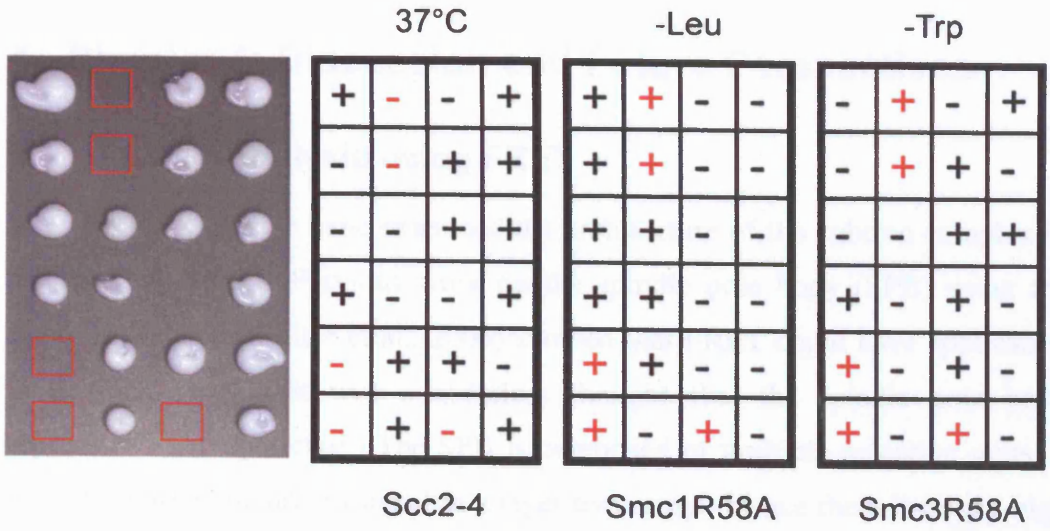

Figure 3.8 *Scc2-4* is synthetic lethal with *smc1R58A smc3R58A*

Strains of Y2266 (*MATa smc1R58A smc3R58A*) were crossed with K7244 (*MATα scc2-4 TetR-GFP::HIS3 TetOs::URA3*) and the resulting diploids were sporulated and dissected on YPD plates. The spores were analysed as being either *smc1R58A::LEU2 smc3R58A::TRP1* or *scc2-4* (dead at 37°C). Spores expected to carry all three mutant alleles are indicated in red boxes.

4 Chapter 4: Discussion and Future Perspectives

4.1 Cohesin analysis using FRET

In this thesis we have examined the architecture of the cohesin complex in live budding yeast. Previous work on the spindle pole body (SPB) using the same technology (Muller et al., 2005) showed that FRET could have application in budding yeast. It was nonetheless thought that the spindle pole body represented a unique case. The SPB is composed of multiple repeating units of the same core structure arranged in a repetitive array. Hence there is a very high local concentration of fluorophores. Here we have performed a very extensive analysis of a less abundant nuclear protein with a more uniform pattern in the yeast nucleus. This shows for the first time that FRET could have application for a whole host of complexes; for both those that form foci in cells e.g. DNA damage foci, transcription foci; as well as for less locally concentrated complexes such as septins, replication proteins or condensins.

Our results are consistent with many of the observations derived from biochemical characterisation of yeast cohesin (Haering et al., 2002; Weitzer et al., 2003; Arumugam et al., 2003). Scc3 can be mapped to the SMC heads of the cohesin complex, with its binding somewhat closer to the C-terminus of Scc1 than to the Scc1 N-terminus consistent with the biochemical results in insect cells (Haering et al., 2002). Scc1 similarly can be mapped around the heads of the cohesin complex, but with a somewhat different conformation than published models. Consistent with the finding that the SMC heads are constitutively together, we find Scc1 C-terminus juxtaposed between the Smc1 and Smc3 heads. The Scc1 N-terminus in turn is slightly closer to the Smc3 head than to Smc1 head. We also find robust intramolecular FRET occurring on Scc1, inconsistent with it adopting an extended conformation. Instead we propose that Scc1 sits in a groove between the Smc1 and Smc3 heads. Pds5 also co-immunoprecipitates with the *S. cerevisiae* cohesin complex in a salt sensitive manner as has been observed in human cells (Sumara et al., 2000) and in Xenopus extracts (Losada et al., 2005). Moreover we observe that Pds5 binding to the cohesin complex is Scc1 dependent. Pds5 failed to map around the heads

of the cohesin complex as might be expected based on the Scc1 dependency for binding. We instead find Pds5 at the distal side of the complex binding near the hinge domains.

What is the functional significance of Pds5 binding? Temperature sensitive alleles of Pds5 when inactivated in G2/M cells display major cohesion defects comparably to other core cohesin subunit mutants (Hartman et al., 2000; Panizza et al., 2000). Furthermore, Pds5 also localises to cohesin associated regions as determined by high density oligonucleotide arrays (Lengronne et al., 2004). We show here that Pds5 co-immunoprecipitates with the cohesin complex as is the case in higher eukaryotes. Hence Pds5 is likely a core component of the cohesin complex. Consistent with this are our findings that (1) Pds5 is stoichiometric with other cohesin components; (2) its localisation in the nucleus is comparable to other cohesin subunits and; (3) the relative amount of Pds5 on chromatin is comparable with other cohesin subunits. How does Pds5 function? It still remains enigmatic as to how Pds5 exerts its function at a molecular level. Still unclear is the role of the HEAT repeats within Pds5 that have been proposed to have a scaffolding function (Neuwald and Hirano, 2000). The role of sumoylation still is poorly understood (Stead et al., 2003). It had been shown previously that Scc1 was a critical determinant for Pds5 binding to chromatin. Repression of Scc1 attenuates Pds5 recruitment as well as other cohesin component recruitment to chromatin (Panizza et al., 2000). Here we have shown that even in soluble extracts, Scc1 is a prerequisite to enable Pds5 to bind to the holo cohesin complex. This result could be interpreted in at least two ways. The result is reminiscent of that of Scc3, which also requires Scc1 to bind to the cohesin complex (Haering et al., 2002). In this case no interaction between Scc3 and Smc1 or Smc3 can be detected in the absence of Scc1. Pds5 could therefore also bind proximal to the heads in an Scc1 dependent manner. Indeed this arrangement would be similar to the recent subunit arrangement of condensin, where both Cap-D2 and Cap-G interact with the holo condensin complex in a Kleisin/Cap-H dependent manner (Onn et al., 2007). We detected however only very low FRET between either N- or C-terminus Pds5 and any of the components around the Smc1 and Smc3 heads. The other interpretation of this result is that Scc1 induces a conformational change through the coiled coils of the cohesin

complex to enable Pds5 to bind to the hinge domains. The concept of a conformational change being transmitted through the coiled coils is not inconsistent with many published results. Rad50 for example undergoes a striking reorganisation in its coiled coils upon DNA binding (Moreno-Herrero et al., 2005). The transmembrane domains of MalK also undergo a tweezer like motion with repeated rounds of ATP binding and association (Chen et al., 2003). Bacterial SMC proteins also have the ability to modulate ATPase events at the heads via their hinge domains (Hirano and Hirano, 2006).

Another very important question, which we have addressed with respect to cohesin architecture, is the orientation of the heads relative to one another. Electron micrographs of *S. cerevisiae* Smc1 and Smc3 expressed in insect cells take on a variety of conformations. Amongst these are rings, open 'V' and 'Y' shaped complexes (Haering et al., 2002). From this one could be led to believe that cohesins exist within the cells in a variety of forms. Do cohesin complexes for example exist as 'open' complexes with the heads apart before transport onto DNA? From our analysis of both soluble and chromatin bound cohesin complexes by FRET we can most likely exclude such possible models. The Smc1 and Smc3 heads appear very proximal in cycling cells, as a function of the cell cycle, in anaphase and even when forced off chromatin by Scc1 C-terminus overexpression. This suggests that the spatial separation of the Smc1 and Smc3 heads does not change in a manner that is detectable by our assay. The idea of the cohesin complex existing in the same conformation while either bound to chromatin or free in the nucleoplasm is in agreement with the same hydrodynamic values that have been observed for both soluble or chromatin bound cohesin in budding yeast (Weitzer et al., 2003).

4.2 Conformational changes within the cohesin complex

Our analysis of key interactions within the cohesion complex throughout the cell cycle suggested that no major structural changes occur during the binding of cohesin to chromosomes or the establishment of sister chromatid cohesion during S-phase. This is based on constant FRET when comparing the diffuse nuclear cohesin pool and the nuclear foci enriched in chromosome bound

cohesin. It is also based on the analysis of FRET as a function of cell cycle progression. Cohesin binds to chromosomes about 15 minutes before S-phase, and any significant change to FRET in the course of cohesion establishment during DNA replication should have become detectable. Our results therefore draw the picture of cohesin as a relatively stable molecular machine, which may undergo conformational changes only on a transient basis.

The nature of any transient structural changes of the cohesin complex during binding to and dissociation from DNA is of great interest. Our measurements of population averages of cohesin in the yeast nucleus does not allow the detection of such transient changes. Any conformational change even if it lasted for a few seconds, long in the time scale of molecular reactions, would go undetected in our measurements. If the total population of cohesin underwent such a change with a synchrony of several minutes, only a few percent of all complexes would be present in an alternative conformation at any one time, an effect too small to be detectable with our technique.

In the future, two advances could allow such reactions to be studied. Ideally, FRET experiments with single molecules in reconstituted DNA binding reactions *in vitro* should allow a more detailed analysis of cohesin's behaviour. This approach is so far limited in that cohesin loading onto DNA in a purified *in vitro* system has not yet been successfully reconstituted. In the interim, it could become possible to take advantage of the genetic amenability of budding yeast to engineer situations in which cohesin accumulates in intermediates of loading or unloading reactions. This could involve the analysis of mutant cohesin complexes, or of the wild type complex in different mutant strain backgrounds. In an attempt to trap cohesin during DNA loading, we tried to analyse cohesin in yeast strains mutant for the cohesin loader Scc2/Scc4 (Ciosk et al., 2000; Lengronne et al., 2004). However, increased background fluorescence at the higher restrictive temperatures required to inactivate the cohesin loader prevented us from analysing these strains further. This obstacle could be overcome by the generation of cold sensitive mutant alleles. The analysis of mutations in cohesin subunits themselves, e.g. the ATPase motifs, poses a similar challenge. Mutant subunits that do not sustain cell viability have been studied after ectopic expression in addition to the wild type copy (Arumugam et al., 2003; Weitzer et

al., 2003). This means that FRET analysis would be limited to a corresponding subset of cohesin complexes with accordingly lower fluorescent and FRET signals. The introduction of more sensitive imaging equipment might open such possibilities in the future.

Our studies so far have shed new insight into the architecture of the cohesin complex *in vivo*, and its behaviour during the cell cycle. Future studies will continue to analyse the molecular action of cohesin, and that of related Smc protein complexes, to understand their mechanisms of action in chromosome structure and dynamics.

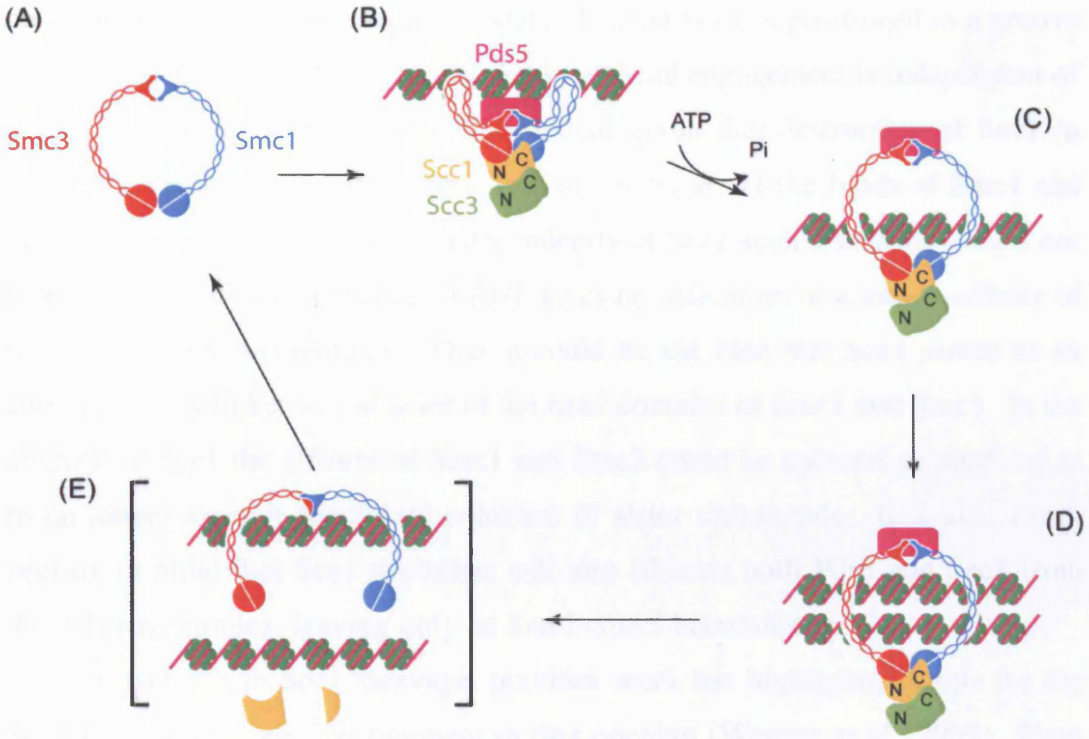

Figure 4.1 Proposed model of cohesin complex architecture and behaviour during the cohesin cycle

(A) Cohesin complexes exist as closed heterodimers in the nucleoplasm in G1 cells. (B) Upon Scc1 re-synthesis in late G1, cohesin complexes are assembled and loaded onto chromatin. Scc1 now facilitates both Pds5 and Scc3 binding to the cohesin complex This initial loading reaction may involve a head-hinge interaction as depicted. (C) Cohesin complexes are DNA bound before cohesion establishment. (D) Cohesion is established with repliaction fork pasage in S phase, now tethering two different DNA molecules. (E) Cohesin removal occurs via Scc1 cleavage. The transient nature of head opening is depicted by the presence of brackets.

4.3 DNA unloading of cohesin

Cohesin unloading from chromatin can proceed via at least two mechanisms as discussed in section 1.5.4. In budding yeast the majority of cohesin is removed at anaphase in an Scc1 cleavage dependent manner. Many current models depict Scc1 as a bridge between the Smc1 and Smc3 heads. This explains whereby cleavage of Scc1 at anaphase onset destroys the integrity of the ring and hence liberates the entrapped sister chromatids. Our results are however not consistent with such bridging models. Instead Scc1 is positioned in a groove between the Smc1 and Smc3 heads, and head-head engagement is independent of Scc1. This result seems at first paradoxical given that destruction of Scc1 in G2/M cells results in a catastrophic loss of cohesion. If the heads of Smc1 and Smc3 were binding one another independently of Scc1 such a scenario would not be predicted to occur. However, FRET gives no indication of a loss in affinity of two proteins for one another. Thus it could be the case that Scc1 serves as an additional crosslinker or stabiliser of the head domains of Smc1 and Smc3. In the absence of Scc1 the affinity of Smc1 and Smc3 could be reduced so much so as to no longer support functional cohesion of sister chromatids. It is also worth bearing in mind that Scc1 depletion will also liberate both Pds5 and Scc3 from the cohesin complex, leaving only an Smc1-Smc3 heterodimer.

In addition to Scc1 cleavage, previous work has highlighted a role for the Scc1 C-terminus cleavage fragment in ring opening (Weitzer et al., 2003). Here we have shown that Scc1 C-terminus overexpression results in the chromatin dissociation of cohesins. This fragment most likely leads to this effect by directly reducing the affinity of the SMC heads for one another. Despite the fact that cohesin were removed from chromatin under our experimental condition, we could not detect 'open' head intermediates by FRET. As discussed, this is probably due to the asynchronous temporal nature of this reaction.

4.4 Cohesin as a monomeric complex *in vivo*

Despite the presence of multiple lines of evidence that cohesin complexes exist as monomers in budding yeast, models whereby cohesin exists as a dimer still continue to champion the literature (Milutinovich and Koshland, 2003; Nasmyth and Haering, 2005; Losada, 2007; Huang et al., 2005). Experiments in diploid yeast strains with differentially tagged copies of the cohesin subunits Smc1, Smc3 failed to co-immunoprecipitate. Likewise, differentially tagged Scc1 or Scc3 fail to co-immunoprecipitate when co-expressed in insect cells (Haering et al., 2002). This suggests that cohesin complexes only contain one copy of each of these proteins and hence exists as a monomer. These experiments performed in yeast were done on both soluble and chromatin released cohesin fractions. It could nonetheless be argued that if dimeric cohesin complexes were to exist, it could be in the context of chromatin or DNA *in vivo*. Therefore it is conceivable that during the preparation of an extract such interactions could be destroyed, and this is the reason they cannot be observed using immunoprecipitation. Further evidence for the monomeric nature of cohesin comes from the observation that chromatin released cohesin or cohesin derived from a soluble fraction migrate on glycerol gradients and on gel filtration columns as a monomer (Weitzer et al., 2003).

Here we have addressed the presence of dimeric cohesin complexes in live cells. This offers the advantage of examining the potential for interactions between different cohesin complexes in their normal environment inside the cell. This eliminates the concerns that were raised earlier about the disruption of interactions between cohesin complexes using extraction techniques. We have found no evidence for interaction between the heads of the different cohesin complexes using differentially tagged FRET pairs on either Smc1 or Smc3 in diploid yeast strains. Furthermore, no evidence for dimerisation in a 'hinge to hinge' orientation can be observed. Lastly, tagging both the Smc1 head (at its C-terminus) and the hinge within the same protein also does not exhibit FRET. This likely excludes the possibility that cohesin complexes dimerise in a 'head to tail' fashion with the head of one complex binding to the hinge region of an adjacent complex. While this analysis is not an exhaustive investigation of all potential interaction sites between different cohesin complexes, it does nonetheless

severely limit the remaining possibilities of putative dimerisation models. Since we have examined the interaction between the 'functional' domains of the SMC protein of cohesin, namely the head and hinge domains, we reason that this is the most likely interaction site that could account for cohesin dimerisation. We cannot formally exclude for example, the possibility that cohesins dimerise via interaction along their coiled coils.

What are the implications of these results for current models of cohesin? These result are easily reconcilable with the so-called 'ring model' of cohesin (Haering et al., 2002; Gruber et al., 2003), whereby cohesin exists as a single ring topologically associated with DNA. What is the evidence for higher order association of other SMC containing protein complexes? The Smc5/6 complex was found to exist in a high molecular weight complex some time ago. The size of this complex is approximately 1.6 MDa and is stable in the presence of salt up to 0.7 M (Fousteri and Lehmann, 2000). The size of a monomeric complex would be approximately 585 KDa including the six non-SMC components of the complex. Bacterial SMC proteins too may exist in higher order structures, especially in the presence of DNA. The *B. subtilis* SMC protein has been shown using cross-linking experiments to be capable of forming protein aggregates in the presence of DNA which is further stimulated by ATP (Hirano et al., 2001). This could be due to direct protein-protein interactions in the context of DNA. Alternatively the condensation reaction of SMCs on DNA could bring separate protein complexes sufficiently close to be subsequently cross-linked. It is noteworthy however to point out that the *E. coli* SMC protein, MukB, forms homodimers and less often multimers. The holo complex, MukBEF, in contrast forms primarily multimeric structures (Matoba et al., 2005). The exact nature of interaction if any between condensin complexes has never been explicitly examined. It is however likely they multimerise given the high degree of co-operativity they exhibit in order to condense DNA (Strick et al., 2004).

Is there really any evidence that cohesin complexes may exist as dimers in yeast? Objectively, the current arguments in favour of dimerisation are not based on any good experimental evidence and are purely theoretical. Whilst condensin may well bind to DNA as a higher order fashion by merit of the fact that its binding to DNA is critically dependent on the stoichiometry of protein versus

DNA (Strick et al., 2004; Stray and Lindsley, 2003), such experiments have not been performed for cohesin. 'Evidence' for dimerisation includes the fact that cohesin associates with chromosomes in clusters (Blat and Kleckner, 1999; Tanaka et al., 1999; Laloraya et al., 2000; Lengronne et al., 2004; Glynn et al., 2004), one interpretation of which could be the existence of cohesin complexes as a filament or as stacks of 'snaps' (Huang et al., 2005). These clusters could of course be due to any number of other explanations. A quick mathematical calculation of the number of cohesin sites in the budding yeast genome is approximately 1357 (305 sites for chromosome III, IV, V and VI which are 2.696 Mb, (Lengronne et al., 2004), and linearly extrapolate this for the 12 Mb yeast genome). If we consider the finding that there are approximately 6000 cohesin complexes per haploid yeast genome (Weitzer et al., 2003), this study), this leaves approximately 4 cohesin complexes per cohesin site. The true value is probably even less given that not all cohesin complexes in the cell are chromatin bound. Since cohesin binding at CARs is in the range of 1-4 Kb bp of DNA (Lengronne et al., 2004), this assumes that 4 or less cohesin complexes are in sufficient proximity to 1-4 Kb of DNA to be cross linked in a ChIP experiment. This is indeed very possible if we consider the packing of DNA into nucleosomes in context of chromatin and this packing relative to the size of a cohesin complex. A recent crystal structure of a tetranucleosome provides a good starting point for this sort of comparison (Schalch et al., 2005). Here 167 bp of DNA wraps round a single nucleosome, which in turn tetramerises. The diameter of the tetranucleosome is 25 nm. If a chromatin fibre is assembled simply by stacking of this tetrameric core one on top of another as the authors propose, the resulting structure might adopt the structure indicated in figure 4.2. The fibre in figure 4.2 would contain 2672 bp of DNA (668 bp DNA per tetranucleosome, four tetranucleosomes shown) and is approximately 45 nm long. Hence it now becomes apparent that a single cohesin complex with a 35-40 nm diameter (Haering et al., 2002) could become cross linked to such a structure at many different sites where it would be in molecular proximity to the fibre. Thus it is reasonable to assume that approximately 4 cohesin complexes could occupy cohesin sites from 1-4 Kb. However we cannot assume that all cohesin sites are occupied in every cell.

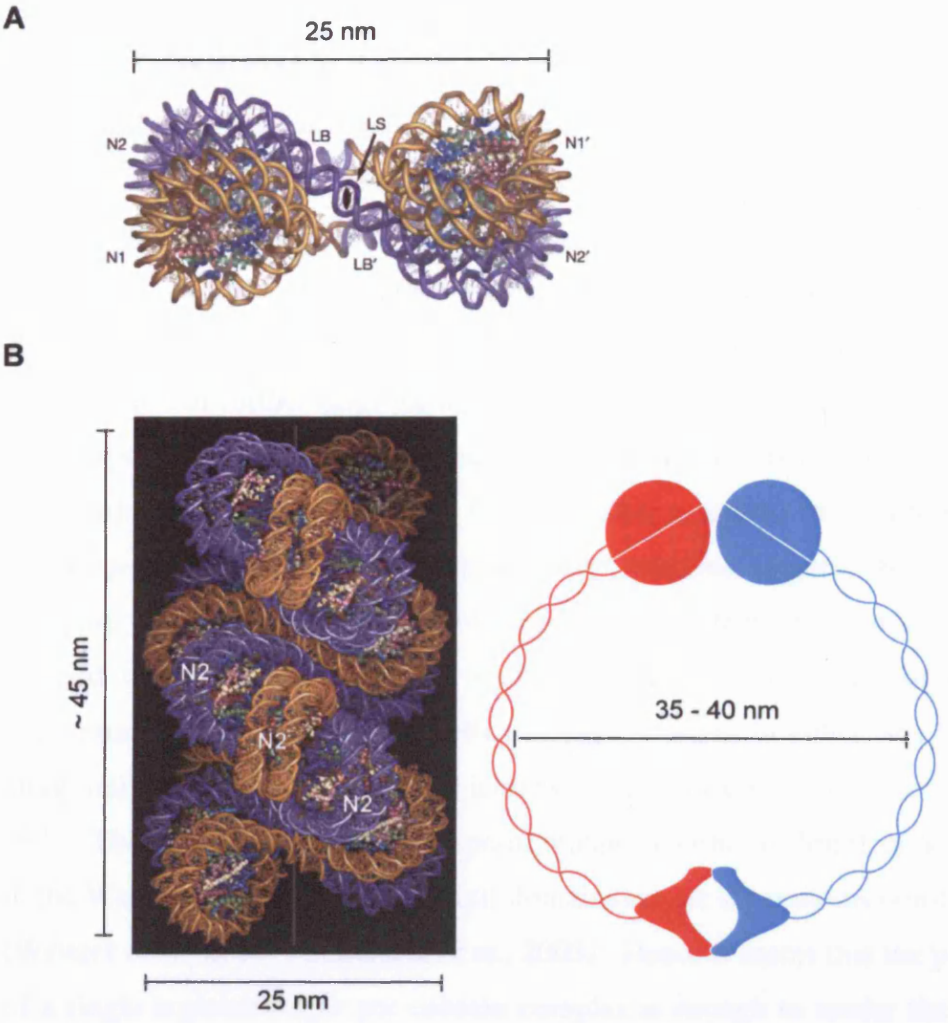

Figure 4.2 Proposed structure of a 30 nm chromatin fibre with respect to that of a cohesin complex

(A) Crystal structure of a tetranucleosome. Nucleosome 1 (N1) packs against N2, and N1' with N2' (from Schalch et al., 2005).
(B) Chromatin fibre models based on the packing of a tetranucleosome core. The fibre is that of a twisted ribbon structure with the tetranucleosome core stacking one on top of another. A schematic of a cohesin complex to scale is indicated.

4.5 ATP hydrolysis during the cohesin cycle

ATP hydrolysis is required for cohesin loading onto DNA in budding yeast (Arumugam et al., 2003; Weitzer et al., 2003). These studies demonstrated that ATPase mutants failed to complement the function of the wild type protein and could also not load onto DNA. However given that cohesin components are essential genes, and the ATPase mutants are not functional, this precluded the investigation of further roles for ATP hydrolysis during the cohesin cycle. Here we have shown using putative attenuated ATPase mutants in Smc1 and Smc3 that ATP hydrolysis is likely important for the loading reaction. In cells bearing both Smc1 and Smc3 mutated in their so called arginine fingers, the kinetics of cohesion loading onto chromatin from late G1 is substantially reduced compared to wild type cells. Predictably, these cells have massive rates of loss of a minichromosome. Interestingly cells bearing mutations in either Smc1 or Smc3 alone only display a very modest increase in chromosome loss over wild type cells. This is intriguing given that point mutant in either of Smc1 or Smc3 alone in the Walker A, Walker B or C-motif domains render the proteins non-functional (Weitzer et al., 2003; Arumugam et al., 2003). Hence it seems that the possession of a single arginine finger per cohesin complex is enough to render the complex largely functional with respect to ATP hydrolysis. We further show that the ATPase mutants can be rescued by allowing more time for cohesin loading before S phase (discussed below). Furthermore attenuated ATPase activities of cohesin seem not required to be required for its chromosomal positioning. This is consistent with the idea of cohesin as a topological entity around sister DNA molecules (Ivanov and Nasmyth, 2005); and with the fact that cohesin can be transported along DNA very rapidly in response to transcription (Lengronne et al., 2004; Glynn et al., 2004) despite the fact that it is seen as a relatively poor ATPase (Arumugam et al., 2006).

4.6 The mechanism of cohesin loading onto chromatin

A schematic depicting the loading reaction of cohesin onto DNA is presented in figure 4.1. In G1 cells, a time when Scc1 is still largely absent from

cells, cohesin complexes should only exist as heterodimers of Smc1 and Smc3. Scc3 and Pds5 should also be absent from this complex as they require Scc1 for complex formation. Upon Scc1 synthesis in late G1 both Pds5 and Scc3 are recruited to the cohesin complex. As part of the loading reaction the hinge may make a transient contact with head domains, potentially as part of a regulatory step of the ATPase cycle as is the case for the bacterial SMC proteins. Scc1 is key for the ATPase reaction, and indeed Smc1 and Smc3 possess negligible ATPase activity in the absence of Scc1 (Arumugam et al., 2006). Upon ATP hydrolysis cohesin complexes are transported onto DNA and await cohesion establishment as part of S phase. This establishment reaction is still probably the most mysterious part of the cohesin cycle and very little is known about the underlying mechanism. We find that the cohesion defect of a putative ATPase mutant with reduced kinetics of loading can be rescued by allowing more time for cohesin loading by means of a HU imposed early S phase arrest. This suggests that an additional round of cohesin loading (and hence ATP hydrolysis) is unlikely to be required during cohesion establishment during S phase. The observed rescue imposed by HU treatment is likely direct, and probably not due to non-specific effects of the drug. For example, cohesins are not ectopically recruited to stalled replication forks in HU imposed arrests (Lengronne et al., 2004), and even if they were this reaction would be predicted to require ATP hydrolysis which is required for all known association of cohesins with DNA (Weitzer et al., 2003; Arumugam et al., 2003).

We here make the assumption that the mutations introduced into budding yeast Smc1 and Smc3 diminish their ATPase activity as is the case for bacteria. We have not explicitly examined their ATPase activity *in vitro*. Nonetheless, what we have shown is that the cohesion defect of a 'slow-loader' version of cohesin can be rescued by allowing time to accumulate cohesin complexes on DNA before cohesion establishment. On the other hand if the cohesion defect could not be rescued by HU, it might indicate that new cohesin loading is required during cohesion establishment.

4.7 A unified model for SMC action on DNA?

Despite an overwhelming body of research on the mechanism of action of SMC proteins in the last decade, a unified model that would reconcile data obtained from all three complexes is still lacking. Will a unified picture on the mechanism of action ever be likely? Based on some very striking differences between the complexes this may indeed be unlikely. Bacteria contain but a single SMC complex that has to presumably deal with many aspects of DNA metabolism that is delegated to three different complexes in higher eukaryotes. Significant advances have been made on the understanding of the mechanism of action of bacterial SMC proteins through extensive biochemical characterisation of these proteins. These studies have proved very central to understanding SMC complexes in higher eukaryotes. Early studies for example, revealed the antiparallel nature of the coiled coils (Melby et al., 1998), the core residues involved in ATP binding and hydrolysis (Hirano et al., 2001) as well as the ability to aggregate DNA (Hirano and Hirano, 1998). It should however not be assumed that biochemical properties of the bacterial SMC are applicable to all three SMC containing complexes in higher eukaryotes. Below is mentioned some very fundamental differences between the different classes of SMC complexes.

A key requirement for the action of SMC complexes is their ability to hydrolyse ATP. This is true for bacterial SMC, cohesin and condensin. Since the Smc5/6 complex also contains Walker A, Walker B and C-Motif residues it is also reasonable to assume they too possess ATPase activity although this has not been explicitly addressed *in vitro*. There are however some marked differences in the requirement for ATP hydrolysis during the mechano chemical cycle of these different complexes. Cohesin for example absolutely requires ATP hydrolysis for all known association with DNA (Weitzer et al., 2003; Arumugam et al., 2003). Both condensin (Kimura and Hirano, 1997; Strick et al., 2004) and the bacterial SMC complex (Hirano and Hirano, 1998) however do not seem to require ATP hydrolysis for the initial DNA binding reaction. Instead they use ATP hydrolysis for the condensation reaction. ATPase mutations have been introduced into the Smc5/6 complex. Amazingly these mutants are viable but still exhibit sensitivity

to DNA damaging agents (Fousteri and Lehmann, 2000). These alleles thus seem to separate between the 'essential' and DNA damage roles of the Smc5/6 complex. Complex assembly in cohesin also depends on the ability of Smc1 to bind ATP (Weitzer et al., 2003; Arumugam et al., 2003) a requirement that is not true at least for condensin (Onn et al., 2007).

From a purely structural point of view, cohesin and condensin display very different overall conformations. Cohesin from EM studies is a ring shaped structure with open arms and significant flexibility at the hinge region. Condensin on the other hand is more closed or rigid at the hinge region and the coiled coils emanate from the hinge at smaller and less variable angles (Anderson et al., 2002). DNA binding studies also reveal differential requirement for DNA binding by different SMC complexes. Condensin and bacterial SMC complexes readily bind to DNA in *in vitro* assays. Cohesin's ability to bind to DNA *in vitro* is very poor (Kagansky et al., 2004; Losada and Hirano, 2001), and may not reflect the real topological association of cohesin with DNA that is likely to occur *in vivo* (Ivanov and Nasmyth, 2005). This poor DNA binding activity may instead reflect the requirement for additional regulators of the loading reaction for example Scc2/4 (Ciosk et al., 2000) without which *in vivo* cohesin likely gets stuck in an intermediate of the loading reaction at Scc2/4 sites (Lengronne et al., 2004). Ultimately, we may have to await a sophisticated *in vitro* system capable of reconstituting the loading and establishment reactions before really having a more complete understanding on the mechanism of cohesin action in the cell.

5 Chapter 5: Materials and Methods

5.1 Biochemistry

5.1.1 Immunoprecipitation

Immunoprecipitation reactions were performed on soluble yeast extracts as described previously (Liang and Stillman, 1997). 250 ml mid log phase culture (OD_{600} = 0.5) were pelleted at 3000 rpm for 10 minutes. Cell pellets were then resuspended in 5 ml PIPES/KOH buffer (100 mM PIPES/KOH pH 9.4, 10 mM DTT, 0.1% DTT) for 10 minutes at room temperature. Cells were then pelleted at 2000rpm for 2 minutes and resuspended in 5ml Kpi/Sorbitol buffer (50 mM K_2HPO_4/KH_2PO_4, 0.6 M Sorbitol, 10 mM DTT). The cells were then spheorblasted by the addition of Zymolase T-100 (MP Biomedicals) to a final concentration of 40 μg/ml for 10 minutes at 37°C. The cells were then collected by centrifugation (800 rpm for 5 minutes), washed with ice cold Spheroblast wash buffer (50 mM HEPES/KOH pH 7.5, 100 mM KCL, 2.5 mM $MgCL_2$, 0.4 M sorbitol), and subsequently resuspended in 450 ml ice-cold EB (50 mM HEPES/KOH pH 7.5, 100 mM KCL, 2.5 mM $MgCL_2$ 1 mM DTT) supplemented with protease inhibitors (1 mM PMSF, 2 μg/ml leupeptin, 2 μg/ml aprotinin, 2 μg/ml pepstatin, 200 μg/ml bacitracin, 2 mM benzamidine, plus complete mini-EDTA free protease inhibitor tablets from Roche. This cell suspension was now lysed by the addition of Triton-X-100 at 0.25% for 3 minutes while vortexing intermittingly. The cell lysate was now carefully layered onto a sucrose cushion of EBXS (EB, plus 30% sucrose) and centrifuged at 4°C for 10 minutes at 12,000 rpm to separate soluble and insoluble fractions. After centrifugation, the soluble extract is seen as the upper yellow layer above the sucrose. This soluble extract is removed for subsequent immunoprecipitation reactions.

The extract is first pre-cleared to prevent non-specific protein binding by the addition of 1/10 volume of Protein-A-sepharose (Sigma) to the extract for 30 minutes on a rotating wheel at 4°C. After centrifugation (800 rpm for 1 minute) the lysate was removed and incubated with either anti-PK (Serotec), anti-myc

(ICRF, 9E10) or HA (ICRF, 12CA5) at concentrations of 1:450, 1:180 and 1:450 respectively. After incubation on ice for 1 hour, Protein-A-Sepharose was added to a final concentration of 1/40 the extract for 30 minutes on a rotating wheel at 4°C. The antibody-coupled beads were then washed 8 times with EBX containing protease inhibitors and 1 mg/ml BSA. The immunoprecipitated proteins were then eluted with 2xSDS loading buffer and analysed by western blotting.

5.1.2 Chromatin fractionation

To analyse protein binding to chromatin, lysates were prepared in the same way as for immunoprecipitation reactions as described in the previous section with a few exceptions. After the separation of the soluble from insoluble material on the sucrose cushion, the soluble extract on the top layer was now aspirated. The remaining chromatin pellet was resuspended in 500 µl EBX. An aliquot of this material was then added to an equal volume of 2x SDS loading buffer for western blotting. As controls for chromatin bound and soluble proteins we used antibodies against Hmo1 (a gift from S. brill) and PSTAIRE (Santa Cruz) respectively.

5.1.3 Protein purification from bacteria

Constructs for expression were cloned into pGEX-KG expression vectors. These constructs were then transformed into BL21 codon plus *E. coli* strains. Cells were grown in L-broth (10 g/L Bacto-Tryptone, 5 g/L Yeast extract, 170 mM NaCl). Protein expression was induced by the addition of 0.1 mM IPTG at 18°C overnight. Cells were harvested by centrifugation (3,000 rpm for 5 minutes). The pellet was then resuspended in 5 – 10 volumes of extraction buffer (50 mM Tris-HCL, pH 8.0, 100 mM NaCl, 0.1% tween 20 and 1 mM PMSF). The cells were then broken by sonication (Sanyo Soniprep 150) on ice using three rounds of 1 minute at 15 microns or until the cells loos their viscosity. A soluble extract was recovered after centrifugation at 17,000 rpm for 30 minutes at 4°C. A loopful of the pellet was then resuspended in 1 ml 6 M Urea, sonicated, and boiled with an equal volume of 2xSDS loading buffer. This represents insoluble proteins. For recovery of hexa-histidine tagged proteins, the extract was

incubated with Ni-NTA beads (Qiagen) pre-equilibrated with extraction buffer. After binding for 2 hours at 4°C on a rotating wheel the beads were washed with 100 volumes of extraction buffer. Proteins were eluted from the beads with extraction buffer spiked with 100mM Imidazole (Sigma).

For the purification of GST tagged proteins, the soluble extract was incubated with pre-equilibrated glutathione-sepharose beads (Amersham). Proteins were eluted with extraction buffer containing 50mM glutathione (Sigma) at 15°C for 10 minutes.

5.1.4 Chromatin Immunoprecipitation followed by hybridization to a high density oligonucleotide array

100 ml log phase culture (OD_{600} = 0.3 – 0.4) cells grown in YPD medium were fixed by the addition of formaldehyde to a final concentration of 1% v/v overnight on a rotating wheel at 4°C. The cell pellets were then washed in ice-cold TBS (200 mM Tris-HCL pH 7.5, 1.5 M NaCl) before transfer to 1.6 ml lysis buffer (50 mM HEPES-KOH, pH 7.5, 140 mM NaCl, 1 mM EDTA, 1% triton-X-100, 0.1% Na-deoxycholate, 1 mM PMSF). The cells were then broken on a multi-bead shocker (MB400U, Yasui Kikai, Osaka, Japan), which was able to keep the extract below 6°C. This soluble extract was now sonicated (Sanyo, Soniprep 150) to obtain DNA fragments of between 400 bp-600 bp. The extract was then incubated with PK (clone SV5-Pk1, Serotec) coupled Protein-A Dyna beads (Dynal) on a rotating wheel at 4°C for 5 hours. The presence of immunoprecipitated protein was confirmed by western blotting. After washing the beads with lysis buffer, the immunoprecipitates were eluted using elution buffer (50 mM Tris-HCL pH 8.0, 10 mM EDTA, 1% SDS) at 65°C for 10 minutes. To one volume of the eluate was now added three volumes of TES (10 mM Tris-HCL, pH 8.0, 1 mM EDTA, 1% SDS) and this mixture was incubated overnight at 65°C to reverse the crosslinks. The immunoprecipitate was incubated with Proteinase K to remove proteins as follows: to 160 µl of the reaction was added 140 µl TE pH 8.0, 3µl Glycogen (10 mg/ml) and 7.5 µl Proteinase K (20 mg/ml). This mixture was then incubated at 37°C for two hours. The DNA was then extracted two times using phenol/chloroform/isamylalcohol, and subsequently ethanol precipitated, dried in

a speed-vac (Savant) and diluted in a final volume of 30 µl TE. This sample was then treated with RNAse A (0.3 µg/µl) at 37°C for 1 hour to remove any contaminating RNA before amplification. The DNA was now further purified over QIAprep spin columns (Qiagen). The volume was reduced by a further round of ethanol precipitation, dried, and resuspended in a final volume of 10 µl. This DNA was amplified by PCR after random priming (Iyer et al., 2001). Approximately 10 µg of amplified DNA was digested with DNAseI to an average size of 100 bp. After DNAseI inactivation at 95°C these DNA fragments were subsequently end-labelled with biotin-N6-ddATP as previously described (Winzeler et al., 1998). Each sample was prepared in a 150 µl reaction containing 6xSSPE, 0.005% triton-X-100, 15 µg denatured salmon sperm DNA (Gibco-BRL), and 1 nmole control oligo B2 that hybridises to specific border regions of the CHiP to facilitate alignment. The samples were boiled at 100°C for 10 minutes before cooling on ice and hybridisation to the microarray in a hybridisation oven (GeneChip hybri oven 320, Affymetrix, CA) at 42°C for 16 hours. Washing and scanning procedures were performed automatically on the affymetric fluidics station (GeneChip fluidics station 400, Affymetrix). Scanning of the microarray was carried out on a HP GeneAray Scanner (Affymetrix).

The chromosome VI CHIP was produced by the Affymetrix custom express service (rikDAF, P/N 510636, Affymetrix). Briefly the CHIP contains sixteen 25mer probes per every 300 bp. To distinguish between positive and negative signals we compared the CHiP fraction a 'SUP' sample representing whole genome DNA, using the criteria as set out in (Katou et al., 2003).

5.1.5 Preparation of yeast extracts

Yeast extracts were prepared according to the NaOH method of Kushnirov, 2000. 10 ml mid log phase culture (OD_{600} = 0.25) was pelleted at 3,000 rpm for 5 minutes. The cell pellets were then washed in 1ml monoQ water before resuspension in 100 µl water. 100 µl 0.2M NaOH was then added to the cell suspension and incubated at room temperature for 2 minutes. The cells were then pelleted at 13,000 rpm for 1 minute and resuspended in 50 µl 2x SDS buffer (100 mM Tris-HCL pH 6.8, 200 mM DTT, 4% SDS, 0.2% bromophenol blue,

20% glycerol) and then boiled at 95°C for 5 minutes. 5-10 µl were then loaded on an SDS-polyacrylamide gel for western blot analysis.

5.1.6 SDS-PAGE electrophoresis and western blotting

Protein samples were resolved on acrylamide/bis-acrylamide (37.5:1, amresco) 375 mM Tris-HCL pH 8.8 and 0.1% SDS. Small proteins of less than 30 kDa were typically resolved on 10% -12% and larger proteins over 100 kDa on 6% -8% gels. A stacking gel was used on top of the separating gel and was composed of 125 mM Tris-HCL pH 6.8, 5% bis-acrylamide and 0.1% SDS.

Proteins were allowed to migrate through the stacking gel at 60 volts and through the separating gel at 110 volts using SDS-PAGE running buffer (25 mM Tris, 250 mM glycine and 0.1% SDS) in electrophoresis tanks from CBS scientific, CA. To monitor the position of the proteins in the gel and subsequently on the membrane, a broad range pre-stained protein marker (New England Biolabs) was used.

Separated protein bands were now transferred onto pre-equilibrated nitrocellulose membranes (Schleicher & Schuell) using either a semi-dry transfer apparatus (Hoefer) or a wet-transfer tank (Biorad). Semi dry transfer buffer contained 14.4 g/L glycine, 3 g/L Tris base, 0.02% SDS and 10% v/v methanol. Wet transfer buffer contained 3.03 g/L Tris base, 14.1 g/L glycine, 0.05% SDS and 20% v/v methanol. Semi-dry transfer was performed at 1.2 mA/cm^2 for 3 hours. Transfer was carried out at 5.3 mA/cm^2 for 40 minutes for the wet transfer protocol. The efficiency of transfer was then checked with ponceau S solution (Sigma). The membrane was then blocked with a 1% skimmed milk solution (Marvel) in PBST (170 mM NaCl, 3 mM KCL, 10 mM Na_2HPO_4, 2 mM KH_2PO_4, 0.01% tween 20) for 1 hour at room temperature. Membranes were then incubated with primary antibodies diluted in PBST containing 5% milk for one hour at room temperature. The concentration of antisera used were as following: anti-HA (12CA5, ICRF 1:5000), anti-myc (9E10, ICRF, 1:2000), anti-PK (Serotec, 1:5000), anti-Hmo1 (From S. Brill, 1:2000), anti-PSTAIRE (Santa Cruz, 1:1000), anti-FLAG (Sigma, M2, 1:1000) and anti-tubulin (Sigma, YOL1/34, 1:1000). Membranes were then washed in an excess of PBST three times for ten minutes. Horseradish peroxidase (HRP) coupled secondary

antibodies (anti-mouse or anti-rabbit, Amersham, 1:5000) were then incubated with the membrane in PBST containing 5% milk for a further hour. Membranes were washed a further three times as before developing with ECL (Amersham) according to the manufacturer's instructions.

5.1.7 Comassie blue staining

Proteins resolved by SDS-PAGE were comassie stained using the Phast-blue system (Amersham Biosciences) according to the manufacturers instructions. After staining the gel was destained using destain solution (20% v/v methanol, 1% v/v acetic acid).

5.2 Molecular Biology

5.2.1 Polymerase chain reaction

5.2.1.1 C-terminal tagging

Epitope tagging of endogenous genes was performed by gene targeting using polymerase chain reaction (PCR) products (Knop et al., 1999). Forward primers contain approximately 50 bp of homology to the 3' end of the gene of interest before the STOP codon. This is followed by 18mer homologous sequence to the vector used for tagging. The reverse primer again contains sequence homologous to 3'UTR region of the gene, followed by sequence to facilitate priming to the vector. The subsequent PCR product contains flanking regions homologous to the gene of interest, thus targeting the epitope containing cassette for in-frame fusion with the desired gene. Transformants were subsequently selected on plates either using Geneticin G418 resistance (in the case of KanMX4), or by using auxotrophic markers. In the case of auxotrophic markers, these are derived from either *K. lactis* or *S. pombe* to minimize the chance of integration at the marker locus. Vectors used for one step tagging are listed in section 5.6.

The PCR reaction was set up as follows:

Template DNA	5-10 ng

Forward primer	0.5 μM
Reverse primer	0.5 μM
dNTP (each of four)	100 μM
10x Expand high fidelity buffer (Roche)	5 μl
Expand high fidelity Taq	3.5 Units
dH_20 up to 50μl	

The PCR reaction was then performed on a Peltier Thermal Cycler (MJ Research) using the following programme:

1 x Cycle	2 min at 95°C
20 x Cycle	30 sec at 95°C
	2 min at 50-60°C (depending on the T_M of the primer)
	2 min at 72°C
1 x Cycle	7 min at 72°C

After completion of the cycle, the PCR products were first checked on agarose gel electrophoresis and then ethanol precipitated. To precipitate the DNA, 1/10 volume of 3 M sodium acetate was added, vortexed briefly, followed by the addition of 2 volumes of 100% ethanol. This mix was then incubated on ice for 1 hour. The DNA was then pelleted at 13,000 rpm for 15 mins before washing with 70% ethanol and drying in a speed vac. The resulting pellet was then resuspended in 15 μl dH_20 for transformation to yeast.

5.2.1.2 N-terminal tagging

N-terminal tagging was performed as described in (Prein et al., 2000). The N-terminal tagging cassette is constructed with a marker gene followed by an epitope tag. The forward primer contains sequence homology to the 3' end of the promoter region of the gene of interest. The reverse primer contains homologous sequences to the 5' end of the gene. The integration of this cassette disrupts expression of the gene, due to the presence of a marker between the promoter and the gene. Thus for essential genes, this must be carried our in diploid yeast

strains. In this case only one copy of the gene is replaced. The marker is flanked by *LoxP* sites on either side, which can be removed from the genome by the expression of the site-specific Cre recombinase. This is achieved by the transformation of the diploid with a centromeric plasmid containing Cre under the control of the *GAL1* promoter. Plating of cells on YP plates supplemented with raffinose and galactose results in efficient removal of the *LoxP* flanked marker. This restores the expression of the tagged gene. Hence, the diploid can now be sporulated to yield haploid spores containing N-terminally tagged genes. Note that this allele does not now have a marker associated with it.

5.2.2 Restriction digest and dephosphorylation of plasmid DNA

Restriction digests were performed using New England Biolabs enzymes and buffers according to the manufactures instructions. Typically approximately 1 – 2 μg of plasmid DNA was digested in a 50 μl reaction for 1 hour at the appropriate temperature for digestion.

To prevent the re-ligation of plasmid DNA, 5' phosphates were removed from plasmid DNA by treatment with Calf Intestinal Phosphatase (CIP, New England Biolabs) according to the manufacturers instructions. This was carried out immediately after the restriction reaction.

5.2.3 Agarose gel electrophoresis

Agarose gels were prepared by the addition of 1-2% w/v agar (depending on the size of the DNA) in 1 x TAE buffer (40 mM Tris base pH 7.5, 2 mM EDTA and 0.115% v/v acetic acid). After boiling and cooling to below 60°C, ethidium bromide was added to a final concentration of 0.5 μg/ml. 6 x DNA loading buffer (0.25% w/v bromophenol blue, 0.25% xylene cyanol FF and 30% v/v glycerol) was added to DNA samples before loading. DNA gels were run at between 1 -5 volts/cm (distance between electrodes) in electrophoresis tanks from anachem biosciences. The position of the DNA within the gel was monitored by running a DNA marker (novagene) sample in parallel. DNA fragments were visualised under a UV transilluminator (BioDoc-It).

5.2.4 Retrieval of DNA fragments from agarose gels

After resolving DNA bands by electrophoresis, bands of interest were excised from the gel using a scalpel. DNA was recovered from these bands using a Qiagen gel extraction kit according to the manufacturers instructions.

5.2.5 DNA ligation reactions

After the quantification of the recovered DNA, ligation reactions were performed. The following formula was used to determine the relative amounts of vector and insert to include in the ligation reaction:

$$Mass_{\text{insert}} = \frac{Base_{\text{insert}}}{Base_{\text{vector}}} \times 3 \times Mass_{\text{vector}}$$

The ligation reaction was set up as follow:

Approximately 50 ng of vector DNA
3x molar excess of insert
800 U T4 DNA ligase (New England Biolabs)
5 µl 10 x T4 DNA ligase buffer (New England Biolabs)
dH20 up to 50 µl

Ligation reactions were performed at 16°C overnight or at room temperature for 2-3 hours. After ligation, 25 µl of this reaction was transformed into 100 µl chemically competent *E. coli* (DH5α) cells.

5.2.6 Transformation of E. coli with plasmid DNA

Chemically competent cells were prepared as follows: DH5α cells were streaked on TY agar (1% w/v Bacto-Tryptone, 1% w/v yeast extract and 85 mM NaCl) plates overnight at 37°C. A single colony was then inoculated into 40 ml L- broth (10% w/v Bacto-Tryptone, 5% w/v yeast extract and 170 mM NaCl) at 37°C overnight. 2 ml of this overnight culture was then used to inoculate a

further 200 ml of L-broth pre-warmed to 18°C, and was grown with vigorous shaking until OD_{600} = 0.5. The culture was then cooled on ice and pelleted at 5,000 rpm for 10 mins using a JA14 rotor. The pellet was then resuspended in 40 ml ice cold TFB I (30 mM $C_2H_3O_2K$, 100 mM RbCl, 10 mM $CaCl_2$, 50 mM $MnCl_2$ ad 15% v/v glycerol) and incubated on ice for 30 mins. The cells were then centrifuged at 5,000 rpm for 10 mins and the resulting pellet resuspended in 8 ml TFB II (10 mM PIPES/KOH, 10 mM RbCl, 75 mM $CaCl_2$ and 15% v/v glycerol) for 15 minutes on ice. Aliquots of cells were then aliquoted and snap frozen in liquid nitrogen and placed at -80°C for long-term storage.

E. coli cells were transformed by the addition of 25 µl of the ligation reaction to 100 µl of bacteria on ice. After incubation on ice for 30 minutes, the cells were heat shocked for 2 minutes at 42°C, followed by an additional 2 minutes on ice. The cells were allowed to recover by the addition of 1 ml LB (10 % w/v Bacto-Tyyptone, 5 % w/v Yeast extract and 170 mM NaCl), before plating on LB agar plates (LB plus 1.5% w/v agar) supplemented with ampicillin at 100 µg/ml. Plates were incubated at 37°C overnight. The resulting colonies were inoculated into 5 ml LB-AMP overnight at 37°C and DNA was extracted from the pellets using Qiagen miniprep kits as described below.

5.2.7 Isolation of plasmid DNA from E. coli

Plasmid DNA was recovered from bacterial pellets using Qiagen miniprep kits according to the manufacturers instructions. The principle of the technique is the alkaline lysis of the bacteria followed by DNA adsorption onto a silica matrix in the presence of high salt. After washing the column with ethanol, the DNA was eluted in TE (10 mM Tris, 1 mM EDTA pH 8).

5.2.8 Generation of a fluorophore conjugated Smc1 hinge

The rationale behind choosing the position of the insertion is discussed in section 1.7.2. To construct a one step replacement vector, a targeting vector was designed as follows. The 472 bp Smc1 promoter up to ARS 603.5 was cloned from a genomic clone as an Nde I/Xma I PCR fragment into YIplac 128 (fragment 1). The *Smc1* open reading frame until proline^{600} was cloned using PCR as an Xma I/Sal I fragment (fragment 2) downstream of fragment 1 and fused to a

Sal I/Sph I fragment encoding the remainder of Smc1 (Fragment 3). Next we inserted into the Sal I site a PCR-amplified YFP (or CFP) flanked by linker peptides of the sequence VDGSTG on both sites (fragment 4). Finally an additional 470 bp sequence upstream of the *Smc1* promoter fragment (fragment 5) was amplified but cloned behind the *Smc1* open reading frame using Sph I and Nla III. This construct was linearised with Sph1 for integration at the Smc1 locus (see figure 5.1).

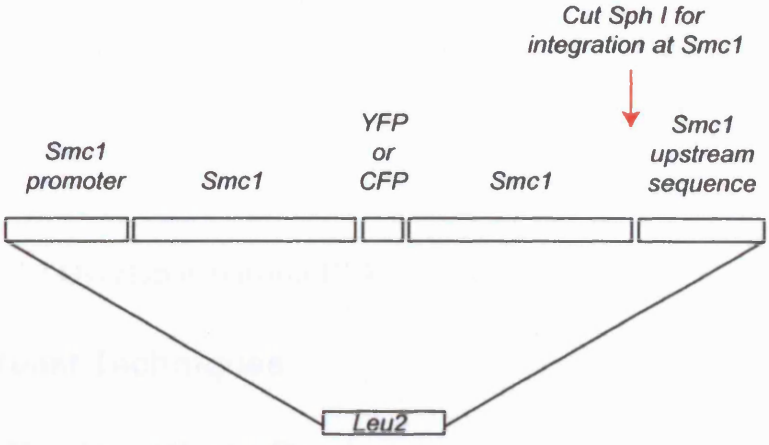

Figure 5.1 One step replacement construct for a fluorophore conjugated SMC1 hinge

5.2.9 Generation of point mutants in Smc1 and Smc3

Point mutations were introduced into Smc1 and Smc3 by overlap extension PCR. To do this, two sets of PCR primers were used. In the first set, the forward primer is located upstream of the intended site of mutation and contains a restriction site to facilitate subsequent cloning. The reverse primer contains the mutation and extends 15 nucleotides on either side of the mutation. The second set is similarly designed with forward primer again harbouring the same mutation in the middle of the primer, and the reverse primer located downstream of the mutation, and containing a restriction site. After running each of these two PCR reactions separately, a small volume of each is mixed, and used as a template, this time using only the upstream and downstream primers for amplification. The PCR product generated in this way was subject to restriction digest and cloning as

described. The successful replacement of the wild type sequence with the point mutant was confirmed by DNA sequencing.

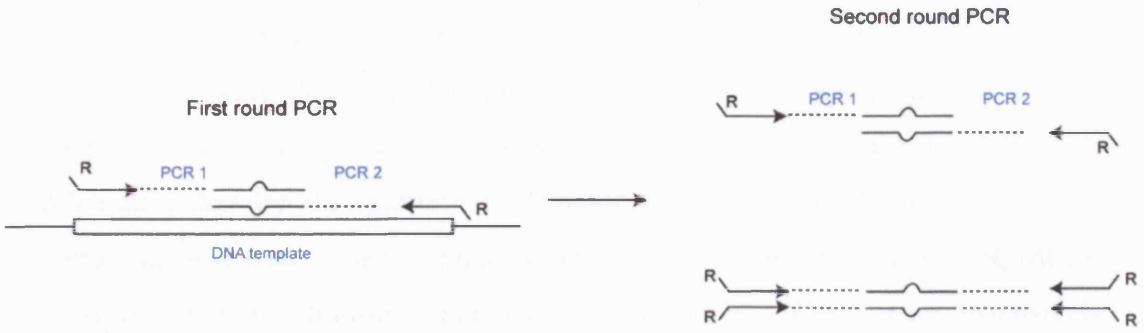

Figure 5.2 Overlap extension PCR

5.3 Yeast Techniques

5.3.1 Yeast growth conditions

Diploid cells were used for FRET experiments and haploids for all other applications. Cells were grown in YP (1.1% w/v yeast extract, 2.2% w/v bacto-peptone and 0.0055 % w/v adenine-HCL) supplemented with 2% w/v glucose (YP-Glu) or 2% w/v raffinose/galactose (YP-Raff/Gal). For growth of strains containing Cdc20 under the control of the methionine repressible *MET3* promoter, cells were grown in synthetic YNB media (Yeast Nitrogen Base: 0.8% w/v yeast nitrogen base, and 60μg/ml of each of the following amino acids: tyrosine, uracil, tryptophan, leucine, adenine, histidine, isoleucine and phenylanine, 3 μg/ml arginine, 4 μg/ml lysine and 5 μg/ml threonine) supplemented with either 2% w/v glucose or 2% w/v raffinose/galactose. For the selection of transformants, YNB agar plates (as per YNB except 2.2% w/v agar) were used lacking the auxotrophic amino acid used for selection. Cells were sporulated on sporulation media (100 mM CH_3COONa, 20 mM NaCl, 25 mM KCl, 1.5 mM $MgSO_4$ and 1.5% w/v agar).

5.3.2 Cell synchronisation

Yeast cells were arrested in G1 with the mating pheremone α-factor. To arrest cells, an early log phase culture (OD_{600} = 0.1) was treated with α -factor (provided by peptide services, Cancer Research UK) at a concentration of 2.5 μg/ml. One and two hours later another 1.8 μg/ml and 1.25 μg/ml of α -factor were added. Arrests were generally complete after two generation times. Cell cycle arrest were determined both cytologically by the appearance of a pear-shaped 'Schmoo' and by FACS analysis of DNA content. G1 arrested cells were released either by the addition of Pronase (50 μg/ml) or by filtration. For filtration, cells were collected on a membrane filter (Schlechter & Schuel, ME28, 1.2μm) using a filtration apparatus from Milipore. Cells were extensively washed with YP before release into YP media supplemented with sugar. For the collection of equal amount of cells post G1 release for chromatin fractionation, the culture was subjected to mild sonication conditions to eliminate clumping of schmooing G1 cells.

For arrest in metaphase, nocodazole (Sigma) was added at 5 μg/ml. Arrests were assessed cytologically by the presence of large budded cells. For arrest using Gal-Cdc20, cells were cultured in media containing 2% raffinose and 2% galactose before being filtered, washed and transfered to media containing only raffinose. For arrest using the repression of *MET3*-Cdc20, cells were grown in YNB supplemented with 2% glucose. To arrest cells, 2% methionine was added. Cell cycle arrests were gain checked cytologically and by DNA content.

Early S phase arrests were performed by the addition of Hydroxyurea (HU, sigma), a ribonucleotide reductase inhibitor, at 200 mM. The presence of small buds indicates S phase arrest.

5.3.3 Protein overexpression and repression from the GAL1 promoter

For overexpression of proteins from the *GAL1* promoter, cells were grown in YP supplemented with 2% raffinose (Sigma) until mid log phase and protein expression was induced by the addition of 2% galactose (Sigma) for 2- 3 hours.

For protein repression (e.g. Scc1 or Cdc20) cultures were grown in YP containing both 2% galactose and 2% raffinose. To repress expression, the culture was filtered, extensively washed with YP, and transferred to YP media

containing raffinose as the sole sugar source. Protein expression was checked by western blotting.

5.3.4 Protein expression and repression from the MET3 promoter

To repress Cdc20 expression from the *MET3* promoter, the endogenous Cdc20 promoter was first replaced by the *MET3* promoter by one step promoter swap PCR reaction. After checking transformants for death on methionine containing media, the cells were grown in complete YNB containing 2% glucose. To repress Cdc20, methionine was added to a final concentration of 2mM.

Alternatively, cells were first arrested in α-factor and then released into media containing methionine to get a synchronous population.

5.3.5 Diploidisation of yeast strains

Haploid yeast cells were diploidised for FRET applications due to increased fluorescent signals with diploids over haploids. To generate diploids, haploid strains were transformed with a centromeric plasmid containing the *HO* gene under the *HO* promoter. *HO* expression causes a double strand break (DSB) at the MAT locus. Repair of the DSB is carried out by gene conversion using one of the silent HM cassettes (HML or HMR) as a template, thus resulting in the substitution of the MAT allele with a sequence of opposite mating type. (Strathern et al., 1982; Simon et al., 2002). After selection of transformants, yeast colonies were streaked for individual colonies once more and tested for their ability to sporulate on sporulatiom media (100 mM CH_3COONa, 20 mM NaCl, 25mM KCl, 25 mM $MgSO_4$ and 1.5 % w/v agar).

5.3.6 Yeast transformation

Transformation of yeast was performed using PCR products as described (section 5.2.1). 50 ml of a mid log phase culture was pelleted at 3,000 rpm for 5 minutes. The cell pellet was washed with 1 ml de-ionized water before washing with 1ml TEL (10 mM Tris/HCL pH 7.5, 100 mM EDTA and 100 mM Lithium acetate) before resuspension in a final volume of 100 µl TEL. To this cell suspension was now added approximately 1 µg of either linearised vector DNA or PCR product and 2 µl of a 10 mg/ml single stranded carrier DNA from salmon

sperm and 600 ml TELP (TEL plus 40% PEG 3350 or 4000), followed by a short vortex. After incubation at 25°C for 2- 3 hours, cells were heat shocked at 42°C for 15 minutes. The cells were then pelleted at 6,000 rpm for 2 minutes, washed in 1 ml sorbitol and plated on selective media. Transformants were checked for the correct integration of the PCR cassette by western blot analysis or death on methionine (in the case of MET-Cdc20) or glucose (Gal-Scc1, Gal-Cdc20) containing media.

5.3.7 Cell cycle analysis using flow cytometry and bud size ratio

To determine cell cycle progression by DNA content, 1 ml of a mid log phase culture (OD_{600} = 0.4) were pelleted and fixed in 70% ethanol on ice for 2 hours. Cells were then RNAse treated in 1 ml 200 mM Tris-HCL pH 7.5 containing 0.1 mg/ml RNAse A overnight at 37°C. After pelleting, DNA was now stained using 400 µl of a propidium iodide containing solution (200 mM Tris-HCL pH 7.5, 211 mM NaCl, 78 mM $MgCL_2$ 50µg/ml propidium iodide). Cells were sonicated (Sanyo, Soniprep 150) before being analysed on a FACScan (Becton Dickinson). Subsequent image preparation was performed using CellQuest software.

For cell cycle determination based on bud size ratio, the diameter of both the mother and daughter bud were determined from DIC images using the SoftWorx software. The diameter of the mother divided by that of the daughter gives an approximate indication of G1 (small values) to G2/M (approximately 1).

5.3.8 Chromosome loss assay

The chromosome loss assay was carried out as per (Hieter et al., 1985). This strain contains a linear minichromosome containing an ochre suppressing form of a tRNA gene, SUP11, of the *ade2-101* allele. Haploid cells carrying one copy of this suppressor remain white. Cells having lost his minichromosome now turn red. To perform the chromosome loss assay, cells were first grown overnight in minimal media lacking uracil so as to retain the suppressor. Cells were then sonicated, counted on a coulter counter and an appropriate density was plated on rich media with minimal adenine to select for the spontaneous loss of the

minichromosome. Loss events were scored as colonies with greater or equal to half sectored colonies, i.e. loss events in the first cell division.

5.4 Cell Biology

5.4.1 Live cell preparation for microscopy

Cells were streaked on YPD plates overnight at 30°C. Plates were supplemented with 150 μg/ml adenine to prevent autofluorescence. *ADE3* was deleted and the growth medium supplemented with adenine to reduce background fluorescence from intermediates of the adenine biosynthesis pathway. Pin-head sized colonies were then scraped from the plate and re-suspended in 12 μl of YNB supplemented with complete amino acids and glucose. 3 μl of the cell suspension was mounted on a 30 μl agarose patch (1% SeaPlaque GTG agarose, Cambrex Bio Science, in SC medium) on a glass slide and covered with a coverslip. Cells were observed on a DeltaVision RT system (Applied Precision) based on an Olympus IX71 microscope. We used a 100x UPUplan Apochromat (NA=1.4) objective, and images were captured with a CoolSNAP HQ camera (Roper scientific). The 100W mercury arc lamp (Olympus, Japan) was changed after 100 hours of usage.

For the generation of stacked images, 15 serial Z sections, each of 0.2 μM and 0.4 sec exposure were projected into a single plane, without deconvolution, using SottWorx software.

5.4.2 Live cell preparation for FRET analysis and data extraction

Cells for FRET were grown in the same way as above. For FRET applications specific band pass filters were used. CFP excitation and emission filters were 440AF21 and 480AF30, YFP excitation and emission filters were 500AF25 and 545AF35, and the dichroic mirror 436-510DBDR (all from Omega Optical). For the acquisition of a FRET image, the sample was excited at the CFP excitation wavelength, with FRET seen as emission at the YFP emission wavelength. The order of image acquisition was critical here, and was recorded in the order of YFP, FRET and lastly CFP. This is due to the very rapid photobleaching of YFP at the CFP excitation energy. Due to the very low

fluorescent signals observed for cohesin fluorophore fusions, all focusing is done using transmitted light. We used 2 x 2 binning, and acquire three sequential 0.4 sec exposure images of YFP, FRET and CFP. Finally, a 0.05 sec DIC image is captured. Approximately 60 – 80 fields of dimensions 512 x 512 pixels are acquired in this way. All image intensity values are calculated on a 5 x 5 pixel box in the fluorescent nucleus, background subtracted by an adjacent box not in the nucleus. Total intensity values from the box were recorded on a data inspector module in SoftWorx.

Subsequently, data is extracted using SoftWorx software. The first step is the calculation of the YFP and CFP spillover factors. This is done in cells only expressing either a YFP or a CFP tagged protein. The CFP spillover factor (CSF) is defined as the signal intensity in the FRET channel divided by that in the CFP channel:

$$\text{Spillover}_{\text{CFP}} = \frac{\text{FRET}_{\text{channel}}}{\text{CFP}_{\text{channel}}}$$

Similarly, the YFP spillover factor (YSF) equals the signal intensity in the FRET channel divided by that in the YFP channel:

$$\text{Spillover}_{\text{YFP}} = \frac{\text{FRET}_{\text{channel}}}{\text{YFP}_{\text{channel}}}$$

For FRET experiments, the sum of these individual spillover factors equals the total baseline spillover. This total spillover is calculated in the experimental strain expressing both fluorophores:

$$\text{Spillover}_{\text{total}} = (\text{Spillover}_{\text{CFP}} \times \text{CFP channel}) + (\text{Spillover}_{\text{YFP}} \times \text{YFP channel})$$

The FRET ratio ($FRET_R$) is defined as the FRET channel divided by this total spillover:

$$FRET_{\text{R}} = \frac{\text{FRET}_{\text{channel}}}{Spillover_{\text{total}}}$$

Thus if the predicted total spillover is accurate, the $FRET_R$ should have a baseline value of 1 in the absence of energy transfer. Subsequent data analysis was performed in JMP software (SAS institute, CA).

5.4.3 Sister chromatid separation assay

Sister chromatid separation was performed using the tetracycline Operator/Repressor GFP system as described in Michaelis et al, 1997. Under conditions when sister chromatids are tightly cohered, the GFP coated tetracycline arrays appear as one dot. Upon separation of sister chromatids, two GFP dots can be seen. 2 ml culture was pelleted (13,000 rpm for 1 min) and resuspended in 1ml ice cold absolute ethanol. Cells were fixed on ice for 2 hours. An aliquot of the cell suspension was placed onto a thin 2% agar pad on a glass slide and covered with a coverslip. GFP dots were imaged on an Axioplan 2 microscope (Zeiss). Cells were kept at -80°C for long-term storage.

5.5 Table of strains

Strains nomenclature is followed as per the guidelines set out on the Saccharomyces Genome Database (http://genome-www.stanford.edu/Saccharomyces/). Briefly, gene names are represented by three italicised upper case letters followed by a number e.g. *SMC1*. Mutant alleles are represented as lower case italicised letters e.g. *smc3-42*. Alleles created by recombinant DNA technology are named by the use of the symbol for the gene that is altered, followed by a symbol to indicate the nature of the alteration: disruption (::), deletion (-Δ) or replacement (Δ::). Additionally, the symbol used after the '::' symbol indicates the marker used for selection whether for one step PCR tagging (*SCC1-Ha6::URA3*), vector integration (*GAL-Ha9-SMC3::TRP1*) or promoter swapping (*GAL-CDC20-TRP1*). Ochre suppressors are indicated by a bold-face suffix **–o**.

If the cell is haploid, just one copy of each gene is listed. If the cell is diploid, one copy is listed for simplicity, even though both copies are tagged unless otherwise stated. (e.g. *SMC1-CFP*).

The presence of an epitope after the gene name denotes C-terminal tagging (*SMC1-CFP*), whereas the presence of the tag before the gene name indicated N-terminal tagging (*CFP-SCC1*).

Unless otherwise stated, all strains are isogenic in the W303 background (*MAT*a, *ade2-1 trp1-1 can1-100 leu2-3, Leu112, his3-11, his15, ura3-52*).

Strain	**Genotype**
Y3087	*MATa/α SCC1-CFP::KAN/SCC1-CFP::KAN ADE3Δ::TRP1/ ADE3Δ::TRP1*
Y2490	*MATa/α SCC3-CFP::KAN/SCC3-CFP::KAN ADE3Δ::LEU2/ ADE3Δ::LEU2*
Y2489	*MATa/α PDS5-CFP::KAN/PDS5-CFP::KAN ADE3Δ::TRP1/ ADE3Δ::TRP1*
Y1967	*MATa/α SMC1-CFP::KAN/SMC1-CFP::KAN ADE3Δ:: LEU2/ ADE3Δ::LEU2*
Y1971	*MATa/α SMC3-CFP::KAN/SMC3-CFP::KAN ADE3Δ:: LEU2/ ADE3Δ::LEU2*
Y1970	*MATa/α SMC1-YFP::HIS5/SMC1-YFP::HIS5 ADE3Δ:: LEU2/ ADE3Δ::LEU2*
Y2587	*MATa/α PDS5-YFP-CFP::KAN/PDS5-YFP-CFP::KAN ADE3Δ:: LEU2/ ADE3Δ::LEU2*
Y2588	*MATa/α SCC3-YFP-CFP::KAN/SCC3-YFP-CFP::KAN ADE3Δ:: LEU2/ ADE3Δ::LEU2*
Y1966	*MATa/α SMC3-CFP::KAN/SMC3-CFP::KAN SMC1-YFP::HIS5 /SMC1-YFP::HIS5 ADE3Δ:: LEU2/ ADE3Δ::LEU2*
Y1972	*MATa/α SMC1-CFP::KAN/SMC1-CFP::KAN SMC3-YFP::HIS5 /SMC3-YFP::HIS5 ADE3Δ:: LEU2/ ADE3Δ::LEU2*
Y2864	*MATa/α SCC1::TRP1/SCC1::TRP1 GAL-SCC1/GAL-SCC1-Ha3::URA3 SMC3-CFP::KAN/SMC3-CFP::KAN SMC1-YFP::HIS5/SMC1-YFP::HIS5 ADE3Δ:: LEU2/ ADE3Δ::LEU2*
Y3254	*MATa/α* GAL-SCC1(Met 269-566)-FLAG::LEU2/GAL-SCC1(Met 269-566)-FLAG::LEU2 *SMC1-CFP::KAN/SMC1-CFP::KAN SMC3-*

	YFP::HIS5 /SMC3-YFP::HIS5 ADE3Δ:: TRP1/ ADE3Δ::TRP1
Y2480	*MATa/α* SCC1-YFP::HIS5/SCC1-YFP::HIS5 *SMC1-CFP::KAN/SMC1-CFP::KAN ADE3Δ:: LEU2/ ADE3Δ::LEU2*
Y2481	*MATa/α* SCC1-YFP::HIS5/SCC1-YFP::HIS5 *SMC3-CFP::KAN/SMC3-CFP::KAN ADE3Δ:: LEU2/ ADE3Δ::LEU2*
Y2482	*MATa/α* SCC1-CFP::KAN/SCC1-CFP::KAN *SMC3-YFP::HIS5/SMC3-YFP::HIS5 ADE3Δ:: LEU2/ ADE3Δ::LEU2*
Y2483	*MATa/α SCC1-CFP::KAN/SCC1-CFP::KAN SMC1-YFP::HIS5/SMC1-YFP::HIS5 ADE3Δ:: LEU2/ ADE3Δ::LEU2*
Y2593	*MATa/α CFP-SCC1/CFP-SCC1 SMC1-YFP::HIS5/SMC1-YFP::HIS5 ADE3Δ:: LEU2/ ADE3Δ::LEU2*
Y2594	*MATa/α CFP-SCC1/CFP-SCC1 SMC3-YFP::HIS5/SMC3-YFP::HIS5 ADE3Δ:: LEU2/ ADE3Δ::LEU2*
Y2589	*MATa/α SMC3-CFP::KAN/SMC3-CFP::KAN SCC3-YFP::HIS5/ SCC3-YFP::HIS5 ADE3Δ:: LEU2/ ADE3Δ::LEU2*
Y2533	*MATa/α SMC1-CFP::KAN/SMC1-CFP::KAN SCC3-YFP::HIS5/ SCC3-YFP::HIS5 ADE3Δ:: LEU2/ ADE3Δ::LEU2*
Y2721	*MATa/α SMC1-CFP::KAN/SMC1-CFP::KAN YFP-SCC3/YFP-SCC3 ADE3Δ:: LEU2/ ADE3Δ::LEU2*
Y2704	*MATa/α SMC3-CFP::KAN/SMC3-CFP::KAN YFP-SCC3/YFP-SCC3 ADE3Δ:: LEU2/ ADE3Δ::LEU2*
Y2534	*MATa/α SCC1-CFP::KAN/SCC1-CFP::KAN SCC3-YFP::HIS5/SCC3-YFP::HIS5 ADE3Δ:: LEU2/ ADE3Δ::LEU2*
Y2591	*MATa/α CFP-SCC1/CFP-SCC1 SCC3-YFP::HIS5/SCC3-YFP::HIS5 ADE3Δ:: LEU2/ ADE3Δ::LEU2*
Y2722	*MATa/α SCC1-CFP::KAN/SCC1-CFP::KAN YFP-SCC3/YFP-SCC3 ADE3Δ:: LEU2/ ADE3Δ::LEU2*
Y2723	*MATa/α CFP-SCC1/CFP-SCC1 YFP-SCC3/YFP-SCC3 ADE3Δ:: TRP1/ ADE3Δ::TRP1*
Y2598	*MATa/α SMC1::LEU/SMC1::LEU SMC1-YFP-hinge/SMC1-YFP-hinge SMC1-CFP::KAN/SMC1-CFP::KAN ADE3Δ:: TRP1/ ADE3Δ::TRP1*

Y2592	*MATa/α CFP-SCC1/CFP-SCC1 SCC1-YFP::HIS5/SCC1-YFP::HIS5 ADE3Δ:: LEU2/ ADE3Δ::LEU2*
Y2872	*MATa/α YFP-SCC3/YFP-SCC3 SCC3-CFP::KAN/ SCC3-CFP::KAN ADE3Δ:: LEU2/ ADE3Δ::LEU2*
Y2865	*MATa/α CFP-PDS5/CFP-PDS5 PDS5-YFP::HIS5/PDS5-YFP::HIS5 ADE3Δ:: LEU2/ ADE3Δ::LEU2*
Y2531	*MATa/α SMC1-CFP::KAN/SMC1-CFP::KAN PDS5-YFP::HIS5/PDS5-YFP::HIS5 ADE3Δ:: LEU2/ ADE3Δ::LEU2*
Y2575	*MATa/α SCC3-YFP::HIS5/SCC3-YFP::HIS5 PDS5-CFP::KAN/PDS5-CFP::KAN ADE3Δ:: LEU2/ ADE3Δ::LEU2*
Y2532	*MATa/α SCC1-CFP::KAN/SCC1-CFP::KAN PDS5-YFP::HIS5/PDS5-YFP::HIS5 ADE3Δ:: LEU2/ ADE3Δ::LEU2*
Y2530	*MATa/α SMC3-CFP::KAN/SMC3-CFP::KAN KAN PDS5-YFP::HIS5/PDS5-YFP::HIS5 ADE3Δ:: LEU2/ ADE3Δ::LEU2*
Y3264	*MATa/α YFP-SCC1/YFP-SCC1 CFP-PDS5/CFP-PDS5 ADE3Δ:: TRP1/ ADE3Δ::TRP1*
Y2574	*MATa/α PDS5-YFP::HIS5/PDS5-YFP::HIS5 SCC3-YFP::HIS5/SCC3-YFP::HIS5 ADE3Δ:: LEU2/ ADE3Δ::LEU2*
Y3275	*MATa/α CFP-PDS5/CFP-PDS5 SCC1-YFP::HIS5/SCC1-YFP::HIS5 ADE3Δ:: TRP1/ ADE3Δ::TRP1*
Y2590	*MATa/α CFP-SCC1/CFP-SCC1 PDS5-YFP::HIS5/PDS5-YFP::HIS5 ADE3Δ:: LEU2/ ADE3Δ::LEU2*
Y2706	*MATa/α SMC1::LEU/SMC1::LEU SMC1-YFP-hinge/SMC1-YFP-hinge PDS5-CFP::KAN/PDS5-CFP::KAN ADE3Δ:: TRP1/ ADE3Δ::TRP1*
Y2705	*MATa/α SMC1::LEU/SMC1::LEU SMC1-YFP-hinge/SMC1-YFP-hinge CFP-PDS5/CFP-PDS5 ADE3Δ:: TRP1/ ADE3Δ::TRP1*
Y3223	*MATa pep4::URA3 bar1::hisG SCC1::TRP1 GAL1-SCC1-HA6::HIS3 SMC-Pk3::KAN*
Y3210	*MATa pep4::URA3 bar1::hisG SCC1::TRP1 GAL1-SCC1-HA6::HIS3 SMC-Pk3::KAN PDS5-Myc18::LEU2*
Y2318	*MATa pep4::URA3 bar1::hisG GAL-SMC3(hinge)-Pk3::TRP1 GAL-*

	Myc9-SMC1(hinge)::HIS3
Y1823	*MATa pep4::URA3 bar1::hisG GAL-SMC3(hinge)-Pk3::TRP1*
Y2319	*MATa pep4::URA3 bar1::hisG GAL-SMC3(hinge)-Pk3::TRP1 GAL-Myc9-SMC1(hinge)::HIS3 GAL-SMC1(head)-Ha3::LEU2*
Y1824	*MATa pep4::URA3 bar1::hisG GAL-SMC1(head)-Ha3::LEU2 GAL-SMC3(hinge)-Pk3::TRP1*
Y3082	*MATa/α SMC1-CFP::KAN/SMC1-YFP::HIS5 ADE3Δ:: TRP1/ ADE3Δ::TRP1*
Y3083	*MATa/α SMC3-YFP::HIS5/SMC1-CFP::KAN ADE3Δ:: TRP1/ ADE3Δ::TRP1*
Y3228	*MATa/α SMC1::LEU/SMC1::LEU SMC1-YFP-hinge/SMC1-CFP-hinge*
BESY131	*MATa/α SMC3-YFP::HIS5/SMC3-YFP::HIS5 SPC29-CFP::KAN/SPC29-CFP::KAN*
Y3239	*MATa SCC1-Pk3::HIS3*
Y2330	*MATa SCC1-Pk3::HIS3 smc1R58A::LEU2 smc3R58A::TRP1*
Y2738	*MATa SCC3-Pk3::KAN TetOs::URA3 TetR-GFP::HIS3 GAL1-CDC20::LEU2*
Y2739	*MATa SCC3-Pk3::KAN TetOs::URA3 TetR-GFP::HIS3 GAL1-CDC20::LEU2 smc1R58A::LEU2 smc3R58A::TRP1*
K5041	*MATa ade2-101 CFIII(CENE.L.YPH278) URA3::SUP11-o*
Y2885	*MATα ade2-101 CFIII(CENE.L.YPH278) URA3::SUP11-o smc3R58A::TRP1*
Y2886	*MATa ade2-101 CFIII(CENE.L.YPH278) URA3::SUP11-o smc1R58A::LEU2*
Y2368	*MATa ade2-101 CFIII(CENE.L.YPH278) URA3::SUP11-o smc1R58A::LEU2 smc3R58A::TRP1*
Y1569	*MATA SCC1-Ha3::TRP*
Y2043	*MATa smc3-42 TetOs::URA3 TetR-GFP::HIS3*
Y2079	*MATa smc3-42 TetOs::URA3 TetR-GFP::HIS3 GAL-Ha9-SMC3::LEU2*
Y2078	*MATa smc3-42 TetOs::URA3 TetR-GFP::HIS3 GAL-Ha9-*

	Smc3R58A::LEU2
K6753	*MATa smc1-259 TetOs::URA3 TetR-GFP::LEU2*
Y754	*MATa smc1-259 TetOs::URA3 TetR-GFP::HIS3 GAL-SMC1-HA6::LEU2*
Y1857	*MATa smc1-259 TetOs::URA3 TetR-GFP::HIS3 GAL-smc1R58A-HA6::LEU2*
Y982	*MATa pep4::URA3 bar1::hisG GAL-SMC1(head)-Ha3::LEU2*
Y1834	*MATa pep4::URA3 bar1::hisG GAL-SMC1(head/WALKER-A)-Ha3::LEU2 GAL-SMC3(hinge)-Pk3::TRP1*
Y1836	*MATa pep4::URA3 bar1::hisG GAL-SMC1(head/C-MOTIF)-Ha3::LEU2 GAL-SMC3(hinge)-Pk3::TRP1*
Y1837	*MATa pep4::URA3 bar1::hisG GAL-SMC1(head/C-MOTIF & WALKER-A)-Ha3::LEU2 GAL-SMC3(hinge)-Pk3::TRP1*
Y2935	*MATa pep4::URA3 bar1::hisG GAL-SMC3(hinge)-Pk3::TRP1 GAL-Myc9-SMC1(hinge)::HIS3 PDS5-Ha3::LEU2*
Y2936	*MATa pep4::URA3 bar1::hisG GAL-SMC3(hinge)-Pk3::TRP1 GAL-Myc9-SMC1(hinge)::HIS3 SCC1-Ha3::LEU2*
K7244	*MATα scc2-4 TetOs::URA3 TetR-GFP::HIS3*
Y1119	*MATa TetOs::URA3 TetR-GFP::HIS3 GAL-CDC20::LEU2*
Y2655	*MATa TetOs::URA3 TetR-GFP::HIS3 GAL-CDC20::LEU2 smc1R58A::LEU2 smc3R58A::TRP1*
Y2185	*MATa smc3R58A::TRP1*
Y2186	*MATa smc1R58A::LEU2*
Y2738	*MATa TetOs::URA3 TetR-GFP::HIS3 GAL-CDC20::LEU2 SCC3-Pk3::KAN*
Y2739	*MATa TetOs::URA3 TetR-GFP::HIS3 GAL-CDC20::LEU2 SCC3-Pk3::KAN smc1R58A::LEU2 smc3R58A::TRP1*
Y27791	*MATa MATa pep4::URA3 bar1::hisG SCC1-Ha6::HIS3 SMC1-Pk3::KAN*
Y3207	*MATa MATa pep4::URA3 bar1::hisG SCC1-Ha6::HIS3 SMC1-Pk3::KAN PDS5-Myc18::LEU2*

5.6 Tables of DNA vectors

Basic vectors for integration in yeast

Number	Name	Description	Origin
1	YIplac 128	*LEU2* based integrative vector	Gietz and Sugino
2	YIplac 204	*TRP1* based integrative vector	Gietz and Sugino
13	YIplac 128	*GAL1* cloned between EcoRI and BamHI in YIplac 128	Frank Uhlmann
9	pRS303	*HIS3* based integrative vector	Sikorski and Hieter
698	pRS303-*GAL1*	*HIS3* based integrative vector with *GAL1* cloned BamHI/EcorI into pRS303	This study

Vectors for epitope tagging in yeast

Number	Name	Description	Origin
285	pDH3	One step C-terminal CFP tagging vector (KAN marker)	Eric Muller, YRC
288	pDH5	One step C-terminal YFP tagging vector (His5 marker)	Eric Muller, YRC
289	pDH18	One step C-terminal YFP-CFP tagging vector (His5 marker)	Eric Muller, YRC
290	pDH22	One step N-terminal YFP tagging vector (Kan marker)	Eric Muller, YRC
284	pBS5	One step N-terminal CFP tagging vector (Kan marker)	Eric Muller, YRC
556	pUC19-Pk3	One step C-terminal Pk tagging vector (Kan marker)	Wolfgang Zachariae
36	pUC19-Ha6	One step C-terminal Ha tagging vector (*S. pombe His5* marker)	Gustav Ammerer
776	pUC19-Myc18	One step C-terminal Myc tagging vector (*K. lactis Leu2* marker)	Toru Higuchi
35	pUC19-Ha3	One step C-terminal Ha tagging vector (*K. lactis Trp1* marker)	Wolfgang Zachariae
555	pUC19-Pk3	One step C-terminal Pk tagging vector (*K. lactis His3* marker)	Wolfgang Zachariae
40	pUC19-Ha3	One step C-terminal Ha tagging vector (*K. lactis Ura3* marker)	Frank Uhlmann

Table of integrative vectors of modified cohesin subunits

Number	Name	Description	Origin
799	YIplac 128-Smc1-YFP-hinge	Construct to replace the endogenous Smc1 with a 'Smc1-YFP-hinge' variant (*Leu2* marker).	This study
806	YIplac 128-	Construct to replace the	This study

	Smc1-CFP-hinge	endogenous Smc1 with a 'Smc1-CFP-hinge' variant (*Leu2* marker).	
645	YIplac 128-*GAL1*-Smc1R58A-Ha6	The arginine point mutant was introduced by overlap extension PCR as a short PCR fragment at the Smc1 5' end (*Leu2* marker).	This study
655	YIplac 128-*GAL1*-Ha9-Smc3R58A	The arginine point mutant was introduced by overlap extension PCR as a short PCR fragment at the Smc3 5' end (*Leu2* marker).	This study
682	YIplac 128 Smc1 R58A	Construct to replace the endogenous Smc1 with Smc1R58A. The 472bp Smc1 promoter was cloned as an NdeI/XmaI into YIplac 128. Downstream of this was cloned an XmaI/XbaI flanked region corresponding to the Smc1 640 N-terminal region. Finally, an Smc1 upstream sequence (474bp) was cloned downstream of Smc1 as an XbaI/SphI fragment. The resulting plasmid was cut XbaI for integration at the Smc1 locus.	This study
687	YIplac 204 Smc3 R58A	Construct to replace the endogenous Smc3 with Smc3R58A. The 1000bp Smc3 promoter was cloned as an NdeI/XmaI into YIplac 204. Downstream of this was cloned an XmaI/XbaI flanked region corresponding to the Smc3 1100bp N-terminal region. Finally, an Smc3 upstream sequence (641bp) was cloned downstream of Smc1 as an XbaI/SphI fragment. The resulting plasmid was cut XbaI for integration at the Smc3 locus.	This study
706	pRS303 *GAL1*-myc9-Smc1 (hinge)	Smc1 hinge flanked 50 amino acids coiled coils under the control of the *GAL1* promoter (*His3* marker)	Stefan Weitzer
??		Smc3 hinge flanked by 50 amino acids coiled coils under the control of the *GAL1* inducible promoter (*Trp1* marker)	Stefan Weitzer
416	YIplac 128 *GAL1*-Smc1	Smc1 N- and C- temninal regions separated by a short peptide linker	Stefan Weitzer

	(head) –Ha3	and under control of the *GAL1* inducible promoter (*Leu2* marker)	
157	pRS305 *GAL1*-Scc1 (MET 269 – 566)	Scc1 C-terminal cleavage frament FLAG tagged and under the *GAL1* promoter (*Leu2* marker)	Hai Rao
457	YIplac 128 *GAL1*-Smc1 –Ha6	Smc1 Ha tagged and under the control of the *GAL1* promoter	Stefan Weitzer
634	YIplac 128 *GAL1*-Ha9-Smc3	Smc3 Ha tagged and under the control of the *GAL1* promoter	Stefan Weitzer

Integrative vectors for one step promoter swapping in yeast

Number	Name	Description	Origin
453	YCplac111 GAL1 cdc20	Construct to replace the endogenous Cdc20 promoter with the *GAL1* inducible promoter (Leu2 marker)	Armelle Lengronne
49	pBS-*GAL1*	Construct for promoter swapping with the *GAL1* inducible promoter (*K. lactis* Trp1 marker)	Frank Uhlmann

Miscellaneous vectors

Number	Name	Description	Origin
657	pRS426-HO	*HO* endonuclease under its endogenous promoter in a centromeric plasmid (*URA3* marker)	Ralf-Peter Jensen
703	pSH47	*Cre* recombinase under the control of the *GAL1* inducible promoter in a centromeric plasmid (*URA3* marker)	Eric Muller, YRC

Numbers listed in these tables refer to DNA or strain number entries in the Uhlmann Lab database.

6 Chapter 6: References

Aguilar, C., Davidson, C., Dix, M., Stead, K., Zheng, K., Hartman, T., and Guacci, V. (2005). Topoisomerase II suppresses the temperature sensitivity of Saccharomyces cerevisiae pds5 mutants, but not the defect in sister chromatid cohesion. Cell Cycle *4*, 1294-1304.

Alexandru, G., Uhlmann, F., Mechtler, K., Poupart, M. A., and Nasmyth, K. (2001). Phosphorylation of the cohesin subunit Scc1 by Polo/Cdc5 kinase regulates sister chromatid separation in yeast. Cell *105*, 459-472.

Anderson, D. E., Losada, A., Erickson, H. P., and Hirano, T. (2002). Condensin and cohesin display different arm conformations with characteristic hinge angles. J Cell Biol *156*, 419-424.

Andrews, E. A., Palecek, J., Sergeant, J., Taylor, E., Lehmann, A. R., and Watts, F. Z. (2005). Nse2, a component of the Smc5-6 complex, is a SUMO ligase required for the response to DNA damage. Mol Cell Biol *25*, 185-196.

Arumugam, P., Gruber, S., Tanaka, K., Haering, C. H., Mechtler, K., and Nasmyth, K. (2003). ATP hydrolysis is required for cohesin's association with chromosomes. Curr Biol *13*, 1941-1953.

Arumugam, P., Nishino, T., Haering, C. H., Gruber, S., and Nasmyth, K. (2006). Cohesin's ATPase activity is stimulated by the C-terminal Winged-Helix domain of its kleisin subunit. Curr Biol *16*, 1998-2008.

Assenmacher, N., and Hopfner, K. P. (2004). MRE11/RAD50/NBS1: complex activities. Chromosoma *113*, 157-166.

Baetz, K. K., Krogan, N. J., Emili, A., Greenblatt, J., and Hieter, P. (2004). The ctf13-30/CTF13 genomic haploinsufficiency modifier screen identifies the yeast chromatin remodeling complex RSC, which is required for the establishment of sister chromatid cohesion. Mol Cell Biol *24*, 1232-1244.

Bell, S. P. (2002). The origin recognition complex: from simple origins to complex functions. Genes Dev *16*, 659-672.

Bernard, P., Maure, J. F., Partridge, J. F., Genier, S., Javerzat, J. P., and Allshire, R. C. (2001). Requirement of heterochromatin for cohesion at centromeres. Science *294*, 2539-2542.

Berney, C., and Danuser, G. (2003). FRET or no FRET: a quantitative comparison. Biophys J *84*, 3992-4010.

Bhat, M. A., Philp, A. V., Glover, D. M., and Bellen, H. J. (1996). Chromatid segregation at anaphase requires the barren product, a novel chromosome-associated protein that interacts with Topoisomerase II. Cell *87*, 1103-1114.

Birkenbihl, R. P., and Subramani, S. (1992). Cloning and characterization of rad21 an essential gene of Schizosaccharomyces pombe involved in DNA double-strand-break repair. Nucleic Acids Res *20*, 6605-6611.

Blat, Y., and Kleckner, N. (1999). Cohesins bind to preferential sites along yeast chromosome III, with differential regulation along arms versus the centric region. Cell *98*, 249-259.

Borck, G., Zarhrate, M., Bonnefont, J. P., Munnich, A., Cormier-Daire, V., and Colleaux, L. (2007). Incidence and clinical features of X-linked Cornelia de Lange syndrome due to SMC1L1 mutations. Hum Mutat *28*, 205-206.

Boue, J., Bou, A., and Lazar, P. (1975). Retrospective and prospective epidemiological studies of 1500 karyotyped spontaneous human abortions. Teratology *12*, 11-26.

Briggs, S. D., Bryk, M., Strahl, B. D., Cheung, W. L., Davie, J. K., Dent, S. Y., Winston, F., and Allis, C. D. (2001). Histone H3 lysine 4 methylation is mediated by Set1 and required for cell growth and rDNA silencing in Saccharomyces cerevisiae. Genes Dev *15*, 3286-3295.

Buonomo, S. B., Clyne, R. K., Fuchs, J., Loidl, J., Uhlmann, F., and Nasmyth, K. (2000). Disjunction of homologous chromosomes in meiosis I depends on proteolytic cleavage of the meiotic cohesin Rec8 by separin. Cell *103*, 387-398.

Chalfie, M., Tu, Y., Euskirchen, G., Ward, W. W., and Prasher, D. C. (1994). Green fluorescent protein as a marker for gene expression. Science *263*, 802-805.

Chan, R. C., Chan, A., Jeon, M., Wu, T. F., Pasqualone, D., Rougvie, A. E., and Meyer, B. J. (2003). Chromosome cohesion is regulated by a clock gene paralogue TIM-1. Nature *423*, 1002-1009.

Chen, J., Lu, G., Lin, J., Davidson, A. L., and Quiocho, F. A. (2003). A tweezers-like motion of the ATP-binding cassette dimer in an ABC transport cycle. Mol Cell *12*, 651-661.

Ciosk, R., Shirayama, M., Shevchenko, A., Tanaka, T., Toth, A., and Nasmyth, K. (2000). Cohesin's binding to chromosomes depends on a separate complex consisting of Scc2 and Scc4 proteins. Mol Cell *5*, 243-254.

Ciosk, R., Zachariae, W., Michaelis, C., Shevchenko, A., Mann, M., and Nasmyth, K. (1998). An ESP1/PDS1 complex regulates loss of sister chromatid cohesion at the metaphase to anaphase transition in yeast. Cell *93*, 1067-1076.

Cohen-Fix, O., Peters, J. M., Kirschner, M. W., and Koshland, D. (1996). Anaphase initiation in Saccharomyces cerevisiae is controlled by the APC-dependent degradation of the anaphase inhibitor Pds1p. Genes Dev *10*, 3081-3093.

Cozzarelli, N. R., Cost, G. J., Nollmann, M., Viard, T., and Stray, J. E. (2006). Giant proteins that move DNA: bullies of the genomic playground. Nat Rev Mol Cell Biol *7*, 580-588.

Davidson, A. L. (2002). Mechanism of coupling of transport to hydrolysis in bacterial ATP-binding cassette transporters. J Bacteriol *184*, 1225-1233.

Dawson, R. J., and Locher, K. P. (2006). Structure of a bacterial multidrug ABC transporter. Nature *443*, 180-185.

de Jager, M., van Noort, J., van Gent, D. C., Dekker, C., Kanaar, R., and Wyman, C. (2001). Human Rad50/Mre11 is a flexible complex that can tether DNA ends. Mol Cell *8*, 1129-1135.

De Piccoli, G., Cortes-Ledesma, F., Ira, G., Torres-Rosell, J., Uhle, S., Farmer, S., Hwang, J. Y., Machin, F., Ceschia, A., McAleenan, A., *et al.* (2006). Smc5-Smc6 mediate DNA double-strand-break repair by promoting sister-chromatid recombination. Nat Cell Biol *8*, 1032-1034.

Dean, M., Hamon, Y., and Chimini, G. (2001). The human ATP-binding cassette (ABC) transporter superfamily. J Lipid Res *42*, 1007-1017.

Deardorff, M. A., Kaur, M., Yaeger, D., Rampuria, A., Korolev, S., Pie, J., Gil-Rodriguez, C., Arnedo, M., Loeys, B., Kline, A. D., *et al.* (2007). Mutations in cohesin complex members SMC3 and SMC1A cause a mild variant of cornelia de Lange syndrome with predominant mental retardation. Am J Hum Genet *80*, 485-494.

Denison, S. H., Kafer, E., and May, G. S. (1993). Mutation in the bimD gene of Aspergillus nidulans confers a conditional mitotic block and sensitivity to DNA damaging agents. Genetics *134*, 1085-1096.

Edwards, S., Li, C. M., Levy, D. L., Brown, J., Snow, P. M., and Campbell, J. L. (2003). Saccharomyces cerevisiae DNA polymerase epsilon and polymerase sigma interact physically and functionally, suggesting a role for polymerase epsilon in sister chromatid cohesion. Mol Cell Biol *23*, 2733-2748.

Erickson, M. G., Moon, D. L., and Yue, D. T. (2003). DsRed as a potential FRET partner with CFP and GFP. Biophys J *85*, 599-611.

Fennell-Fezzie, R., Gradia, S. D., Akey, D., and Berger, J. M. (2005). The MukF subunit of Escherichia coli condensin: architecture and functional relationship to kleisins. Embo J *24*, 1921-1930.

Fleming, W. (1882). Zellsubstanz, Kern und Zelltheilung (F .C. W. Vogel, Leipzig.

Fousteri, M. I., and Lehmann, A. R. (2000). A novel SMC protein complex in Schizosaccharomyces pombe contains the Rad18 DNA repair protein. Embo J *19*, 1691-1702.

Fujioka, Y., Kimata, Y., Nomaguchi, K., Watanabe, K., and Kohno, K. (2002). Identification of a novel non-structural maintenance of chromosomes (SMC) component of the SMC5-SMC6 complex involved in DNA repair. J Biol Chem *277*, 21585-21591.

Funabiki, H., Yamano, H., Kumada, K., Nagao, K., Hunt, T., and Yanagida, M. (1996). Cut2 proteolysis required for sister-chromatid seperation in fission yeast. Nature *381*, 438-441.

Furuse, M., Nagase, Y., Tsubouchi, H., Murakami-Murofushi, K., Shibata, T., and Ohta, K. (1998). Distinct roles of two separable in vitro activities of yeast Mre11 in mitotic and meiotic recombination. Embo J *17*, 6412-6425.

Gandhi, R., Gillespie, P. J., and Hirano, T. (2006). Human Wapl is a cohesin-binding protein that promotes sister-chromatid resolution in mitotic prophase. Curr Biol *16*, 2406-2417.

Gerbi, S. A., and Bielinsky, A. K. (2002). DNA replication and chromatin. Curr Opin Genet Dev *12*, 243-248.

Gerlich, D., Koch, B., Dupeux, F., Peters, J. M., and Ellenberg, J. (2006). Live-cell imaging reveals a stable cohesin-chromatin interaction after but not before DNA replication. Curr Biol *16*, 1571-1578.

Gillespie, P. J., and Hirano, T. (2004). Scc2 couples replication licensing to sister chromatid cohesion in Xenopus egg extracts. Curr Biol *14*, 1598-1603.

Glynn, E. F., Megee, P. C., Yu, H. G., Mistrot, C., Unal, E., Koshland, D. E., DeRisi, J. L., and Gerton, J. L. (2004). Genome-wide mapping of the cohesin complex in the yeast Saccharomyces cerevisiae. PLoS Biol *2*, E259.

Gordon, G. W., Berry, G., Liang, X. H., Levine, B., and Herman, B. (1998). Quantitative fluorescence resonance energy transfer measurements using fluorescence microscopy. Biophys J *74*, 2702-2713.

Gottesman, M. M., Pastan, I., and Ambudkar, S. V. (1996). P-glycoprotein and multidrug resistance. Curr Opin Genet Dev *6*, 610-617.

Greenfeder, S. A., and Newlon, C. S. (1992). Replication forks pause at yeast centromeres. Mol Cell Biol *12*, 4056-4066.

Gruber, S., Arumugam, P., Katou, Y., Kuglitsch, D., Helmhart, W., Shirahige, K., and Nasmyth, K. (2006). Evidence that loading of cohesin onto chromosomes involves opening of its SMC hinge. Cell *127*, 523-537.

Gruber, S., Haering, C. H., and Nasmyth, K. (2003). Chromosomal cohesin forms a ring. Cell *112*, 765-777.

Gruss, C., Wu, J., Koller, T., and Sogo, J. M. (1993). Disruption of the nucleosomes at the replication fork. Embo J *12*, 4533-4545.

Guacci, V., Hogan, E., and Koshland, D. (1997a). Centromere position in budding yeast: evidence for anaphase A. Mol Biol Cell *8*, 957-972.

Guacci, V., Koshland, D., and Strunnikov, A. (1997b). A direct link between sister chromatid cohesion and chromosome condensation revealed through the analysis of MCD1 in S. cerevisiae. Cell *91*, 47-57.

Ha, T. (2001). Single-molecule fluorescence methods for the study of nucleic acids. Curr Opin Struct Biol *11*, 287-292.

Haering, C. H., Lowe, J., Hochwagen, A., and Nasmyth, K. (2002). Molecular architecture of SMC proteins and the yeast cohesin complex. Mol Cell *9*, 773-788.

Haering, C. H., Schoffnegger, D., Nishino, T., Helmhart, W., Nasmyth, K., and Lowe, J. (2004). Structure and stability of cohesin's Smc1-kleisin interaction. Mol Cell *15*, 951-964.

Hagstrom, K. A., and Meyer, B. J. (2003). Condensin and cohesin: more than chromosome compactor and glue. Nat Rev Genet *4*, 520-534.

Hailey, D. W., Davis, T. N., and Muller, E. G. (2002). Fluorescence resonance energy transfer using color variants of green fluorescent protein. Methods Enzymol *351*, 34-49.

Hakimi, M. A., Bochar, D. A., Schmiesing, J. A., Dong, Y., Barak, O. G., Speicher, D. W., Yokomori, K., and Shiekhattar, R. (2002). A chromatin remodelling complex that loads cohesin onto human chromosomes. Nature *418*, 994-998.

Hanna, J. S., Kroll, E. S., Lundblad, V., and Spencer, F. A. (2001). Saccharomyces cerevisiae CTF18 and CTF4 are required for sister chromatid cohesion. Mol Cell Biol *21*, 3144-3158.

Hartman, T., Stead, K., Koshland, D., and Guacci, V. (2000). Pds5p is an essential chromosomal protein required for both sister chromatid cohesion and condensation in Saccharomyces cerevisiae. J Cell Biol *151*, 613-626.

Harvey, S. H., Sheedy, D. M., Cuddihy, A. R., and O'Connell, M. J. (2004). Coordination of DNA damage responses via the Smc5/Smc6 complex. Mol Cell Biol *24*, 662-674.

Hassold, T., Chen, N., Funkhouser, J., Jooss, T., Manuel, B., Matsuura, J., Matsuyama, A., Wilson, C., Yamane, J. A., and Jacobs, P. A. (1980). A cytogenetic study of 1000 spontaneous abortions. Ann Hum Genet *44*, 151-178.

Hauf, S., Roitinger, E., Koch, B., Dittrich, C. M., Mechtler, K., and Peters, J. M. (2005). Dissociation of cohesin from chromosome arms and loss of arm cohesion during early mitosis depends on phosphorylation of SA2. PLoS Biol *3*, e69.

Hauf, S., Waizenegger, I. C., and Peters, J. M. (2001). Cohesin cleavage by separase required for anaphase and cytokinesis in human cells. Science *293*, 1320-1323.

Heim, R., and Tsien, R. Y. (1996). Engineering green fluorescent protein for improved brightness, longer wavelengths and fluorescence resonance energy transfer. Curr Biol *6*, 178-182.

Hieter, P., Mann, C., Snyder, M., and Davis, R. W. (1985). Mitotic stability of yeast chromosomes: a colony color assay that measures nondisjunction and chromosome loss. Cell *40*, 381-392.

Higgins, D. G., Thompson, J. D., and Gibson, T. J. (1996). Using CLUSTAL for multiple sequence alignments. Methods Enzymol *266*, 383-402.

Hirano, M., Anderson, D. E., Erickson, H. P., and Hirano, T. (2001). Bimodal activation of SMC ATPase by intra- and inter-molecular interactions. Embo J *20*, 3238-3250.

Hirano, M., and Hirano, T. (1998). ATP-dependent aggregation of single-stranded DNA by a bacterial SMC homodimer. Embo J *17*, 7139-7148.

Hirano, M., and Hirano, T. (2002). Hinge-mediated dimerization of SMC protein is essential for its dynamic interaction with DNA. Embo J *21*, 5733-5744.

Hirano, M., and Hirano, T. (2006). Opening closed arms: long-distance activation of SMC ATPase by hinge-DNA interactions. Mol Cell *21*, 175-186.

Hirano, T. (2006). At the heart of the chromosome: SMC proteins in action. Nat Rev Mol Cell Biol *7*, 311-322.

Hirano, T., Kobayashi, R., and Hirano, M. (1997). Condensins, chromosome condensation protein complexes containing XCAP-C, XCAP-E and a Xenopus homolog of the Drosophila Barren protein. Cell *89*, 511-521.

Hirano, T., and Mitchison, T. J. (1994). A heterodimeric coiled-coil protein required for mitotic chromosome condensation in vitro. Cell *79*, 449-458.

Holt, C. L., and May, G. S. (1996). An extragenic suppressor of the mitosis-defective bimD6 mutation of Aspergillus nidulans codes for a chromosome scaffold protein. Genetics *142*, 777-787.

Hopfner, K. P., Craig, L., Moncalian, G., Zinkel, R. A., Usui, T., Owen, B. A., Karcher, A., Henderson, B., Bodmer, J. L., McMurray, C. T., *et al.* (2002). The Rad50 zinc-hook is a structure joining Mre11 complexes in DNA recombination and repair. Nature *418*, 562-566.

Hopfner, K. P., Karcher, A., Craig, L., Woo, T. T., Carney, J. P., and Tainer, J. A. (2001). Structural biochemistry and interaction architecture of the DNA double-strand break repair Mre11 nuclease and Rad50-ATPase. Cell *105*, 473-485.

Hopfner, K. P., Karcher, A., Shin, D. S., Craig, L., Arthur, L. M., Carney, J. P., and Tainer, J. A. (2000). Structural biology of Rad50 ATPase: ATP-driven conformational control in DNA double-strand break repair and the ABC-ATPase superfamily. Cell *101*, 789-800.

Hornig, N. C., and Uhlmann, F. (2004). Preferential cleavage of chromatin-bound cohesin after targeted phosphorylation by Polo-like kinase. Embo J *23*, 3144-3153.

Hou, F., and Zou, H. (2005). Two human orthologues of Eco1/Ctf7 acetyltransferases are both required for proper sister-chromatid cohesion. Mol Biol Cell *16*, 3908-3918.

Hu, B., Liao, C., Millson, S. H., Mollapour, M., Prodromou, C., Pearl, L. H., Piper, P. W., and Panaretou, B. (2005). Qri2/Nse4, a component of the essential Smc5/6 DNA repair complex. Mol Microbiol *55*, 1735-1750.

Huang, C. E., Milutinovich, M., and Koshland, D. (2005). Rings, bracelet or snaps: fashionable alternatives for Smc complexes. Philos Trans R Soc Lond B Biol Sci *360*, 537-542.

Huang, J., Hsu, J. M., and Laurent, B. C. (2004). The RSC nucleosome-remodeling complex is required for Cohesin's association with chromosome arms. Mol Cell *13*, 739-750.

Hung, L. W., Wang, I. X., Nikaido, K., Liu, P. Q., Ames, G. F., and Kim, S. H. (1998). Crystal structure of the ATP-binding subunit of an ABC transporter. Nature *396*, 703-707.

Indjeian, V. B., Stern, B. M., and Murray, A. W. (2005). The centromeric protein Sgo1 is required to sense lack of tension on mitotic chromosomes. Science *307*, 130-133.

Ivanov, D., and Nasmyth, K. (2005). A topological interaction between cohesin rings and a circular minichromosome. Cell *122*, 849-860.

Ivanov, D., Schleiffer, A., Eisenhaber, F., Mechtler, K., Haering, C. H., and Nasmyth, K. (2002). Eco1 is a novel acetyltransferase that can acetylate proteins involved in cohesion. Curr Biol *12*, 323-328.

Iyer, V. R., Horak, C. E., Scafe, C. S., Botstein, D., Snyder, M., and Brown, P. O. (2001). Genomic binding sites of the yeast cell-cycle transcription factors SBF and MBF. Nature *409*, 533-538.

Jallepalli, P. V., and Lengauer, C. (2001). Chromosome segregation and cancer: cutting through the mystery. Nat Rev Cancer *1*, 109-117.

Jares-Erijman, E. A., and Jovin, T. M. (2003). FRET imaging. Nat Biotechnol *21*, 1387-1395.

Johnson, A., and O'Donnell, M. (2005). Cellular DNA replicases: components and dynamics at the replication fork. Annu Rev Biochem *74*, 283-315.

Kagansky, A., Freeman, L., Lukyanov, D., and Strunnikov, A. (2004). Histone tail-independent chromatin binding activity of recombinant cohesin holocomplex. J Biol Chem *279*, 3382-3388.

Katis, V. L., Galova, M., Rabitsch, K. P., Gregan, J., and Nasmyth, K. (2004). Maintenance of cohesin at centromeres after meiosis I in budding yeast requires a kinetochore-associated protein related to MEI-S332. Curr Biol *14*, 560-572.

Katou, Y., Kanoh, Y., Bando, M., Noguchi, H., Tanaka, H., Ashikari, T., Sugimoto, K., and Shirahige, K. (2003). S-phase checkpoint proteins Tof1 and Mrc1 form a stable replication-pausing complex. Nature *424*, 1078-1083.

Kerrebrock, A. W., Moore, D. P., Wu, J. S., and Orr-Weaver, T. L. (1995). Mei-S332, a Drosophila protein required for sister-chromatid cohesion, can localize to meiotic centromere regions. Cell *83*, 247-256.

Kiburz, B. M., Reynolds, D. B., Megee, P. C., Marston, A. L., Lee, B. H., Lee, T. I., Levine, S. S., Young, R. A., and Amon, A. (2005). The core centromere and Sgo1 establish a 50-kb cohesin-protected domain around centromeres during meiosis I. Genes Dev *19*, 3017-3030.

Kim, J. S., Krasieva, T. B., LaMorte, V., Taylor, A. M., and Yokomori, K. (2002). Specific recruitment of human cohesin to laser-induced DNA damage. J Biol Chem *277*, 45149-45153.

Kimura, K., Hirano, M., Kobayashi, R., and Hirano, T. (1998). Phosphorylation and activation of 13S condensin by Cdc2 in vitro. Science *282*, 487-490.

Kimura, K., and Hirano, T. (1997). ATP-dependent positive supercoiling of DNA by 13S condensin: a biochemical implication for chromosome condensation. Cell *90*, 625-634.

Kimura, K., and Hirano, T. (2000). Dual roles of the 11S regulatory subcomplex in condensin functions. Proc Natl Acad Sci U S A *97*, 11972-11977.

Kimura, K., Rybenkov, V. V., Crisona, N. J., Hirano, T., and Cozzarelli, N. R. (1999). 13S condensin actively reconfigures DNA by introducing global positive writhe: implications for chromosome condensation. Cell *98*, 239-248.

Kitagawa, R., Bakkenist, C. J., McKinnon, P. J., and Kastan, M. B. (2004). Phosphorylation of SMC1 is a critical downstream event in the ATM-NBS1-BRCA1 pathway. Genes Dev *18*, 1423-1438.

Kitajima, T. S., Hauf, S., Ohsugi, M., Yamamoto, T., and Watanabe, Y. (2005). Human Bub1 defines the persistent cohesion site along the mitotic chromosome by affecting Shugoshin localization. Curr Biol *15*, 353-359.

Kitajima, T. S., Kawashima, S. A., and Watanabe, Y. (2004). The conserved kinetochore protein shugoshin protects centromeric cohesion during meiosis. Nature *427*, 510-517.

Kitajima, T. S., Miyazaki, Y., Yamamoto, M., and Watanabe, Y. (2003a). Rec8 cleavage by separase is required for meiotic nuclear divisions in fission yeast. Embo J *22*, 5643-5653.

Kitajima, T. S., Sakuno, T., Ishiguro, K., Iemura, S., Natsume, T., Kawashima, S. A., and Watanabe, Y. (2006). Shugoshin collaborates with protein phosphatase 2A to protect cohesin. Nature *441*, 46-52.

Kitajima, T. S., Yokobayashi, S., Yamamoto, M., and Watanabe, Y. (2003b). Distinct cohesin complexes organize meiotic chromosome domains. Science *300*, 1152-1155.

Kitamura, E., Blow, J. J., and Tanaka, T. U. (2006). Live-cell imaging reveals replication of individual replicons in eukaryotic replication factories. Cell *125*, 1297-1308.

Klein, F., Mahr, P., Galova, M., Buonomo, S. B., Michaelis, C., Nairz, K., and Nasmyth, K. (1999). A central role for cohesins in sister chromatid cohesion, formation of axial elements, and recombination during yeast meiosis. Cell *98*, 91-103.

Knop, M., Siegers, K., Pereira, G., Zachariae, W., Winsor, B., Nasmyth, K., and Schiebel, E. (1999). Epitope tagging of yeast genes using a PCR-based strategy: more tags and improved practical routines. Yeast *15*, 963-972.

Krantz, I. D., McCallum, J., DeScipio, C., Kaur, M., Gillis, L. A., Yaeger, D., Jukofsky, L., Wasserman, N., Bottani, A., Morris, C. A., *et al.* (2004). Cornelia de Lange syndrome is caused by mutations in NIPBL, the human homolog of Drosophila melanogaster Nipped-B. Nat Genet *36*, 631-635.

Kueng, S., Hegemann, B., Peters, B. H., Lipp, J. J., Schleiffer, A., Mechtler, K., and Peters, J. M. (2006). Wapl controls the dynamic association of cohesin with chromatin. Cell *127*, 955-967.

Kushnirov, V. V. (2000). Rapid and reliable protein extraction from yeast. Yeast *16*, 857-860.

Lakowicz, J. R. (1999). Principles of Fluorescence Spectroscopy. Plenum Press, New York.

Laloraya, S., Guacci, V., and Koshland, D. (2000). Chromosomal addresses of the cohesin component Mcd1p. J Cell Biol *151*, 1047-1056.

Lam, W. W., Peterson, E. A., Yeung, M., and Lavoie, B. D. (2006). Condensin is required for chromosome arm cohesion during mitosis. Genes Dev *20*, 2973-2984.

Lammens, A., Schele, A., and Hopfner, K. P. (2004). Structural biochemistry of ATP-driven dimerization and DNA-stimulated activation of SMC ATPases. Curr Biol *14*, 1778-1782.

Lavoie, B. D., Hogan, E., and Koshland, D. (2002). In vivo dissection of the chromosome condensation machinery: reversibility of condensation distinguishes contributions of condensin and cohesin. J Cell Biol *156*, 805-815.

Lehmann, A. R. (2005). The role of SMC proteins in the responses to DNA damage. DNA Repair (Amst) *4*, 309-314.

Lehmann, A. R., Walicka, M., Griffiths, D. J., Murray, J. M., Watts, F. Z., McCready, S., and Carr, A. M. (1995). The rad18 gene of Schizosaccharomyces pombe defines a new subgroup of the SMC superfamily involved in DNA repair. Mol Cell Biol *15*, 7067-7080.

Lemon, K. P., and Grossman, A. D. (2000). Movement of replicating DNA through a stationary replisome. Mol Cell *6*, 1321-1330.

Lengronne, A., Katou, Y., Mori, S., Yokobayashi, S., Kelly, G. P., Itoh, T., Watanabe, Y., Shirahige, K., and Uhlmann, F. (2004). Cohesin relocation from sites of chromosomal loading to places of convergent transcription. Nature *430*, 573-578.

Lengronne, A., McIntyre, J., Katou, Y., Kanoh, Y., Hopfner, K. P., Shirahige, K., and Uhlmann, F. (2006). Establishment of sister chromatid cohesion at the S. cerevisiae replication fork. Mol Cell *23*, 787-799.

Liang, C., and Stillman, B. (1997). Persistent initiation of DNA replication and chromatin-bound MCM proteins during the cell cycle in cdc6 mutants. Genes Dev *11*, 3375-3386.

Lindroos, H. B., Strom, L., Itoh, T., Katou, Y., Shirahige, K., and Sjogren, C. (2006). Chromosomal association of the Smc5/6 complex reveals that it functions in differently regulated pathways. Mol Cell *22*, 755-767.

Lisby, M., Barlow, J. H., Burgess, R. C., and Rothstein, R. (2004). Choreography of the DNA damage response: spatiotemporal relationships among checkpoint and repair proteins. Cell *118*, 699-713.

Lisby, M., Rothstein, R., and Mortensen, U. H. (2001). Rad52 forms DNA repair and recombination centers during S phase. Proc Natl Acad Sci U S A *98*, 8276-8282.

Locher, K. P., Lee, A. T., and Rees, D. C. (2002). The E. coli BtuCD structure: a framework for ABC transporter architecture and mechanism. Science *296*, 1091-1098.

Losada, A. (2007). Cohesin regulation: fashionable ways to wear a ring. Chromosoma.

Losada, A., Hirano, M., and Hirano, T. (1998). Identification of Xenopus SMC protein complexes required for sister chromatid cohesion. Genes Dev *12*, 1986-1997.

Losada, A., Hirano, M., and Hirano, T. (2002). Cohesin release is required for sister chromatid resolution, but not for condensin-mediated compaction, at the onset of mitosis. Genes Dev *16*, 3004-3016.

Losada, A., and Hirano, T. (2001). Intermolecular DNA interactions stimulated by the cohesin complex in vitro: implications for sister chromatid cohesion. Curr Biol *11*, 268-272.

Losada, A., and Hirano, T. (2005). Dynamic molecular linkers of the genome: the first decade of SMC proteins. Genes Dev *19*, 1269-1287.

Losada, A., Yokochi, T., and Hirano, T. (2005). Functional contribution of Pds5 to cohesin-mediated cohesion in human cells and Xenopus egg extracts. J Cell Sci *118*, 2133-2141.

Losada, A., Yokochi, T., Kobayashi, R., and Hirano, T. (2000). Identification and characterization of SA/Scc3p subunits in the Xenopus and human cohesin complexes. J Cell Biol *150*, 405-416.

Lowe, J., Cordell, S. C., and van den Ent, F. (2001). Crystal structure of the SMC head domain: an ABC ATPase with 900 residues antiparallel coiled-coil inserted. J Mol Biol *306*, 25-35.

Marston, A. L., Tham, W. H., Shah, H., and Amon, A. (2004). A genome-wide screen identifies genes required for centromeric cohesion. Science *303*, 1367-1370.

Mascarenhas, J., Soppa, J., Strunnikov, A. V., and Graumann, P. L. (2002). Cell cycle-dependent localization of two novel prokaryotic chromosome segregation and condensation proteins in Bacillus subtilis that interact with SMC protein. Embo J *21*, 3108-3118.

Matoba, K., Yamazoe, M., Mayanagi, K., Morikawa, K., and Hiraga, S. (2005). Comparison of MukB homodimer versus MukBEF complex molecular architectures by electron microscopy reveals a higher-order multimerization. Biochem Biophys Res Commun *333*, 694-702.

Mayer, M. L., Gygi, S. P., Aebersold, R., and Hieter, P. (2001). Identification of RFC(Ctf18p, Ctf8p, Dcc1p): an alternative RFC complex required for sister chromatid cohesion in S. cerevisiae. Mol Cell *7*, 959-970.

Mayer, M. L., Pot, I., Chang, M., Xu, H., Aneliunas, V., Kwok, T., Newitt, R., Aebersold, R., Boone, C., Brown, G. W., and Hieter, P. (2004). Identification of protein complexes required for efficient sister chromatid cohesion. Mol Biol Cell *15*, 1736-1745.

McDonald, W. H., Pavlova, Y., Yates, J. R., 3rd, and Boddy, M. N. (2003). Novel essential DNA repair proteins Nse1 and Nse2 are subunits of the fission yeast Smc5-Smc6 complex. J Biol Chem *278*, 45460-45467.

McGuinness, B. E., Hirota, T., Kudo, N. R., Peters, J. M., and Nasmyth, K. (2005). Shugoshin prevents dissociation of cohesin from centromeres during mitosis in vertebrate cells. PLoS Biol *3*, e86.

Megee, P. C., Mistrot, C., Guacci, V., and Koshland, D. (1999). The centromeric sister chromatid cohesion site directs Mcd1p binding to adjacent sequences. Mol Cell *4*, 445-450.

Melby, T. E., Ciampaglio, C. N., Briscoe, G., and Erickson, H. P. (1998). The symmetrical structure of structural maintenance of chromosomes (SMC) and MukB proteins: long, antiparallel coiled coils, folded at a flexible hinge. J Cell Biol *142*, 1595-1604.

Mendelsohn, A. R., and Brent, R. (1999). Protein interaction methods--toward an endgame. Science *284*, 1948-1950.

Mengiste, T., Revenkova, E., Bechtold, N., and Paszkowski, J. (1999). An SMC-like protein is required for efficient homologous recombination in Arabidopsis. Embo J *18*, 4505-4512.

Michaelis, C., Ciosk, R., and Nasmyth, K. (1997). Cohesins: chromosomal proteins that prevent premature separation of sister chromatids. Cell *91*, 35-45.

Milutinovich, M., and Koshland, D. E. (2003). Molecular biology. SMC complexes--wrapped up in controversy. Science *300*, 1101-1102.

Milutinovich, M., Unal, E., Ward, C., Skibbens, R. V., and Koshland, D. (2007). A Multi-Step Pathway for the Establishment of Sister Chromatid Cohesion. PLoS Genet *3*, e12.

Moldovan, G. L., Pfander, B., and Jentsch, S. (2006). PCNA controls establishment of sister chromatid cohesion during S phase. Mol Cell *23*, 723-732.

Moncalian, G., Lengsfeld, B., Bhaskara, V., Hopfner, K. P., Karcher, A., Alden, E., Tainer, J. A., and Paull, T. T. (2004). The rad50 signature motif: essential to ATP binding and biological function. J Mol Biol *335*, 937-951.

Moreno-Herrero, F., de Jager, M., Dekker, N. H., Kanaar, R., Wyman, C., and Dekker, C. (2005). Mesoscale conformational changes in the DNA-repair complex Rad50/Mre11/Nbs1 upon binding DNA. Nature *437*, 440-443.

Morikawa, H., Morishita, T., Kawane, S., Iwasaki, H., Carr, A. M., and Shinagawa, H. (2004). Rad62 protein functionally and physically associates with the smc5/smc6 protein complex and is required for chromosome integrity and recombination repair in fission yeast. Mol Cell Biol *24*, 9401-9413.

Mosser, J., Douar, A. M., Sarde, C. O., Kioschis, P., Feil, R., Moser, H., Poustka, A. M., Mandel, J. L., and Aubourg, P. (1993). Putative X-linked adrenoleukodystrophy gene shares unexpected homology with ABC transporters. Nature *361*, 726-730.

Muller, E. G., Snydsman, B. E., Novik, I., Hailey, D. W., Gestaut, D. R., Niemann, C. A., O'Toole, E. T., Giddings, T. H., Jr., Sundin, B. A., and Davis, T. N. (2005). The organization of the core proteins of the yeast spindle pole body. Mol Biol Cell *16*, 3341-3352.

Nasim, A., and Smith, B. P. (1975). Genetic control of radiation sensitivity in Schizosaccharomyces pombe. Genetics *79*, 573-582.

Nasmyth, K. (2002). Segregating sister genomes: the molecular biology of chromosome separation. Science *297*, 559-565.

Nasmyth, K., and Haering, C. H. (2005). The structure and function of SMC and kleisin complexes. Annu Rev Biochem *74*, 595-648.

Neuwald, A. F., and Hirano, T. (2000). HEAT repeats associated with condensins, cohesins, and other complexes involved in chromosome-related functions. Genome Res *10*, 1445-1452.

Niki, H., Jaffe, A., Imamura, R., Ogura, T., and Hiraga, S. (1991). The new gene mukB codes for a 177 kd protein with coiled-coil domains involved in chromosome partitioning of E. coli. Embo J *10*, 183-193.

Noble, D., Kenna, M. A., Dix, M., Skibbens, R. V., Unal, E., and Guacci, V. (2006). Intersection Between the Regulators of Sister Chromatid Cohesion Establishment and Maintenance in Budding Yeast Indicates a Multi-Step Mechanism. Cell Cycle *5*.

Nonaka, N., Kitajima, T., Yokobayashi, S., Xiao, G., Yamamoto, M., Grewal, S. I., and Watanabe, Y. (2002). Recruitment of cohesin to heterochromatic regions by Swi6/HP1 in fission yeast. Nat Cell Biol *4*, 89-93.

Obmolova, G., Ban, C., Hsieh, P., and Yang, W. (2000). Crystal structures of mismatch repair protein MutS and its complex with a substrate DNA. Nature *407*, 703-710.

Onn, I., Aono, N., Hirano, M., and Hirano, T. (2007). Reconstitution and subunit geometry of human condensin complexes. Embo J *26*, 1024-1034.

Ono, T., Fang, Y., Spector, D. L., and Hirano, T. (2004). Spatial and temporal regulation of Condensins I and II in mitotic chromosome assembly in human cells. Mol Biol Cell *15*, 3296-3308.

Ono, T., Losada, A., Hirano, M., Myers, M. P., Neuwald, A. F., and Hirano, T. (2003). Differential contributions of condensin I and condensin II to mitotic chromosome architecture in vertebrate cells. Cell *115*, 109-121.

Onoda, F., Takeda, M., Seki, M., Maeda, D., Tajima, J., Ui, A., Yagi, H., and Enomoto, T. (2004). SMC6 is required for MMS-induced interchromosomal and sister chromatid recombinations in Saccharomyces cerevisiae. DNA Repair (Amst) *3*, 429-439.

Ormo, M., Cubitt, A. B., Kallio, K., Gross, L. A., Tsien, R. Y., and Remington, S. J. (1996). Crystal structure of the Aequorea victoria green fluorescent protein. Science *273*, 1392-1395.

Palecek, J., Vidot, S., Feng, M., Doherty, A. J., and Lehmann, A. R. (2006). The Smc5-Smc6 DNA repair complex. bridging of the Smc5-Smc6 heads by the KLEISIN, Nse4, and non-Kleisin subunits. J Biol Chem *281*, 36952-36959.

Panizza, S., Tanaka, T., Hochwagen, A., Eisenhaber, F., and Nasmyth, K. (2000). Pds5 cooperates with cohesin in maintaining sister chromatid cohesion. Curr Biol *10*, 1557-1564.

Parisi, S., McKay, M. J., Molnar, M., Thompson, M. A., van der Spek, P. J., van Drunen-Schoenmaker, E., Kanaar, R., Lehmann, E., Hoeijmakers, J. H., and Kohli, J. (1999). Rec8p, a meiotic recombination and sister chromatid cohesion phosphoprotein of the Rad21p family conserved from fission yeast to humans. Mol Cell Biol *19*, 3515-3528.

Paull, T. T., and Gellert, M. (1998). The 3' to 5' exonuclease activity of Mre 11 facilitates repair of DNA double-strand breaks. Mol Cell *1*, 969-979.

Pebernard, S., McDonald, W. H., Pavlova, Y., Yates, J. R., 3rd, and Boddy, M. N. (2004). Nse1, Nse2, and a novel subunit of the Smc5-Smc6 complex, Nse3, play a crucial role in meiosis. Mol Biol Cell *15*, 4866-4876.

Pebernard, S., Wohlschlegel, J., McDonald, W. H., Yates, J. R., 3rd, and Boddy, M. N. (2006). The Nse5-Nse6 dimer mediates DNA repair roles of the Smc5-Smc6 complex. Mol Cell Biol *26*, 1617-1630.

Peter, M., and Ameer-Beg, S. M. (2004). Imaging molecular interactions by multiphoton FLIM. Biol Cell *96*, 231-236.

Petronczki, M., Chwalla, B., Siomos, M. F., Yokobayashi, S., Helmhart, W., Deutschbauer, A. M., Davis, R. W., Watanabe, Y., and Nasmyth, K. (2004). Sister-chromatid cohesion mediated by the alternative RF-CCtf18/Dcc1/Ctf8, the helicase Chl1 and the polymerase-alpha-associated protein Ctf4 is essential for chromatid disjunction during meiosis II. J Cell Sci *117*, 3547-3559.

Petronczki, M., Siomos, M. F., and Nasmyth, K. (2003). Un menage a quatre: the molecular biology of chromosome segregation in meiosis. Cell *112*, 423-440.

Pezzi, N., Prieto, I., Kremer, L., Perez Jurado, L. A., Valero, C., Del Mazo, J., Martinez, A. C., and Barbero, J. L. (2000). STAG3, a novel gene encoding a protein involved in meiotic chromosome pairing and location of STAG3-related genes flanking the Williams-Beuren syndrome deletion. Faseb J *14*, 581-592.

Potts, P. R., Porteus, M. H., and Yu, H. (2006). Human SMC5/6 complex promotes sister chromatid homologous recombination by recruiting the SMC1/3 cohesin complex to double-strand breaks. Embo J *25*, 3377-3388.

Prein, B., Natter, K., and Kohlwein, S. D. (2000). A novel strategy for constructing N-terminal chromosomal fusions to green fluorescent protein in the yeast Saccharomyces cerevisiae. FEBS Lett *485*, 29-34.

Rabitsch, K. P., Gregan, J., Schleiffer, A., Javerzat, J. P., Eisenhaber, F., and Nasmyth, K. (2004). Two fission yeast homologs of Drosophila Mei-S332 are required for chromosome segregation during meiosis I and II. Curr Biol *14*, 287-301.

Rankin, S., Ayad, N. G., and Kirschner, M. W. (2005). Sororin, a substrate of the anaphase-promoting complex, is required for sister chromatid cohesion in vertebrates. Mol Cell *18*, 185-200.

Rao, H., Uhlmann, F., Nasmyth, K., and Varshavsky, A. (2001). Degradation of a cohesin subunit by the N-end rule pathway is essential for chromosome stability. Nature *410*, 955-959.

Riedel, C. G., Gregan, J., Gruber, S., and Nasmyth, K. (2004). Is chromatin remodeling required to build sister-chromatid cohesion? Trends Biochem Sci *29*, 389-392.

Riedel, C. G., Katis, V. L., Katou, Y., Mori, S., Itoh, T., Helmhart, W., Galova, M., Petronczki, M., Gregan, J., Cetin, B., *et al.* (2006). Protein phosphatase 2A protects centromeric sister chromatid cohesion during meiosis I. Nature.

Riordan, J. R., Rommens, J. M., Kerem, B., Alon, N., Rozmahel, R., Grzelczak, Z., Zielenski, J., Lok, S., Plavsic, N., Chou, J. L., and et al. (1989). Identification of the cystic fibrosis gene: cloning and characterization of complementary DNA. Science *245*, 1066-1073.

Saka, Y., Sutani, T., Yamashita, Y., Saitoh, S., Takeuchi, M., Nakaseko, Y., and Yanagida, M. (1994). Fission yeast cut3 and cut14, members of a ubiquitous protein family, are required for chromosome condensation and segregation in mitosis. Embo J *13*, 4938-4952.

Sakai, A., Hizume, K., Sutani, T., Takeyasu, K., and Yanagida, M. (2003). Condensin but not cohesin SMC heterodimer induces DNA reannealing through protein-protein assembly. Embo J *22*, 2764-2775.

Salic, A., Waters, J. C., and Mitchison, T. J. (2004). Vertebrate shugoshin links sister centromere cohesion and kinetochore microtubule stability in mitosis. Cell *118*, 567-578.

Schalch, T., Duda, S., Sargent, D. F., and Richmond, T. J. (2005). X-ray structure of a tetranucleosome and its implications for the chromatin fibre. Nature *436*, 138-141.

Scheffzek, K., Ahmadian, M. R., Kabsch, W., Wiesmuller, L., Lautwein, A., Schmitz, F., and Wittinghofer, A. (1997). The Ras-RasGAP complex: structural basis for GTPase activation and its loss in oncogenic Ras mutants. Science *277*, 333-338.

Schleiffer, A., Kaitna, S., Maurer-Stroh, S., Glotzer, M., Nasmyth, K., and Eisenhaber, F. (2003). Kleisins: a superfamily of bacterial and eukaryotic SMC protein partners. Mol Cell *11*, 571-575.

Schmitz, J., Watrin, E., Lenart, P., Mechtler, K., and Peters, J. M. (2007). Sororin is required for stable binding of cohesin to chromatin and for sister chromatid cohesion in interphase. Curr Biol *17*, 630-636.

Schwob, E., and Nasmyth, K. (1993). CLB5 and CLB6, a new pair of B cyclins involved in DNA replication in Saccharomyces cerevisiae. Genes Dev *7*, 1160-1175.

Sergeant, J., Taylor, E., Palecek, J., Fousteri, M., Andrews, E. A., Sweeney, S., Shinagawa, H., Watts, F. Z., and Lehmann, A. R. (2005). Composition and architecture of the Schizosaccharomyces pombe Rad18 (Smc5-6) complex. Mol Cell Biol *25*, 172-184.

Shepherd, A. J., Gorse, D., and Thornton, J. M. (1999). Prediction of the location and type of beta-turns in proteins using neural networks. Protein Sci *8*, 1045-1055.

Shih, I. M., Zhou, W., Goodman, S. N., Lengauer, C., Kinzler, K. W., and Vogelstein, B. (2001). Evidence that genetic instability occurs at an early stage of colorectal tumorigenesis. Cancer Res *61*, 818-822.

Shimada, K., and Gasser, S. M. (2007). The origin recognition complex functions in sister-chromatid cohesion in Saccharomyces cerevisiae. Cell *128*, 85-99.

Shintomi, K., and Hirano, T. (2007). How are cohesin rings opened and closed? Trends Biochem Sci.

Shroff, R., Arbel-Eden, A., Pilch, D., Ira, G., Bonner, W. M., Petrini, J. H., Haber, J. E., and Lichten, M. (2004). Distribution and dynamics of chromatin modification induced by a defined DNA double-strand break. Curr Biol *14*, 1703-1711.

Simon, P., Houston, P., and Broach, J. (2002). Directional bias during mating type switching in Saccharomyces is independent of chromosomal architecture. Embo J *21*, 2282-2291.

Sjogren, C., and Nasmyth, K. (2001). Sister chromatid cohesion is required for postreplicative double-strand break repair in Saccharomyces cerevisiae. Curr Biol *11*, 991-995.

Skibbens, R. V. (2004). Chl1p, a DNA helicase-like protein in budding yeast, functions in sister-chromatid cohesion. Genetics *166*, 33-42.

Skibbens, R. V., Corson, L. B., Koshland, D., and Hieter, P. (1999). Ctf7p is essential for sister chromatid cohesion and links mitotic chromosome structure to the DNA replication machinery. Genes Dev *13*, 307-319.

Smith, P. C., Karpowich, N., Millen, L., Moody, J. E., Rosen, J., Thomas, P. J., and Hunt, J. F. (2002). ATP binding to the motor domain from an ABC transporter drives formation of a nucleotide sandwich dimer. Mol Cell *10*, 139-149.

Sonoda, E., Matsusaka, T., Morrison, C., Vagnarelli, P., Hoshi, O., Ushiki, T., Nojima, K., Fukagawa, T., Waizenegger, I. C., Peters, J. M., *et al.* (2001). Scc1/Rad21/Mcd1 is required for sister chromatid cohesion and kinetochore function in vertebrate cells. Dev Cell *1*, 759-770.

Stead, K., Aguilar, C., Hartman, T., Drexel, M., Meluh, P., and Guacci, V. (2003). Pds5p regulates the maintenance of sister chromatid cohesion and is sumoylated to promote the dissolution of cohesion. J Cell Biol *163*, 729-741.

Strachan, T. (2005). Cornelia de Lange Syndrome and the link between chromosomal function, DNA repair and developmental gene regulation. Curr Opin Genet Dev *15*, 258-264.

Strathern, J. N., Klar, A. J., Hicks, J. B., Abraham, J. A., Ivy, J. M., Nasmyth, K. A., and McGill, C. (1982). Homothallic switching of yeast mating type cassettes is initiated by a double-stranded cut in the MAT locus. Cell *31*, 183-192.

Stray, J. E., and Lindsley, J. E. (2003). Biochemical analysis of the yeast condensin Smc2/4 complex: an ATPase that promotes knotting of circular DNA. J Biol Chem *278*, 26238-26248.

Strick, T. R., Kawaguchi, T., and Hirano, T. (2004). Real-time detection of single-molecule DNA compaction by condensin I. Curr Biol *14*, 874-880.

Strom, L., Lindroos, H. B., Shirahige, K., and Sjogren, C. (2004). Postreplicative recruitment of cohesin to double-strand breaks is required for DNA repair. Mol Cell *16*, 1003-1015.

Strom, L., and Sjogren, C. (2005). DNA damage-induced cohesion. Cell Cycle *4*, 536-539.

Strunnikov, A. V., Hogan, E., and Koshland, D. (1995). SMC2, a Saccharomyces cerevisiae gene essential for chromosome segregation and condensation, defines a subgroup within the SMC family. Genes Dev *9*, 587-599.

Stryer, L. (1978). Fluorescence energy transfer as a spectroscopic ruler. Annu Rev Biochem *47*, 819-846.

Sumara, I., Vorlaufer, E., Gieffers, C., Peters, B. H., and Peters, J. M. (2000). Characterization of vertebrate cohesin complexes and their regulation in prophase. J Cell Biol *151*, 749-762.

Sumara, I., Vorlaufer, E., Stukenberg, P. T., Kelm, O., Redemann, N., Nigg, E. A., and Peters, J. M. (2002). The dissociation of cohesin from chromosomes in prophase is regulated by Polo-like kinase. Mol Cell *9*, 515-525.

Sutani, T., Yuasa, T., Tomonaga, T., Dohmae, N., Takio, K., and Yanagida, M. (1999). Fission yeast condensin complex: essential roles of non-SMC subunits for condensation and Cdc2 phosphorylation of Cut3/SMC4. Genes Dev *13*, 2271-2283.

Suter, B., Tong, A., Chang, M., Yu, L., Brown, G. W., Boone, C., and Rine, J. (2004). The origin recognition complex links replication, sister chromatid cohesion and transcriptional silencing in Saccharomyces cerevisiae. Genetics *167*, 579-591.

Takahashi, K., Yamada, H., and Yanagida, M. (1994). Fission yeast minichromosome loss mutants mis cause lethal aneuploidy and replication abnormality. Mol Biol Cell *5*, 1145-1158.

Takahashi, T. S., Yiu, P., Chou, M. F., Gygi, S., and Walter, J. C. (2004). Recruitment of Xenopus Scc2 and cohesin to chromatin requires the pre-replication complex. Nat Cell Biol *6*, 991-996.

Takemoto, A., Kimura, K., Yanagisawa, J., Yokoyama, S., and Hanaoka, F. (2006). Negative regulation of condensin I by CK2-mediated phosphorylation. Embo J *25*, 5339-5348.

Tanaka, K., Hao, Z., Kai, M., and Okayama, H. (2001). Establishment and maintenance of sister chromatid cohesion in fission yeast by a unique mechanism. Embo J *20*, 5779-5790.

Tanaka, K., Yonekawa, T., Kawasaki, Y., Kai, M., Furuya, K., Iwasaki, M., Murakami, H., Yanagida, M., and Okayama, H. (2000). Fission yeast Eso1p is required for establishing sister chromatid cohesion during S phase. Mol Cell Biol *20*, 3459-3469.

Tanaka, T., Cosma, M. P., Wirth, K., and Nasmyth, K. (1999). Identification of cohesin association sites at centromeres and along chromosome arms. Cell *98*, 847-858.

Tang, Z., Sun, Y., Harley, S. E., Zou, H., and Yu, H. (2004). Human Bub1 protects centromeric sister-chromatid cohesion through Shugoshin during mitosis. Proc Natl Acad Sci U S A *101*, 18012-18017.

Terret, M. E., Wassmann, K., Waizenegger, I., Maro, B., Peters, J. M., and Verlhac, M. H. (2003). The meiosis I-to-meiosis II transition in mouse oocytes requires separase activity. Curr Biol *13*, 1797-1802.

Tonkin, E. T., Wang, T. J., Lisgo, S., Bamshad, M. J., and Strachan, T. (2004). NIPBL, encoding a homolog of fungal Scc2-type sister chromatid cohesion proteins and fly Nipped-B, is mutated in Cornelia de Lange syndrome. Nat Genet *36*, 636-641.

Torres-Rosell, J., Machin, F., Farmer, S., Jarmuz, A., Eydmann, T., Dalgaard, J. Z., and Aragon, L. (2005). SMC5 and SMC6 genes are required for the segregation of repetitive chromosome regions. Nat Cell Biol *7*, 412-419.

Toth, A., Ciosk, R., Uhlmann, F., Galova, M., Schleiffer, A., and Nasmyth, K. (1999). Yeast cohesin complex requires a conserved protein, Eco1p(Ctf7), to establish cohesion between sister chromatids during DNA replication. Genes Dev *13*, 320-333.

Truong, K., and Ikura, M. (2001). The use of FRET imaging microscopy to detect protein-protein interactions and protein conformational changes in vivo. Curr Opin Struct Biol *11*, 573-578.

Tsuyama, T., Inou, K., Seki, M., Seki, T., Kumata, Y., Kobayashi, T., Kimura, K., Hanaoka, F., Enomoto, T., and Tada, S. (2006). Chromatin loading of Smc5/6 is induced by DNA replication but not by DNA double-strand breaks. Biochem Biophys Res Commun *351*, 935-939.

Uhlmann, F., Lottspeich, F., and Nasmyth, K. (1999). Sister-chromatid separation at anaphase onset is promoted by cleavage of the cohesin subunit Scc1. Nature *400*, 37-42.

Uhlmann, F., and Nasmyth, K. (1998). Cohesion between sister chromatids must be established during DNA replication. Curr Biol *8*, 1095-1101.

Uhlmann, F., Wernic, D., Poupart, M. A., Koonin, E. V., and Nasmyth, K. (2000). Cleavage of cohesin by the CD clan protease separin triggers anaphase in yeast. Cell *103*, 375-386.

Unal, E., Arbel-Eden, A., Sattler, U., Shroff, R., Lichten, M., Haber, J. E., and Koshland, D. (2004). DNA damage response pathway uses histone modification to assemble a double-strand break-specific cohesin domain. Mol Cell *16*, 991-1002.

van Heemst, D., James, F., Poggeler, S., Berteaux-Lecellier, V., and Zickler, D. (1999). Spo76p is a conserved chromosome morphogenesis protein that links the mitotic and meiotic programs. Cell *98*, 261-271.

Varshavsky, A. (1996). The N-end rule: functions, mysteries, uses. Proc Natl Acad Sci U S A *93*, 12142-12149.

Vergani, P., Lockless, S. W., Nairn, A. C., and Gadsby, D. C. (2005). CFTR channel opening by ATP-driven tight dimerization of its nucleotide-binding domains. Nature *433*, 876-880.

Verkade, H. M., Bugg, S. J., Lindsay, H. D., Carr, A. M., and O'Connell, M. J. (1999). Rad18 is required for DNA repair and checkpoint responses in fission yeast. Mol Biol Cell *10*, 2905-2918.

Verni, F., Gandhi, R., Goldberg, M. L., and Gatti, M. (2000). Genetic and molecular analysis of wings apart-like (wapl), a gene controlling heterochromatin organization in Drosophila melanogaster. Genetics *154*, 1693-1710.

Vogel, S. S., Thaler, C., and Koushik, S. V. (2006). Fanciful FRET. Sci STKE *2006*, re2.

Vrabioiu, A. M., and Mitchison, T. J. (2006). Structural insights into yeast septin organization from polarized fluorescence microscopy. Nature *443*, 466-469.

Waizenegger, I. C., Hauf, S., Meinke, A., and Peters, J. M. (2000). Two distinct pathways remove mammalian cohesin from chromosome arms in prophase and from centromeres in anaphase. Cell *103*, 399-410.

Wang, Z., Castano, I. B., De Las Penas, A., Adams, C., and Christman, M. F. (2000). Pol kappa: A DNA polymerase required for sister chromatid cohesion. Science *289*, 774-779.

Warren, C. D., Eckley, D. M., Lee, M. S., Hanna, J. S., Hughes, A., Peyser, B., Jie, C., Irizarry, R., and Spencer, F. A. (2004). S-phase checkpoint genes safeguard high-fidelity sister chromatid cohesion. Mol Biol Cell *15*, 1724-1735.

Watanabe, Y. (2005). Shugoshin: guardian spirit at the centromere. Curr Opin Cell Biol *17*, 590-595.

Watanabe, Y., and Nurse, P. (1999). Cohesin Rec8 is required for reductional chromosome segregation at meiosis. Nature *400*, 461-464.

Watrin, E., Schleiffer, A., Tanaka, K., Eisenhaber, F., Nasmyth, K., and Peters, J. M. (2006). Human Scc4 is required for cohesin binding to chromatin, sister-chromatid cohesion, and mitotic progression. Curr Biol *16*, 863-874.

Weber, S. A., Gerton, J. L., Polancic, J. E., DeRisi, J. L., Koshland, D., and Megee, P. C. (2004). The kinetochore is an enhancer of pericentric cohesin binding. PLoS Biol *2*, E260.

Weitzer, S., Lehane, C., and Uhlmann, F. (2003). A model for ATP hydrolysis-dependent binding of cohesin to DNA. Curr Biol *13*, 1930-1940.

Williams, B. C., Garrett-Engele, C. M., Li, Z., Williams, E. V., Rosenman, E. D., and Goldberg, M. L. (2003). Two putative acetyltransferases, san and deco, are required for establishing sister chromatid cohesion in Drosophila. Curr Biol *13*, 2025-2036.

Winzeler, E. A., Richards, D. R., Conway, A. R., Goldstein, A. L., Kalman, S., McCullough, M. J., McCusker, J. H., Stevens, D. A., Wodicka, L., Lockhart, D. J., and Davis, R. W. (1998). Direct allelic variation scanning of the yeast genome. Science *281*, 1194-1197.

Yamamoto, A., Guacci, V., and Koshland, D. (1996). Pds1p is required for faithful execution of anaphase in the yeast, Saccharomyces cerevisiae. J Cell Biol *133*, 85-97.

Yamazoe, M., Onogi, T., Sunako, Y., Niki, H., Yamanaka, K., Ichimura, T., and Hiraga, S. (1999). Complex formation of MukB, MukE and MukF proteins involved in chromosome partitioning in Escherichia coli. Embo J *18*, 5873-5884.

Yazdi, P. T., Wang, Y., Zhao, S., Patel, N., Lee, E. Y., and Qin, J. (2002). SMC1 is a downstream effector in the ATM/NBS1 branch of the human S-phase checkpoint. Genes Dev *16*, 571-582.

Yu, X., VanLoock, M. S., Poplawski, A., Kelman, Z., Xiang, T., Tye, B. K., and Egelman, E. H. (2002). The Methanobacterium thermoautotrophicum MCM protein can form heptameric rings. EMBO Rep *3*, 792-797.

Yuan, Y. R., Blecker, S., Martsinkevich, O., Millen, L., Thomas, P. J., and Hunt, J. F. (2001). The crystal structure of the MJ0796 ATP-binding cassette. Implications for the structural consequences of ATP hydrolysis in the active site of an ABC transporter. J Biol Chem *276*, 32313-32321.

Zhao, X., and Blobel, G. (2005). A SUMO ligase is part of a nuclear multiprotein complex that affects DNA repair and chromosomal organization. Proc Natl Acad Sci U S A *102*, 4777-4782.

Zou, H., and Rothstein, R. (1997). Holliday junctions accumulate in replication mutants via a RecA homolog-independent mechanism. Cell *90*, 87-96.